UNIVERSITY OF OKLAHOMA

GRADUATE COLLEGE

ANTIBIOTIC COMBINATION THERAPY AGAINST MULTIDRUG-RESISTANT *STAPHYLOCOCCUS EPIDERMIDIS* BIOFILMS AND BROADENING ANTIBIOTIC SPECTRUM USING POLYETHYLENIMINE

A DISSERTATION

SUBMITTED TO THE GRADUATE FACULTY

in partial fulfillment of the requirements for the

Degree of

DOCTOR OF PHILOSOPHY

By

ANH KIM LAM
Norman, Oklahoma
2020

Downloaded from SHAREOK. Persistent Handle URL: https://hdl.handle.net/11244/325287

ANTIBIOTIC COMBINATION THERAPY AGAINST MULTIDRUG-RESISTANT *STAPHYLOCOCCUS EPIDERMIDIS* BIOFILMS AND BROADENING ANTIBIOTIC SPECTRUM USING POLYETHYLENIMINE

A DISSERTATION APPROVED FOR THE
DEPARTMENT OF CHEMISTRY AND BIOCHEMISTRY

BY
THE COMMITTEE CONSISTING OF

Dr. Charles V. Rice, Chair

Dr. Si Wu

Dr. Zhibo Yang

Dr. Yihan Shao

Dr. Mark Nanny

© Copyright by ANH KIM LAM 2020
All Rights Reserved.

Dedicated to my *mom*
and all teachers, scientists, researchers, health care providers, policy makers, and others
who are supporting science.

Acknowledgements

The completion of this graduate-school journey could not have been possible without the guidance and support of many people. Although my words are fallen short in expressing boundless gratitude for them whose names may not all be enumerated, I am immensely grateful!

The most special thankfulness goes to my family, Quen Nguyen (Mẹ/Mother), Tai Lam (Ba/Father), Nhan Bunn (Cô-2/Aunt), and Travis Bunn (Daddle) for their strong and rooted support.

My sincere thanks also arise for my cherished and valued friends who have become my adopted family: Melissa Hill, Anita Ly, Hannah Panlilio, and Dai & Ninh Nguyen!

I feel deeply grateful to all the colleagues and members in the Rice Lab for each of them helped me in ways that I could never fully express: Erika Moen, Casey Wouters, Jennifer Pusavat, Beatrice Wilson, Andrew Neel, Tristan Haight, and Neda Heydarian.

A special word of appreciation also goes to Prof. Bob (Robert) Brennan from the University of Central Oklahoma (UCO) for his assistance, guidance, and intellectual suggestions during my last project with human cells.

I extend my thankfulness to my graduate committee members: Prof. Mark Nanny, Prof. Yihan Shao, Prof. Zhibo Yang, and Prof. Si Wu, for their thoughtful and valuable advice and suggestions.

Thanks are also due to Dr. Preston Larson, Dr. Phil Bourne, Dr. Erwin Abucayon, Dr. Naga Rama Kothapalli, and Dr. Steven Foster for their help and co-operation in their research expertise.

I will fail in my duty if I do not thank my undergraduate professors: Prof. Fakhrildeen Albahadily, Prof. Wei Chen, Prof. Hari Kotturi, and Prof. Lilian Chooback for seeding/nurturing the love of science in me and providing me every help to further reach my dreamed-goal.

My heartfelt appreciation also goes to my partner, Sam Wood, for always being there, putting up with me, and encouraging/supporting me.

Finally and most importantly, I immensely thank my idol and respectful mentor, Prof. Charles V. Rice, for his mentorship, guidance, support, encouragement, and constructive criticism at every stage of this journey. His keen personal interest (and dad jokes) inspired me even more for a positive work attitude in science and research and to work more diligently and efficiently. I cannot conclude my acknowledgements without my heartful gratitude to his wife, Toni Rice, for her priceless advice and encouragements beyond academic subjects. They – my lab parents – both have welcomed and treated me like family, and their generous supports have made my time here incredibly joyous!

Table of Contents

Acknowledgements iv

List of Tables xi

List of Figures xii

Abstract xxii

Chapter 1: *Staphylococcus epidermidis,* an opportunistic pathogen 1

Antibiotic Resistance 2

The Emergence of MRSE 5

The Cell Wall and The Gram Stain Characteristics 7

β-Lactam Antibiotic Resistance 11

The Need for New Strategies 15

Chapter 2: 600-Da Branched Polyethylenimine (BPEI) and Its Effect on Human Inflammatory Responses 17

Background 17

Chemistry and Applications of BPEI 18

600-Da BPEI's Cytotoxicity and Biocompatibility 19

Purpose of Experiment 20

Experimental Procedures 21

High Performance Liquid Chromatography (HPLC) 21

Mass Spectrometry (MS) 21

Fourier-transform infrared spectroscopy (FTIR) 21

Effects of BPEI on human epithelia's inflammatory cytokines 22

Results and Discussion 23

Instrumental Analyses 23
Inflammatory Response of Human Epithelial Keratinocytes exposed to BPEI . 26
Therapeutic Potentials of 600-Da BPEI 32
Conclusions 33
Chapter 3: Synergy between β-lactam antibiotics and BPEI against planktonic MRSE 34
Background 34
Purpose of Experiment 36
Experimental Procedures 36
Materials 36
In vitro Checkerboard Assays 36
Growth Curves 37
Scanning Electron Microscopy (SEM) 37
Transmission Electron Microscopy (TEM) 38
Results and Discussion 39
Checkerboard assays indicate synergistic effects between BPEI and β-lactams 39
Growth curves confirm antimicrobial activity of oxacillin was restored 42
Scanning and transmission electron microscopies confirm BPEI's mechanism of action 44
Conclusions 49
Chapter 4: BPEI potentiates β-lactam antibiotics against MRSE biofilms 52
Background 52
Biofilms and Multidrug Resistance 52

Purpose of Experiment 56
Experimental Procedures 56
Materials 56
MBEC Assay 57
Biofilm Disrupting Assay 59
Minimum Biofilm Inhibitory Concentration (MBIC) 60
Biofilm Kill Curve 60
Results and Discussion 61
Confirmation of MRSE Biofilms 62
Efficacy of BPEI and β-lactams Against MRSE Biofilms 64
BPEI Possesses Biofilm-Disrupting Potential 66
Biofilm Inhibition and Eradication Using Combination of BPEI + β-Lactams . 69
Efficacy of BPEI on 3-Day-Old Biofilms 72
Conclusions 74
Chapter 5: BPEI potentiates ampicillin against MRSA biofilms 76
Background 76
Prevalence and Pathogeneses 76
Purpose of Experiment 79
Experimental Procedures 80
Materials: 80
MBEC Assay 80
Biofilm Disrupting Assay 81
Scanning Electron Microscopy (SEM) 81

SEM of Biofilms on Polycarbonate Membrane Filters 82
Results and Discussion 83
Conclusion 91
Chapter 6: Broadening the spectrum of antibiotics capable of killing multidrug-resistant *Staphylococcus aureus* and *Pseudomonas aeruginosa* 93
Background 93
Bacterial Membranes and The Non-β-Lactam Antibiotics 94
Purpose of Experiment 97
Experimental Procedures 97
Materials 97
In Vitro Checkerboard Assay 98
Cell-permeation Assay / bisBenzimide H33342 Intracellular Accumulation 98
Cell viability assays 99
IL-8 responses 99
Results and Discussion 100
Conclusions 111
Chapter 7: Overcoming multidrug resistance and biofilms of *Pseudomonas aeruginosa* with a single dual-function potentiator 113
Background 113
Pathogeneses and Virulence 114
Purpose of Experiment 115
Experimental Procedures 115
Materials 115

Checkerboard Assays and Growth Curves 116
MBEC Assay: 116
Scanning Electron Microscopy 117
H33342 Bisbenzimide and NPN Accumulation Assays 118
Results and Discussion 119
BPEI synergizes β-lactams against multidrug-resistant Pseudomonas aeruginosa 119
Mechanisms of action of BPEI on the influx and efflux effects 122
SEM images demonstrate adverse effects of 600-Da BPEI on morphology 128
Eradicating P. aeruginosa biofilms 131
Conclusions 132
References 134

List of Tables

Table 1. Distinct antibacterial drugs and their targets 3

Table 2: Characteristics of Gram-positive and Gram-negative bacteria 10

Table 3. Synergy of 600-Da BPEI and antibiotics against MRSE 40

Table 4: MRSA clinical isolates susceptibility data 79

Table 5. Synergistic effects between BPEI and ampicillin against MRSA biofilms 84

Table 6. Synergy of 600-Da BPEI and antibiotics against MRSA and MDR-PA clinical isolates 102

Table 7. MIC and FICI values for *P. aeruginosa* treated with 600-Da BPEI, piperacillin, and their combination. 121

List of Figures

Figure 1. Antibiotic discovery timeline and the “discovery void.” Years shown are first reported patented antibiotics. 3

Figure 2. Cell wall structure of Gram-positive and Gram-negative bacteria. 9

Figure 3. A core chemical structure of penicillin with the β-lactam ring (square-shape ring in blue frame). The ring is a four-membered cyclic amide. It holds each bond at 90° angle and is reactive to binding covalently to bacterial penicillin binding proteins (PBPs). 11

Figure 4. Chemical structure of D-ala-D-ala peptidoglycan terminus, which has structural similarity to β-lactam ring. 12

Figure 5. Illustration of the cell wall peptidoglycan crosslinking in MRSE. Penicillin binding proteins (PBPs and PBP2a) crosslink the subunits of the peptidoglycan, completing the last stage of cell wall synthesis. 14

Figure 6. Illustration of β-lactam resistance factor, PBP2a, in MRSE. Regular PBPs are inhibited by β-lactam antibiotics, except PBP2a. PBP2a has low affinity to β-lactams and thereby can still crosslink the cell wall without being affected. A cofactor of PBP2a is the wall teichoic acid (WTA) which localizes PBP2a. 14

Figure 7. Chemical structure of 600-Da BPEI. The repeating unit of an amine group and an ethyl 2-carbon spacer continues on for larger molecular-weight BPEIs. 18

Figure 8. HPLC chromatogram of 600-Da BPEI solution (2.56 mg/mL). Retention time of BPEI peaks at 2.09 min. 24

Figure 9. Mass spectrum of 600-Da BPEI. Most abundant peaks are around ~500 m/z which are the most ionized fragments of 600-Da BPEI. Most peaks have a similar

difference of 43 m/z from their adjacent peaks, which is equal to the m/z ratio of one amine and an ethyl repeating unit of the polymer BPEI (i.e. 534.5 – 491.5 = 43 m/z).. 25

Figure 10. FTIR spectrum of 600-Da BPEI (in CCl_4)..... 26

Figure 11. Standard curves of the three cytokines tested (IL-8, IL-6, and TNF-α). Linear fitted equations are shown with their corresponding R-squared values. These equations were used to calculate the amount of the cytokines released by HEKa cells..... 29

Figure 12. Cytokines released (picograms - pg/mL) by human epithelial keratinocytes (HEKa cells) in responses to peptidoglycan (PG), lipopolysaccharides (LPS), and 600-Da BPEI. Data shown the average of triplicate trials. Error bars denote standard deviation. (*) indicates significant difference found between that sample and the untreated control (t-test, p-value < 0.05)..... 31

Figure 13. Illustrations of cell wall peptidoglycan in MRSE. PBPs crosslink the peptidoglycan subunits finishing the last stage of cell wall synthesis unless inhibited by β-lactams. MRSE's methicillin-resistant factor is the extra PBP2a, which is not affected by β-lactams. 600-Da BPEI binds WTA and blocks PBP2a's localization, thereby disabling the resistance..... 35

Figure 14. Checkerboard assays testing the synergy of BPEI and antibiotics on MRSE 35984, MRSE 29887, and MSSE 12228. Synergy between BPEI and β-lactams was observed on MRSE 35984 (A, B) and MRSE 29887 (C, D), but not on MSSE 12228 (F). No synergy was found between BPEI and vancomycin on MRSE 29887 (E). Each heat map is the average of three trials in the change of OD_{600}..... 41

Figure 15. BPEI restores bactericidal activity of oxacillin in the combination treatment (yellow curve) against both MRSE 29887 and MRSE 35984. Each growth curve is the average of three separate trials. Error bars denote standard deviation (n=3). 44

Figure 16. Scanning electron micrographs of MRSE 35984; scale bar = 1 µm. Untreated control cells appear smooth and rounded with clear division septa (arrows) (A). BPEI (256 µg/ml) treated cells (B) and oxacillin (2 µg/ml) treated cells (C) show no significant difference. Combination of BPEI+oxacillin (256 µg/ml + 2 µg/ml) treated cells (D) show extreme distortions and thicker division septa (inset). 45

Figure 17. Scanning electron micrographs of MSSE 12228; scale bar = 1 µm. Untreated control (A), BPEI (32 µg/ml) treated (B), oxacillin (0.003 µg/ml) treated (C), and combination of BPEI+oxacillin (32 µg/ml + 0.003 µg/ml) treated cells (D) show no noticeable differences. 46

Figure 18. Cell size measurements of MSSE 12228 and MRSE 35984 from SEM images among four treated groups: untreated control, BPEI (256 µg/ml) treated, oxacillin (2 µg/ml) treated, and combination BPEI + oxacillin treated. N=100 cells/group. Mean value, X-marker; median value, center line; lower quartile and upper quartile, lower and upper ends of the box; minimum and maximum values, whiskers outside the box. No significant difference in cell size among treated groups in MSSE 12228 (ANOVA, *p-value* > 0.001) (A). Significant difference in cell size among treated groups in MRSE 35984 (ANOVA, *p-value* < 0.001) (B)..... 47

Figure 19. Transmission electron micrographs of MRSE 35984; scale bar = 200nm; arrows show division septa. Untreated control cells appear rounded with complete division septa (A). BPEI (256µg/ml) treated cells (B) and oxacillin treated (2 µg/ml)

cells (C) show incomplete division septa. Combination of BPEI + oxacillin (256 µg/ml + 2 µg/ml) treated cells (D) appear to be the largest with abnormal division septa and concave morphology. 48

Figure 20. Biofilm formation stages and biofilm-disrupting ability of BPEI. BPEI disrupts established biofilm by collapsing the structure of EPS, releasing the cells into planktonic stage so that β-lactam antibiotics can actively target and eradicate them. ... 54

Figure 21. A schematic experimental procedure of our microtiter biofilm model for synergistic effect screening against methicillin-resistant *S. epidermidis* (MRSE) biofilms. MBEC assays were carried out using MBEC inoculator, which is a microtiter plate lid with protruding prongs attached. Each prong fits into each well and allows bacterial biofilm to form and grow. Details are given in the Experimental Procedures. The method of CFU counting is detailed in Biofilm Kill Curve..... 56

Figure 22. Scanning Electron Micrographs of the tip of MBEC prongs. A control prong with no bacteria is shown (A). MRSE 35984 biofilm colonies were formed after 24 hours of inoculation (B); the arrows highlight some of the biofilm microcolonies. Scale bars = 200 µm. 63

Figure 23. Scanning electron micrographs of MRSE 35984 biofilm. The intercellular matrices of EPS are captured as they wrap around every bacterium (A). At higher magnification, the EPS matrix is clearly shown to be sheltering the whole bacterial colony in an amorphous coat (B). Scale bars = 2 µm. 64

Figure 24. Synergistic effects of BPEI and antibiotics against MRSE 35984 (A) and MRSE 29887 (B) on a 96-well checkerboard pattern. The synergy was seen both on the

planktonic challenge plates (A,a and B,a) and the biofilm MBEC assays (A,b and B,b). 66

Figure 25. Established MRSE 35984 biofilms stained with crystal violet were treated with 600-Da BPEI for 20 hours, as well as the negative and positive controls. The dissolved biofilm solutions were transferred to a new plate, and the biofilm remainders are shown as top-down view, (A). The mean OD_{550} of the dissolved biofilms was measured, (B). Error bars denote standard deviation (*n = 10*). The MRSE biofilms were significantly dissolved by 600-Da BPEI (*t-Test*, *p-value* < 0.01, significant difference between the negative control and each treatment is indicated with an asterisk). 67

Figure 26. Established MRSE 35984 biofilms stained with crystal violet were treated with 10,000-Da BPEI for 20 hours, as well as the negative and positive controls. The dissolved biofilm solutions were transferred to a new plate, and the biofilm remainders are shown as top-down view, (A). The mean OD_{550} of the dissolved biofilms was measured, (B). Error bars denote standard deviation (*n = 10*). The MRSE biofilms were significantly dissolved by 10,000-Da BPEI (*t-Test*, *p-value* < 0.01, significant difference between the negative control and each treatment is indicated with an asterisk). 69

Figure 27. Crystal violet absorbance represents MRSE 35984 biofilm biomass. Strong antibiofilm formation synergy between BPEI and piperacillin was observed, compared to individual piperacillin or BPEI treated samples. Error bars denote standard deviation (*n = 3*). PIP, piperacillin. 70

Figure 28. Biofilm kill curve of MRSE 35984. Only the combination treatment of BPEI+oxacillin (64 µg/mL + 16 µg/mL) – the diamond-curve – could eradicate MRSE

35984 biofilms. Error bars denote standard deviation (*n = 2*). CFU, colonies forming units. 72

Figure 29. Scanning electron micrographs of established MRSE 35984 biofilms (3-day old). The untreated control sample shows thick EPS enfolding every bacterial cell (A). BPEI-treated sample shows disrupted EPS and significant number of exposed cells without the EPS (B). At lower magnification, the untreated control (C) biofilms appear with full and tightly occupied biofilms, while the BPEI-treated sample (D) shows disjointed biofilms by many revealed surfaces. Scale bars (A and B) = 1 µm. Scale bars (C and D) = 100 µm. 73

Figure 30. Synergy between BPEI and ampicillin against MRSA 43300 (A), MRSA OU6 (B), and MRSA OU11 (C). Checkerboard assay data on planktonic bacteria are shown on the left (Ai, Bi, and Ci), and corresponding biofilm data are shown on the right (Aii, Bii, and Cii). 86

Figure 31. Established MRSA OU6 biofilms stained with crystal violet were treated with polymyxin B (PmB) and 600 Da BPEI for 20 hours, as well as the negative control (water only) and positive control (30% acetic acid). The dissolved biofilm solutions were transferred to a new plate, and the biofilm remainders are shown as top-down view, (A). The mean OD_{550} of the dissolved biofilm solution was measured, (B). Error bars denote standard deviation (*n = 10*). 88

Figure 32. SEM images of MRSA OU11 biofilms on glass coverslips. Untreated control biofilms are shown to be covered and wrapped around in the matrix of EPS (A and C). BPEI-treated samples have much less EPS with many cells being exposed (B and D). Scale bars in A and B = 2 µm. Scale bars in C and D = 1 µm. 89

Figure 33. SEM images of established MRSA OU6 biofilms on PC membranes. Very thick coat of the EPS matrix is present in the untreated control biofilm on the PC membrane which also blocks the bacterial cells from being captured in the microscope (A). BPEI-treated sample has a much clearer view as the EPS removed and even the membrane surface is exposed as many nano-size pores are seen at the bottom (B). Scale bars in A and B = 1 μm. 90

Figure 34. Graphical presentation of 600-Da BPEI's mechanisms of action on Gram-positive and Gram-negative cell wall and membrane. Cationic BPEI not only binds anionic wall teichoic acid (WTA) to indirectly disable penicillin binding proteins PBP2a/4 (which only function properly by localization of WTA), it also electrostatically binds the phosphate heads of the lipid membrane, causing a partial loss of the permeability barrier. Consequently, BPEI can potentiate both β-lactams and non-β-lactams (those target intracellular machinery) against MRSA (Gram-positive). In *Pseudomonas* (Gram-negative), BPEI binds anionic LPS, creating new hydrophilic conduits to enhance drug-influx 95

Figure 35. Absorbance (OD.600) of erythromycin (eryth) MIC scan on MRSA OU6 and OU11 shows that the two bacterial strains had high resistance to erythromycin (both MICs are over 2000 μg/mL since no inhibitory effect was found; n = 3)..... 101

Figure 36. Checkerboard data presentation of bacterial growth inhibition from the combination of erythromycin and 600-Da BPEI. The MICs in these checkerboard assays can be used to show synergy in the clinical isolates MRSA OU6 (A), MRSA OU11 (B), and PA OU19 (C). Each assay was performed in triplicate and the data presented above are the average of these assays. 102

Figure 37. H33342 permeation curves show the addition of BPEI (128 µg/mL) enhances the cell-membrane permeability of MRSA OU6 and OU11 as the fluorescence of H33342 increased, compared to their untreated control. Error bars denote standard deviation (n = 5). 103

Figure 38. H33342 permeation curves show the addition of of 128 µg/mL polymyxin B (PmB) drastically increases the dye uptake more than twice of that 128 µg/mL BPEI does on P. aeruginosa PA OU19. Error bars denote standard deviation (n = 6). 104

Figure 39. H33342 permeation curves show the addition of 128 µg/mL polymyxin B (PmB) drastically increases the dye uptake by MRSA OU11, more than twice of that 128 µg/mL BPEI does. Error bars denote standard deviation (n = 5). 106

Figure 40. Resazurin assay indicates cell viability of MRSA OU11 (at the cell density of ~$7*10^9$ CFU/mL) treated with either BPEI or polymyxin B (PmB). Resazurin is converted to resorufin by cellular metabolism product $NADH/H^+$ and thus provide an indication of cell viability. Error bars denote standard deviation (n=8)..... 107

Figure 41. ELISA assays show the amount of cytokine IL-8 released by human epithelial keratinocytes (HEKa cells) in responses to: peptidoglycan (PGN) and 600-Da BPEI (A); combinations of PGN and 600-Da BPEI (B). Data are shown as average of triplicate trials. Error bars denote standard deviation. Statistical analysis with the student's t-test generates p-values of < 0.05% (95% confidence, denoted by ∗) and <0.01 (99% confidence, denoted by ∗∗). nd = no statistical difference. 110

Figure 42. Checkerboard assay data demonstrating that sub-lethal amounts of 600-Da BPEI lower the piperacillin MIC against a MDR clinical isolate of *P. aeruginosa*, OU1.

The MIC of piperacillin (64 μg/mL) is resistant but 2 μg/mL of 600-Da BPEI (3.3 μM) reduces the β-lactam MIC to 4 μg/mL which is interpreted as susceptibility. 120

Figure 43. Growth curves of PA BAA-47 shows that sub-lethal amounts of 600-Da BPEI and piperacillin slow bacterial growth but do not kill the culture. However, treating the culture with a combination of 600-Da BPEI and piperacillin, each at sub-lethal concentrations, is. Error bars denote standard deviation (*n = 2*). 121

Figure 44. Effect of 600-Da BPEI on the intracellular accumulation of the DNA-binding H33342 by *P. aeruginosa* BAA-47. Real-time kinetics of H33342 uptake show that 600-Da BPEI significantly increased the H33342 accumulation (closed red circles) into the bacterial cells, compared to the untreated control (open red circles). Similar effects are seen with the efflux deficient mutant PaΔ3 (open and closed blue diamonds). The intracellular concentration of H33342 in the treated cells is higher than the wild-type cells indicating that 600-Da BPEI does not hinder efflux processes. Error bars denote standard deviation (*n = 5*). 124

Figure 45. Incubation of PA BAA-47 cells at high cell density (~$6x10^9$ CFU/mL) with resazurin produces the fluorescence molecule resorufin via cellular metabolism. Treating these cells with 600-Da BPEI prior to resazurin addition results in lower emission that indicates (a) the cells are alive, (b) BPEI has affected the growth rate in a concentration-dependent manner, and (c) the cells are not depolarized. This contrasts with cells treated with polymyxin-B, which kills the cell culture at all concentrations tested. Error bar denotes standard deviation (n = 8)..... 126

Figure 46. The dye 1-*N*-phenylnaphthylamine (NPN) accumulates in hydrophobic regions and fluoresces when bound to phosphate groups. Polymyxin-B (PmB) allows greater uptake of NPN than 600-Da BPEI. Error bars denote standard deviation. 127

Figure 47. Scanning electron micrograph images of PA BAA-47. Untreated control cells appear with regular rod-shape of about 2-3 µm long (A). 600-Da BPEI treated cells (B) and piperacillin treated cells (C) show inconsistency in their size with longer lengths but the rod-shape remains. Combination of 600-Da BPEI + piperacillin treated cells (D) show extreme distortions both in size and shape with insets (E) and (F) for higher magnifications. Scale bars = 2µm. 130

Figure 48. Biofilm eradication assay data using collected with the Calgary biofilm device. EPS creates additional barriers to piperacillin efficacy and thus 256 µg/mL are required to kill the bacteria. However, 600-Da BPEI disrupts the biofilm EPS and increases β-lactam access to the cells, reducing the MBEC to 8 µg/mL..... 132

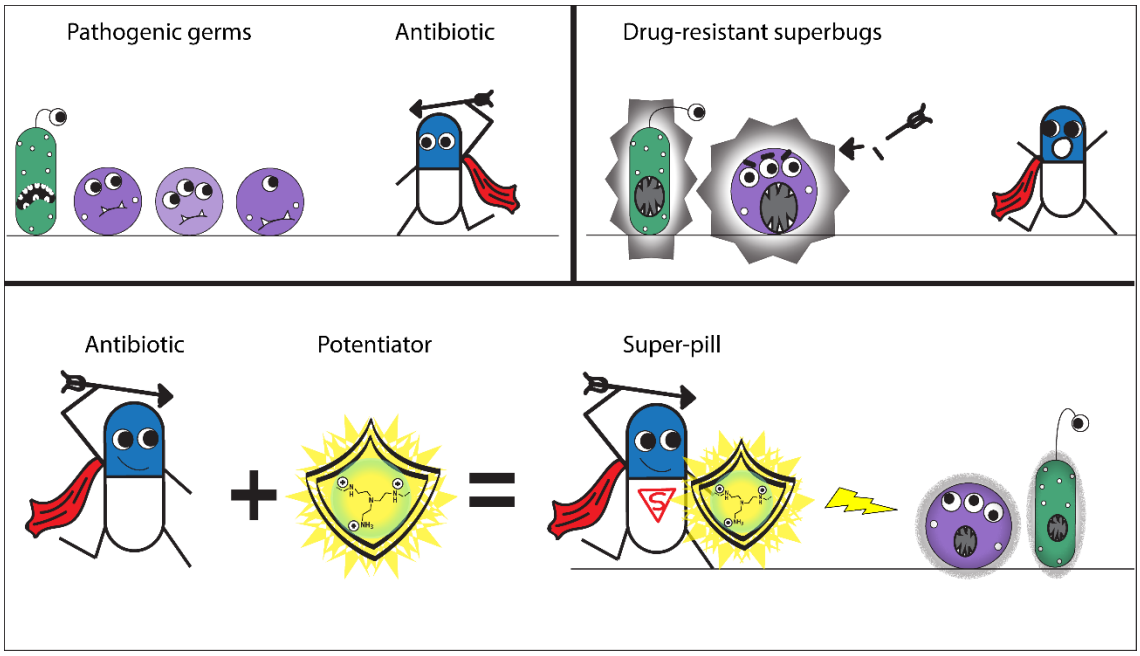
Abstract

Antibiotic resistance (AR) is a serious growing threat around the globe. There has been no new antibiotic class developed in the past 30 years, while antibiotic-resistant superbugs are emerging everywhere and becoming more and more life-threatening. In 2019, AR pathogens took away about 35,000 lives and infected over 2.8 million people a year in the United States alone. Experts predict that, by 2050, AR will be the top leading cause of death, claiming 10 million lives a year.

Motivated and dedicated to thousands of families who lose their loved ones each year to antibiotic-resistant infections, our research lab studies the defense mechanisms of superbugs. Instead of finding a new antibiotic, we study how to remove their resistance using a potentiator called BPEI (**b**ranched **p**oly**e**thylen**i**mine). BPEI is a chemical compound that can disable the resistance factors of superbugs while traditional antibiotics (i.e. amoxicillin) can now actively target the vulnerable pathogens. It is called “combination therapy”. My initial specific contribution is study to fight one of the most commonly clinical isolates of Staph infections—multidrug-resistant *Staphylococcus epidermidis*. Previously known as a harmless commensal species on human skin, *Staphylococcus epidermidis* is now the first-ranking causative agent of hospital-related infections, with 24% mortality. It has become resistant to many antibiotics and thus acquired the name MRSE (Methicillin- Resistant *Staphylococcus epidermidis*). Additionally, MRSE bacteria can form dangerous biofilms – extra layers of self-made material – that protects them from antibiotics and helps them live on inanimate surfaces like medical devices for weeks to months. Persistent biofilms are also a leading cause of chronic wound infections. In the United States, a cost of $2

billion/year is estimated for *S. epidermidis* vascular-catheter-related bloodstream infections. This resistance is mainly governed by a protein called PBP2a, which the susceptible Staph bacteria do not have. The protein PBP2a has a very low affinity for traditional β-lactam antibiotics, thereby making first-choice antibiotics ineffective. Here, the use of BPEI becomes effective because exposure to BPEI molecules inhibits the function of PBP2a of MRSE, and therefore making them susceptible to existing antibiotics.

Many experiments and analyses were conducted by using multiple biochemical techniques including microtiter plate assays, growth and time-killing curves, bacterial colony forming units, visible and fluorescence spectroscopies, electron microscopies, Fourier-transform infrared spectroscopy, and mass spectrometry. Not only being effective against MRSE, BPEI can also broaden antibiotic spectrum against other bacterial species like MRSA, *Pseudomonas aeruginosa*, *E. coli* and their biofilms. Exact concentrations of each combination treatment were found for each bacterial strain. New mechanisms of action of BPEI against different bacteria and its effects on human inflammatory responses were also elucidated and reported in this dissertation. Better understanding of how superbugs react to each treatment helps us to design more and more powerful potentiators. The efficacy of BPEI in combination therapy has shown to be effective against more than 20 clinical isolates (patients' swab from OUHSC) of drug-resistant pathogens. This enables BPEI to function as a broad-spectrum antibiotic potentiator which expands the opportunities to improve drug design (synthesis of BPEI analogs), antibiotic development, and therapeutic approaches (i.e. anti-inflammatory) against pathogenic germs.



-Abstract art of the research-

Chapter 1: *Staphylococcus epidermidis,* an opportunistic pathogen

Staphylococcus epidermidis is one of the most prevalent prokaryotic species on human skin and mucosal membranes that constitute the commensal flora. *S. epidermidis* has become one of the most common causes of primary bacteremia and healthcare-related biofilm infections. Infections are difficult to diagnose because the pathogen has natural niches on human skin and the ability to adhere to inanimate surfaces via biofilms. No antibiotic currently on the market can eradicate pathogenic biofilms, which contain complex defense mechanisms composed of slime-like extracellular polymeric substances (EPS). Alarmingly, *S. epidermidis* has acquired resistance to many antibiotics, which presents a danger to human health. Known as methicillin-resistant *S. epidermidis* (MRSE), most clinical isolates of MRSE in North America exhibit β-lactam resistance primarily due to the presence of *mecA*, a gene that bestows β-lactam antibiotic resistance in a manner similar to methicillin-resistant *Staphylococcus aureus* (MRSA). *MecA* encodes for expression of penicillin-binding protein 2a (PBP2a), which is absent in β-lactam susceptible strains of *S. epidermidis*. Our research objective is to disable this resistance factor in MRSE with 600-Da branched polyethylenimine (BPEI). Cationic BPEI not only targets anionic wall teichoic acid (WTA), an essential cofactor for proper functioning of PBP2a, BPEI also reduces the EPS formation of MRSE biofilms rendering the bacteria vulnerable. We found that BPEI disables resistance in MRSE and potentiates β-lactam antibiotics against both planktonic and biofilm MRSE. Therefore, first line clinical treatments can be effective against MRSE infections when used in combination with 600-Da BPEI. This study also provides a better understanding to further extend the technology against other superbugs, which has been documented and published in the

Journal of *ChemMedChem*, *ACS Biomacromolecules*, *ACS MedChem Letters*, and *ACS Infectious Diseases*.[1-5]

Antibiotic Resistance

Antibiotic resistance (AR) is the ability of germs that overpowers the drugs intended to kill them. In 2013, the Centers of Disease Control (CDC) estimated around 2 million people in the United States were infected with antibiotic-resistant germs and at least 23,000 Americans died each year. In a current update from the CDC's Antibiotic Resistance Threats Report in 2019, that number has increased to almost 3 million cases infected with AR and 35,000 of them died.[6] These numbers are only estimation in the US, a country with one of the best medicine and research technologies. Experts in the U.K predict that antibiotic resistance will be the top leading cause of deaths by 2050, which will kill 10 million lives a year, exceeding the number caused by cancer today. This alarming estimation would likely to come true unless a global response to the AR problem is initiated in time.[7] Clearly, AR is already here. The challenges to antimicrobial discovery and optimization of novel drugs have lead AR become one of the greatest threats to global public health. Over the past three decades, there has been no successful discoveries of novel antibiotic classes naming the time as "the discovery void." After the first antibiotic discovery of penicillin in 1928,[8] a "golden age" of many new antimicrobial discoveries unexpectedly arose. Until 1960s, this process slowed down due to limited screening methods. The latest registered antibacterial class was the lipopeptides (i.e.

daptomycin) which was patented in 1987.[9] A timeline of distinct antibiotic discoveries is adapted from Silver[10] and shown in Figure 1 with their modes of action[11-12] in Table 1.

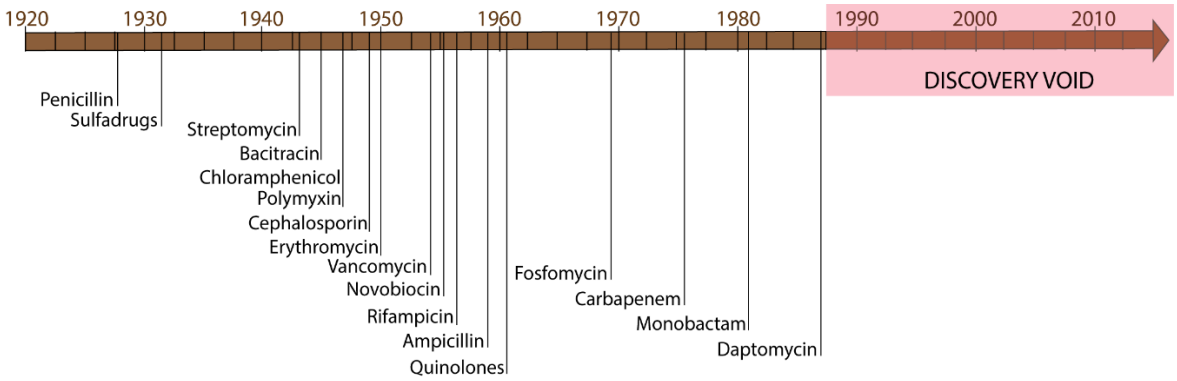


Figure 1. Antibiotic discovery timeline and the "discovery void." Years shown are first reported patented antibiotics.

Table 1. Distinct antibacterial drugs and their targets

Antibiotic	Class	Mechanism	Target	Notes
Penicillin	β-Lactam	Inhibit cell wall synthesis	PBPs	Penams, narrow spectrum
Oxacillin				Penams, β-lactamase resistant
Ampicillin				Penams, broad spectrum
Amoxicillin				Penams, broad spectrum
Piperacillin				Penams, against Gram-negatives
Imipenem				Carbapenems, very broad spectrum
Cephalothin				Cephalosporins, injection
Cefixime				Cephalosporins, oral use
Vancomycin	Glycopeptide		D-Ala-D-Ala (lipid II)	Reserved drug, against MRSA/MRSE, intravenous application
Erythromycin	Macrolide	Inhibit protein synthesis	rRNA of 50S	Alternative to penicillin
Azithromycin				Broader spectrum, better tissue penetration

Chloramphenicol	Chloramphenicol			Broad spectrum, considered toxic
Linezolid	Oxazolidinone			Reserved drug, against MRSA/MRSE
Neomycin **Gentamycin**	Aminoglycoside		rRNA of 30S	Broad spectrum, topical use Broad spectrum, against *Pseudomonas*
Tetracycline	Tetracycline			Broad spectrum, animal feed additives
Rifampicin	Rifamycin	Inhibit nucleic acid synthesis	RNA polymerase	Treatment of tuberculosis
Norfloxacin **Ciprofloxacin**	Fluoroquinolone		DNA gyrase	Broad spectrum, treatment of urinary tract infections, and also in animal husbandry
Polymyxin B **Colistin (**or Polymyxin E**)**	Polymyxin	Injure plasma membrane	LPS and cytoplasmic membrane	Topical use, against *Pseudomonas*. Reserved drug, against multidrug-resistant Gram-negatives
Daptomycin	Lipopeptide		Cytoplasmic membrane	Against multidrug-resistant Gram-positives

Since then, experimentation, innovation, and efforts for new antibacterial drugs have implemented, but little has reached clinical trials. The biggest reason for the discovery void is the withdrawal of pharmaceutical companies due to regulatory and scientific obstacles. Besides financial cost, a massive number of required standards and criteria that pharmaceutical companies must meet to develop an antimicrobial agent has shifted the investment equation towards other therapies. In many developing countries,

antibiotics are sold over the counter, and their use in livestock is poorly regulated. Lack of regulation can lead to overexposure, thereby encouraging acquired antimicrobial resistance. As the most common agricultural pathogens in developing countries, antibiotic resistance has another convenient means of spreading to humans.[13]

On top of these challenges, the fitness of resistant mutants is yet another reason. Bacteria always find ways (fitness and mutations) to survive and defeat the drugs designed to kill them. Most of the life-threatening infamous superbugs belong to the ESKAPE pathogens: *Enterococcus*, *Staphylococcus*, *Klebsiella*, *Acinetobacter*, *Pseudomonas*, and *Enterobacter* species. These pathogens are commonly drug-resistant isolates which often lead to amputation or death once complications arise and no effective drugs are available.[14] Not stopping at resisting conventional β-lactam antibiotics (i.e. ampicillin), they have made their way to resist all available classes of antibiotics including the drugs of last-resort (vancomycin and linezolid).[15] Evidently, antibiotic resistance has been found in every country and every US state.[6] The need for antibiotic resistance solutions is urgent. Each person, each organization, and each country can affect antibiotic resistance development. Even though there is no safe place from antibiotic resistance, actions can be taken to mitigate, slow down, and prevent it from disarming us especially with research and science.

The Emergence of MRSE

Staphylococcus epidermidis belongs to the Gram-positive *Staphylococcus* genus, which has a thick peptidoglycan cell wall. *S. epidermidis* is the most abundant microorganism among the human commensal microflora of the skin and mucosal membranes. Typically, around 10-24 different strains of *S. epidermidis* are carried by a

normal average person. Previously known as a harmless species, *Staphylococcus epidermidis* is now a frequent causative agent of nosocomial infections, along with *Staphylococcus aureus*.[16] Because human skin characteristics (pH range, temperature, water/moisture, and nutrient contents) are widely different from person to person, their ability to adapt to a large range of environmental conditions make *S. epidermidis* an intrinsic opportunistic pathogen. With the widespread use of indwelling medical devices and implanted foreign bodies, as well as the rising number of immunocompromised patients,[17] *S. epidermidis* has become a significant threat to the public health. In the U.S., *S. epidermidis* vascular catheter-related bloodstream infections create an economic burden of approximately $2 billion/year.[18] Unlike the more aggressively virulent and coagulase-positive *Staphylococcus aureus*, *S. epidermidis* belongs to the coagulase-negative staphylococci and is rarely a life-threatening infection outside of hospital settings. However, its prevalence in hospitals and the commensal lifestyle on human skin have granted *S. epidermidis* resilience against treatments.

Complications in treatment are often due to the presence of specific antibiotic resistance genes and the production of biofilms (biofilms are agglomerations of bacteria enclosed in a protective matrix of extra-polymeric substances). *S. epidermidis* has been reported to colonize fabrics and abiotic surfaces, such as medical devices, for weeks to months.[19] Polysaccharide intercellular adhesin, also known as poly-N-acetyl glucosamine (PIA/PNAG), was found to have a major function in *S. epidermidis* biofilm formation. PIA/PNAG is governed by the *ica*ADBC operon, which appears more frequently in isolates of *S. epidermidis* from hospital-related infections than isolates from healthy individuals. As a permanent skin-colonizer, *S. epidermidis* may also have elaborate

mechanisms that allow it to attach to cardiac devices, surgical sites, central nervous system shunts, prosthetic joints, and vascular grafts.[18-20] Resistance to certain antibiotics and disinfectants in many clinical isolates is due to the presence of selective-pressure-exerted efflux *quaternary ammonium compound (qac)* genes found both in *S. aureus* and *S. epidermidis*.[21-22] Encoding for efflux (or export) proteins, *qac* genes are responsible for antiseptic-resistance and are more prevalent in hospital/nursing environment due to the pressure of regular disinfectant/antiseptic usage. Additionally, *mecA* gene is found in all *S. epidermidis* isolates that are resistant to β-lactam antibiotics (methicillin resistance), therefore the name MRSE (methicillin-resistant *Staphylococcus epidermidis*) has emerged.[23]

As the top leading cause, coagulase-negative staphylococci are responsible for a third of hospital-related bacteremia infections. *S. epidermidis* is the second most common cause of prosthetic valve endocarditis with 24% mortality, surpassed in frequency only by *S. aureus*.[20] In orthopedic prosthetic device infections, *S. epidermidis* accounts for 30-43% of cases. Inoculation of infections occurs at the time of surgery, and their infections usually stay indolent (symptoms of pain at the surgical site) without fever. Hospital isolates of *S. epidermidis* are methicillin resistant at significantly higher rates (75–90%) than *S. aureus* (40–60%).[18] The emergence of MRSE infections emphasizes the need for antimicrobial drug design to yield new treatments before the pathogens become resistant to the last-resort antibiotics.

The Cell Wall and The Gram Stain Characteristics

Bacteria are single-cell prokaryotes which are chemically similar to eukaryotes with the compositions of carbohydrates, lipids, proteins, and nucleic acids. Mainly their

complicated cell walls and membranes structure and the absence of organelles make them distinct from eukaryotic cells. The bacterial cell wall is a complex structure that shapes the morphology of the cell. All prokaryotes have cell walls, except the *Mycoplasma* genus. The semirigid cell wall surrounds and protects the fragile cytoplasmic membrane and the interior of the cell from cytoplasmic osmosis and physical changes from their environment. The composition of the bacterial cell wall primarily has a macromolecular network of peptidoglycan, which consists of a repeating disaccharide of N-acetylglucosamine (NAG) and N-acetylmuramic acid (NAM). Rows of 10-65 linked NAG and NAM sugars form the "glycan" backbone. Polypeptides link adjacent glycan rows together and make up the "peptide" portion of peptidoglycan. The differences in the cell wall classify bacteria into two large groups: Gram-positive and Gram-negative (Figure 2), which was originally based on the technique of Gram-staining. The Gram stain procedure was invented by Han Christian Gram in 1884, and it is now one of the most useful techniques in microbiology to differentiate bacteria. Basically, Gram-positive bacteria have a thick multilayer of peptidoglycan and therefore will retain the purple color of a primary stain (crystal violet). On the other hand, Gram-negative bacteria can't retain crystal violet after alcohol washing due to their thin monolayer peptidoglycan, and therefore they will have a contrast pink color of a counter stain (safranin).[11, 24-25]

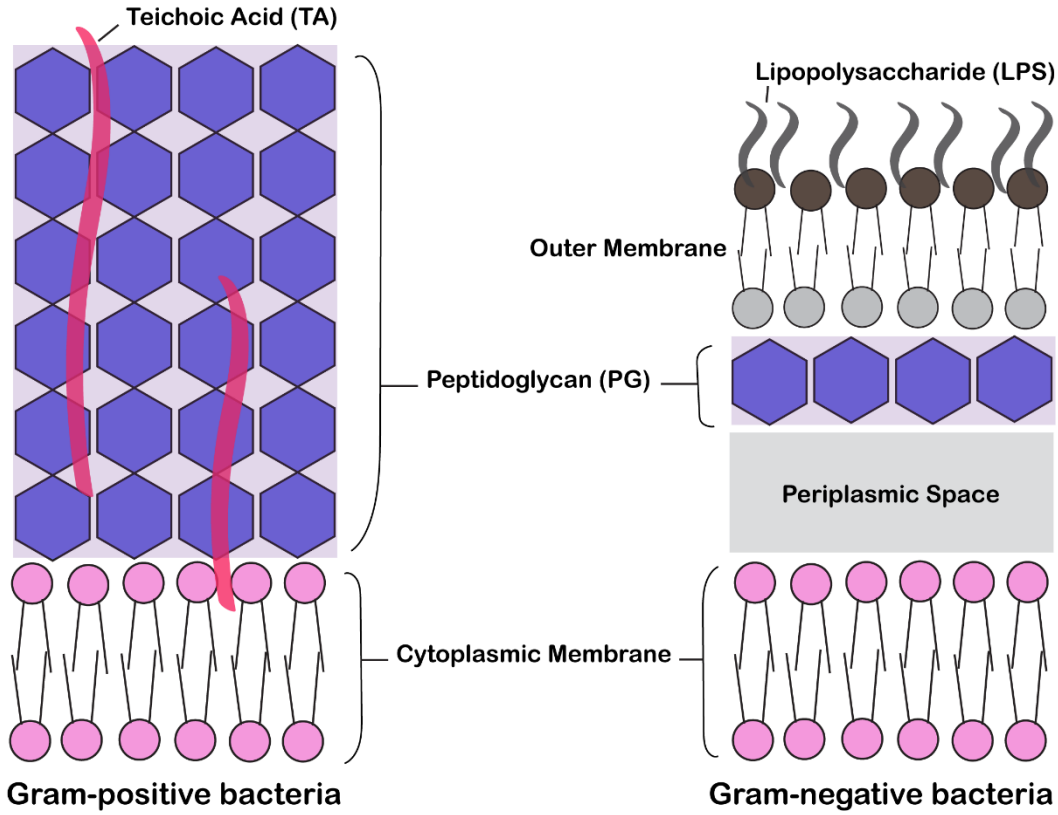


Figure 2. Cell wall structure of Gram-positive and Gram-negative bacteria.

Unique characteristics of the Gram-positive and Gram-negative bacteria are summarized in Table 2.[11] In Gram-positive strains, the thick peptidoglycan layers compose the entire cell wall. Embedded within the peptidoglycan are the negatively charged teichoic acids (wall teichoic acids and lipoteichoic acids) which regulate the essential cations in and out of the cell. In Gram-negative bacteria, an additional outer membrane is present on top of their thin peptidoglycan monolayer. They do not have teichoic acids in the cell wall. The outer membrane consists of phospholipids, lipoproteins, and lipopolysaccharides (LPS), and it also provides an extra barrier to antibiotics, lysozyme enzymes (in tear, mucus, and saliva), and certain detergents. Between the peptidoglycan and the cytoplasmic membrane, periplasmic space (or periplasm) is a gel-like liquid containing many enzymes and transport proteins. Because

of their uniqueness, many antibiotics (β-lactams) target the bacterial cell walls by interfering with the peptide cross-linking of peptidoglycan. Consequently, the weaken cell wall would lyse due to rupture of fragile cell membrane, resulting in cell death.

Table 2: Characteristics of Gram-positive and Gram-negative bacteria

Characteristics	**Gam-positive**	**Gram-negative**
Gram stain reaction	(+) retain the purple color of crystal violet dye	(-) does not retain crystal violet dye after a counterstain, safranin, decolorizes into pink
Peptidoglycan layer	Multilayer, thick	Monolayer, thin
Teichoic acid	Present in most	Absent
Outer membrane	Absent	Present
Lipopolysaccharide	Absent	Present
Toxins	Exotoxins	Endotoxins
Cell wall disruption by lysozyme	Easy	Hard (due to outer membrane)

Most Gram-positive bacteria produce exotoxins—proteins that are metabolic products of cell growth. Exotoxins are highly toxic to hosts but usually heat-unstable and can be easily neutralized by antitoxins. Typical diseases caused by exotoxins are gas gangrene, scarlet fever, and tetanus. In contrast, endotoxins are primarily produced by Gram-negative bacteria.[26] Endotoxins are the lipid A portions of the LPS of outer membrane. They are released when cells divide or lyse. Endotoxins have low toxicity compared to exotoxins, but they can withstand extreme heat (121°C) for an hour. They

are hard to be neutralized by antitoxins. Representative diseases by endotoxins are urinary tract infections and typhoid fever.

β-Lactam Antibiotic Resistance

In 1928, Alexander Fleming noticed a large fungal contamination on a petri dish of *Staphylococcus aureus*. The mold inhibited *S. aureus* colonies from growing. The incident led Fleming to the discovery of the first antiseptic drug, penicillin, which is named after the isolated fungus *Penicillium notatum (*later renamed as *P. chrysogenum)*.[27] In March 1942, a near-death patient—Anne Miller—had blood poisoning (bacteria reach the bloodstream) and was administered experimental penicillin. She recovered in hours and became the first American saved by an antibiotic.[6] Until the end of World War II in 1945, penicillin finally made its way through commercialization, reached the general public, and saved millions of lives. Since then, a great number of penicillin-derivative antibiotics were developed: the β-lactams. All β-lactams have a core β-lactam ring in its chemical structure (Figure 3).

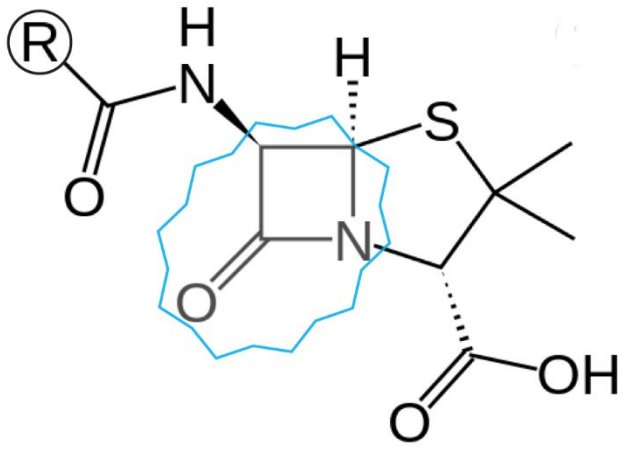


Figure 3. A core chemical structure of penicillin with the β-lactam ring (square-shape ring in blue frame). The ring is a four-membered cyclic amide. It holds each bond at 90°

angle and is reactive to binding covalently to bacterial penicillin binding proteins (PBPs).

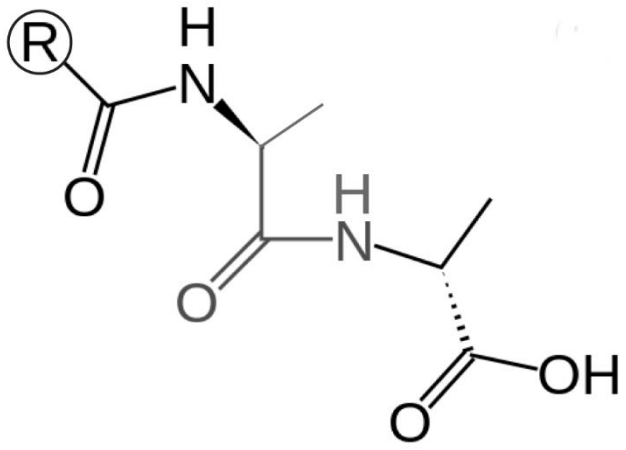


Figure 4. Chemical structure of D-ala-D-ala peptidoglycan terminus, which has structural similarity to β-lactam ring.

The β-lactam ring is a four-membered cyclic amide that is able to covalently bind to penicillin binding proteins (PBPs) within bacteria because the ring has a very similar structure to D-ala-D-ala terminus of the peptidoglycan (Figure 4). PBPs misrecognize β-lactams for the serine transpeptidase catalytic site, and so their chemical interaction prevents transpeptidase enzymes (PBPs) from finishing the last stage of bacterial cell wall synthesis: crosslinking the peptidoglycan layers (Figure 5 and 6). The peptidoglycan plays a vital role for cell wall integrity, especially in Gram-positive bacteria. Without a strong cell wall, bacteria lyse and die from excessive cytoplasmic pressure. Antibiotics have saved a countless number of lives and are an important factor in raising the lifespan of humans over the past 80 years. However, evolution has its rules. Bacterial reproduction rate is extremely faster than human's, and so is their mutation rate. In a given environment of antibiotic presence, bacterial fitness by natural and mutational selections favor the ones

survive and resist injurious drugs, leading to the emergence of more and more drug-resistant pathogens. MRSE is one of them.

In 2015, the US had 269.3 million antibiotic prescriptions given by healthcare providers, which is equivalent to 838 prescriptions per 1000 people. Among them, β-lactams were the most popular prescribed antibiotics with amoxicillin top the chart at 171 prescriptions per 1000 people.[28] This rate isn't going to change soon because today we depend heavily on antibiotics. From treatments of common illnesses (sinus/throat infections) to many medical advances (organ transplants, surgeries, and cancer therapies), we are dependent on antibiotics every day to fight bacterial infections before bacteria reach our blood and kill us. Despite how quick a new antibiotic drug was discovered; resistant germs were always identified after several years or even before the drug released to the market.[29] Penicillin was first introduced to the public in 1943, but penicillin-resistant *Staphylococcus* was found in 1940. Methicillin was discovered in 1960, and shorty after in 1962 methicillin-resistant *Staphylococcus* was identified. Today, almost 90% of all hospital isolates of *Staphylococcus epidermidis* are methicillin-resistant (MRSE). The staphylococcal cassette chromosome *mec* (SCC*mec*) is the root of methicillin resistance. SCC*mec* contains *mecA* gene which is eventually translated into PBP2a proteins that are resistant to β-lactams. In *S. epidermidis*, ten different structures of SCC*mec* were found, in which SCC*mec* type IV element was the most common and the most problematic. SCC*mec* type IV can be acquired and spread without the presence of antibiotic pressure.[18] This SCC*mec* is also found to be a one-way horizontal gene transfer from *S. epidermidis* to MRSA.[30]

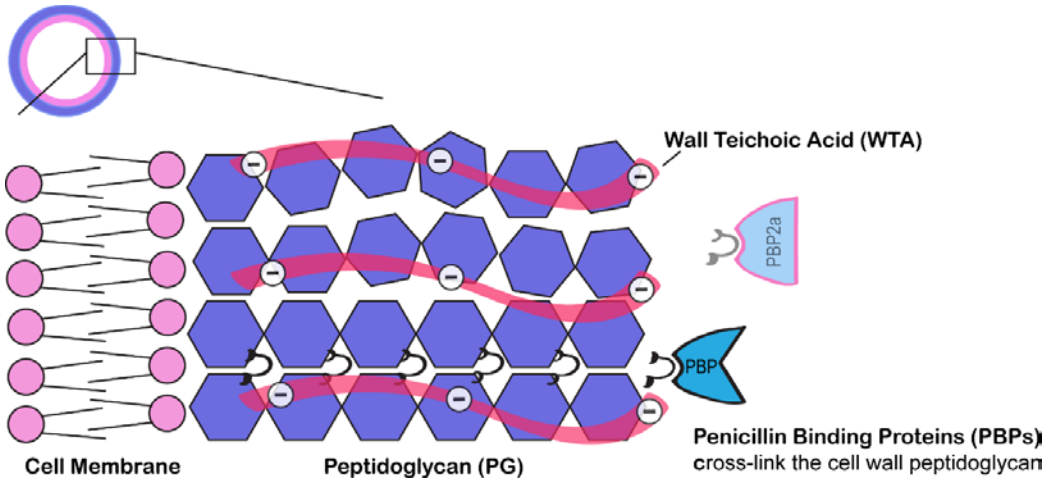


Figure 5. Illustration of the cell wall peptidoglycan crosslinking in MRSE. Penicillin binding proteins (PBPs and PBP2a) crosslink the subunits of the peptidoglycan, completing the last stage of cell wall synthesis.

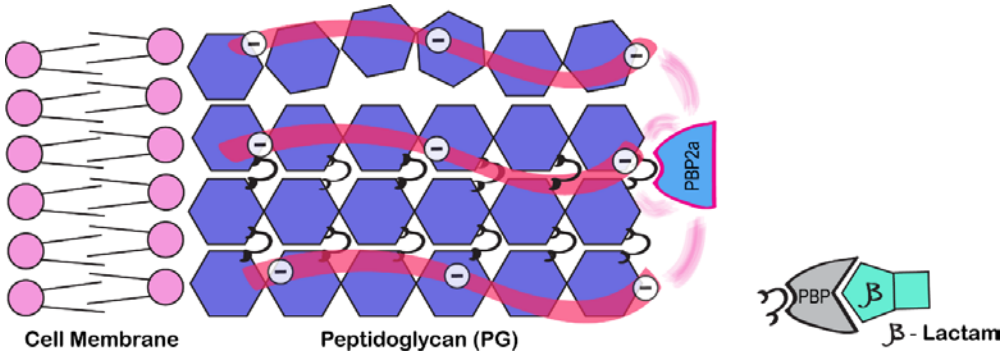


Figure 6. Illustration of β-lactam resistance factor, PBP2a, in MRSE. Regular PBPs are inhibited by β-lactam antibiotics, except PBP2a. PBP2a has low affinity to β-lactams and thereby can still crosslink the cell wall without being affected. A cofactor of PBP2a is the wall teichoic acid (WTA) which localizes PBP2a.

In addition to the SCC*mec*, the second most important determinant for MRSE's invasiveness is the intercellular adhesion *ica* genes that regulate poly-*N*-acetylglucosamine (PNAG) production.[31-32] As the main component of the protective biofilm's exopolymer substances (EPS), PNAG has a pivotal role in *S. epidermidis* biofilm formation and immune evasion *in vitro* and *in vivo*. The regulation of PNAG production is less well understood, and some reports on the necessity of PNAG in biofilm-

forming bacteria are contradictory.[18, 33] However, the biofilm EPS has been found to protect *S. epidermidis* from host immune defense molecules, antimicrobial peptides (AMP), and antibiotic attack.[34-35]

The Need for New Strategies

Drug development takes at least a decade to get FDA approval and reach the market. The process first starts in the laboratory where new discovery occurs, and if the discovery is promising then many following steps will proceed: preclinical research (efficacy and safety on animal models), then clinical phase 1, phase 2, and phase 3 (on human volunteers). Each step can take from 1 to 4 years and can cost millions of dollars. With this costly and time-consuming process, there are clearly too few antibiotics to meet patient demands. Besides that, natural and acquired drug-resistance via horizontal gene transfer in bacteria indeed add up to the urgent need for new strategies. Alternative treatments that combine existing drugs with potentiators have become a topic of interest. Potentiators remove the resistance or restore the susceptibility of pathogens, while antibiotics attack the vulnerable germs. These strategies can potentially be as effective as new antibiotics because they have lower risk and quicker development process.

As a ubiquitous commensal species of the human microflora, opportunistic *S. epidermidis* carry an optimum reservoir pool of genetic information (including the methicillin resistant gene SCC*mec*) that is ready to express and spread to other bacteria at any time. Hundreds of thousands of Americans are infected with MRSE each year, especially patients with prosthetic devices or intravenous catheters. With a dwindling arsenal of new antibiotics, we are motivated to combine existing antibiotics with potentiators (low-molecular weight branched polyethylenimine, Chapter 2.) and re-

evaluated as combination treatments against multidrug-resistant superbugs: MRSE, MRSA, and *Pseudomonas aeruginosa*.

Chapter 2: 600-Da Branched Polyethylenimine (BPEI) and Its Effect on Human Inflammatory Responses

Background

Polyethylenimine (PEI) or also known as polyaziridine is a polymer of repeating units of an amine group and an ethyl spacer. PEI was first commercially produced in 1938 by a chemical company Badische Anilin und Soda Fabrik in Germany and by Chemirad Corporation in the US.[36] Its linear form contains only secondary amines with a chemical formula of $(C_2H_5N)_n$ and is solid at room temperature. Branched PEIs, on the other hand, can contain primary, secondary, and tertiary amine groups and are viscous liquids at room temperature. PEIs are mainly obtained by homopolymerization of aziridine (saturated three-membered cyclic compound including one nitrogen and two carbons) and are available in different molecular masses. PEIs are useful in many applications including the manufacturing of paper, textile, adhesives, detergents, and cosmetics. In biochemical research, scientists have found valuable roles of PEIs for tissue culture and gene delivery.[37-39] Almost all documented reports focused on large-molecular PEIs (> 10000 Da), while the lower molecular weight PEIs (< 2000 Da) are less cytotoxic and less well understood. Our lab started studying PEIs as metal-interfering agents in bacteria and accidentally discovered their abilities to restore susceptibility to antibiotic-resistant bacteria, especially the branched polyethylenimines (BPEI).[40-41] This finding laid the foundation and shifted our research into combinational treatments against multidrug-resistant pathogens (*Staphylococcus aureus*, *Staphylococcus epidermidis*, and *Pseudomonas aeruginosa*) using low-molecular weight BPEI (the 600-Da or unless otherwise noted). This chapter summarizes BPEI's

chemical characteristics, cytotoxicity, and its effects on inflammatory responses of human epithelial keratinocytes.

Chemistry and Applications of BPEI

Polyethylenimine (PEI) can be synthesized from 300 to 10^6 Da using different alkylating agents during ring opening of polymerization of aziridine. The amine distribution (primary/secondary/tertiary) or the branching of BPEI can also be obtained by special techniques (addition of acids and reactants).[37, 42] 600-Da BPEI used in our research was purchased from Polysciences[Inc] which has a ratio of primary/secondary/tertiary amines of 1/2/1 (Figure 7). It's highly branched polymer with roughly spherical shape. BPEI is miscible in water. In aqueous solution, primary amines of BPEI are protonated at neutral pH, making the solution cationic.

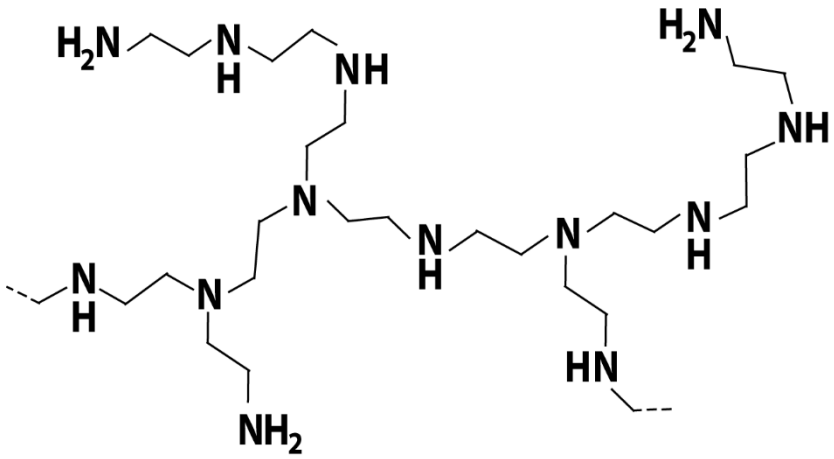


Figure 7. Chemical structure of 600-Da BPEI. The repeating unit of an amine group and an ethyl 2-carbon spacer continues on for larger molecular-weight BPEIs.

PEIs are used primarily in manufacturing a variety of products.[37] PEIs have been used in the paper industry for decades as retention and drainage agents. Today, the rising of paper recycling industry makes PEIs more important fixing agents for

flocculating contaminants. In the coating industry, PEIs are used in a variety of coating purposes: tie-coat adhesives, laminated films, primers, pigment dispersants, and amine components of epoxy resins. PEIs are also used as chelating agents of heavy metals like zinc and copper, and as metal surface brighteners for galvanic baths. In water treatment applications, PEIs are used as clarifying aids. PEIs are also used in air purification as absorbents of ozone and acidic gas molecules. In textile industry, PEIs are used as dye-fixation agents and to reduce static properties of fabric. In biological research, cationic PEIs have attracted great attentions in gene therapy and hence opened up a myriad of therapeutic opportunities. Extensive studies have investigated and concluded that the 5-25 kDa BPEI as the most suitable candidates for gene delivery due to high cellular uptake, great solubility in water, good transfection, and inexpensive synthesis. Less effectively, low-molecular-weight BPEI (<2000 Da) loses their charge density to compact and protect the genetic material.[39]

600-Da BPEI's Cytotoxicity and Biocompatibility

In a biological system, low toxicity is required for any applications, especially on the human body. Despite their high transfection efficiency, *in vitro* cytotoxicity of PEIs appears to increase with increasing polymer size, remaining a challenging issue clinically.[38-39, 43-44] However, documented studies only tested relatively large PEIs (10-25 kDa) because they are the most effective in gene therapy. Deviated from the large interest, we focus on using the smallest commercially available BPEIs in *combination antibiotic therapy* against difficult-to-treat bacterial infections where the high charge density of large-sized BPEI is not needed. Therefore, our lab examined the cytotoxicity of 600, 1200, 1800, and 10000-Da BPEIs on human cell lines.[45] The results suggested

that the smallest (600-Da) BPEI could be the lead potentiator for combination antibiotic treatments. 600-Da BPEI had the lowest *in vitro* cytotoxicity with the IC_{50} of 1090 and 690 µg/mL on human HeLa cells and HEK293, respectively. The IC_{50} of 10000-Da BPEI was much smaller: 6.6 and 1.9 µg/mL on HeLa cells and HEK293 cells, indicating a more cytotoxicity than 600-Da BPEI. Additionally, lactate dehydrogenase (LDH) assays showed that 600-Da BPEI gave the lowest nephrotoxicity of 3.5% at 63 µg/mL (even lower than Polymyxin E/Colistin which was >20% nephrotoxicity at the same concentration tested).[45] These data highlight the safety of 600-Da BPEI on human cell lines as it is the lowest cytotoxic BPEI that's commercially available. Low-molecular-weight BPEI's biocompatibility has been reported with the highest tolerance on dermal applications.[46] Thus, 600-Da BPEI is chosen to be the lead potentiator in our studies for coupling with existing antibiotics against antibiotic-resistant pathogens as a promising therapeutic agent.

Purpose of Experiment

The purpose of this experiment is *to characterize* 600-Da BPEI using instrumental analyses—high performance liquid chromatography (HPLC), mass spectrometry (MS), and Fourier-transform infrared spectroscopy (FTIR)—and *to examine* the inflammatory responses of human epithelial keratinocytes exposed to 600-Da BPEI.

Experimental Procedures

High Performance Liquid Chromatography (HPLC)

Mobile phase: A ratio of acetyl nitrile (ACN): water: phosphoric acid = 10:90:0.1 was used to make the mobile phase by mixing them with their respective volumes of 100mL of ACN, 900 mL of water, and 1mL of H_3PO_4. The pH was 3.5.

Chromatographic conditions: Flow rate: 1.0 mL/min; Wavelength: 260nm; Injection Volume: 15 µL; Column: ODS-AQ C18, S-5 micron, 120 Angstrom, (4.6 x 250mm)

The purity of 600-Da BPEI stock solution (2.56 mg/mL) was measured using a DIONEX HPLC with UVD340U, ASI 100, and P680 Pump.

Mass Spectrometry (MS)

600-Da BPEI sample (1mg/mL) was made using HPLC-graded water as solvent. The sample (2µL) was injected using Waters Acquity M-Class refrigerated (4°C) autosampler and UPLC with methanol as the isocratic mobile phase at 20.0 µL/min. The sample was introduced into a Waters SYNAPT G2-Si Q-TOF Mass Spectrometer equipped with an electrospray ionization (ESI) source in positive mode. Nitrogen was used as a nebulizing and a drying gas with a capillary voltage of 3.20 kV. Data were collected and analyzed with MassLynx (V4) software.

Fourier-transform infrared spectroscopy (FTIR)

600-Da was deposited on a KBr salt plate using CCl_4 solvent. BPEI's spectra were collected using a Bruker Tensor II FTIR spectrometer equipped with attenuated total reflectance (ATR) and liquid nitrogen cooled mercury cadmium telluride (MCT) detector.

Effects of BPEI on human epithelia's inflammatory cytokines

Materials: HEKa cells (primary human epithelial keratinocytes; Invitrogen), Epilife Medium and growth supplement (Invitrogen), lipopolysaccharides from *Escherichia coli* O111:B4 (Sigma), peptidoglycan from *Staphylococcus aureus* (Sigma), and Human (IL-8/CXCL8, IL-6, TNF-alpha, IL-1 beta/IL-1F2) Quantikine ELISA Kits (R&D).

Methods: HEKa cells were seeded in T-75 tissue culture flasks with Epilife media supplemented with human keratinocyte growth supplement 100ug/mL and 100 U/mL of pen/strep and incubated at 37°C in a CO_2 incubator. Fresh media was replaced every 2 days. Until the cell confluence reach 80-90%, they were split into a new passage. To avoid cell senescent, all experiments were performed with cells at passage 3-7. HEKa cells were cultured in a new 24-well plate until 80-90% confluence (total V = 1mL/ well). Then treatments of 600-Da BPEI (64, 128, 256, 512, and 1024 µg/mL), LPS (lipopolysaccharide from *E. coli*; 5 µg/mL), PG (peptidoglycan from *S. aureus*; 5 µg/mL) were added in triplicate cultures for 24 hr. The cell media was collected in 1.5 mL Eppendorf microtubes and stored at -20°C until ELISA assays were performed. Concentrations of IL-8, IL-6, TNF-α cytokines released into the media were quantified followed the instructions of Quantikine Colorimetric ELISA assay kits (R&D Systems). Absorbance was measured at 450 nm and 570 nm. Final corrected absorbance was the subtraction at 450 nm from the one at 570 nm.

Results and Discussion

Instrumental Analyses

Instrumental analysis is an important and powerful method in analytical chemistry for obtaining qualitative and quantitative data about the structure and composition of matters. For a better understanding of the chemistry itself as well as laying a foundation for future BPEI-derivative syntheses, 600-Da BPEI was instrumentally analyzed using HPLC, MS, and FTIR.

Chromatography is a sophisticated technique that has applications in all shape and size of science, and high-performance liquid chromatography (HPLC) is one of the most popular separation techniques by using a liquid mobile phase. The working principle of HPLC can be described as a mass transfer process with the adsorption of the analytes to a column filled with adsorbent. The interactions are based on hydrophilic, hydrophobic, dipole-dipole, ionic, or the sum of all in which are influenced mostly by different stationary phase, mobile phase, pH, temperature, pressure, and flow rate. A peristaltic pump drives both solvent and sample through a column, which is the stationary phase, where separation takes place. Right after the column, a detector detects those separated species and displays on computerized charts.[47-48] Here, 600-Da BPEI solution used in all testing was run through a reverse-phase HPLC to determine its purity as well as its retention time in the non-polar column used. As shown in Figure 8, the peak at 2.09 min indicates that the BPEI solution was highly pure (single peak) and very hydrophilic (eluted quickly, less than 3 min).

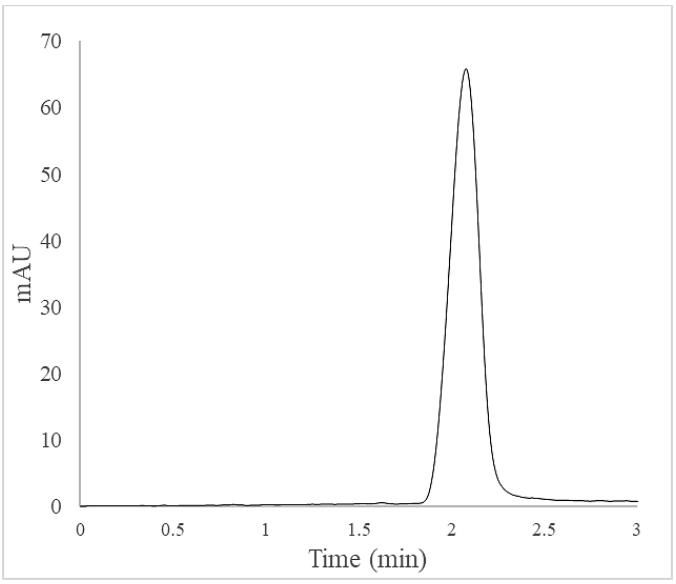


Figure 8. HPLC chromatogram of 600-Da BPEI solution (2.56 mg/mL). Retention time of BPEI peaks at 2.09 min.

Characterization of the BPEI molecule was further examined using a Q-TOF (quadrupole-time-of-flight) mass spectrometry (MS), one of the most sophisticated instruments for accurate mass-to-charge-ratio (m/z) characterization. As shown in Figure 9, 600-Da BPEI fragmentation gave most of its abundant ionized peaks at around 500 m/z. A common difference of 43 m/z exists between one peak to the adjacent another, indicating the repeating unit of the polymer tested BPEI: an amine plus an ethyl group. This repetitive pattern confirming the purity and polymerized chemical structure of 600-Da BPEI.

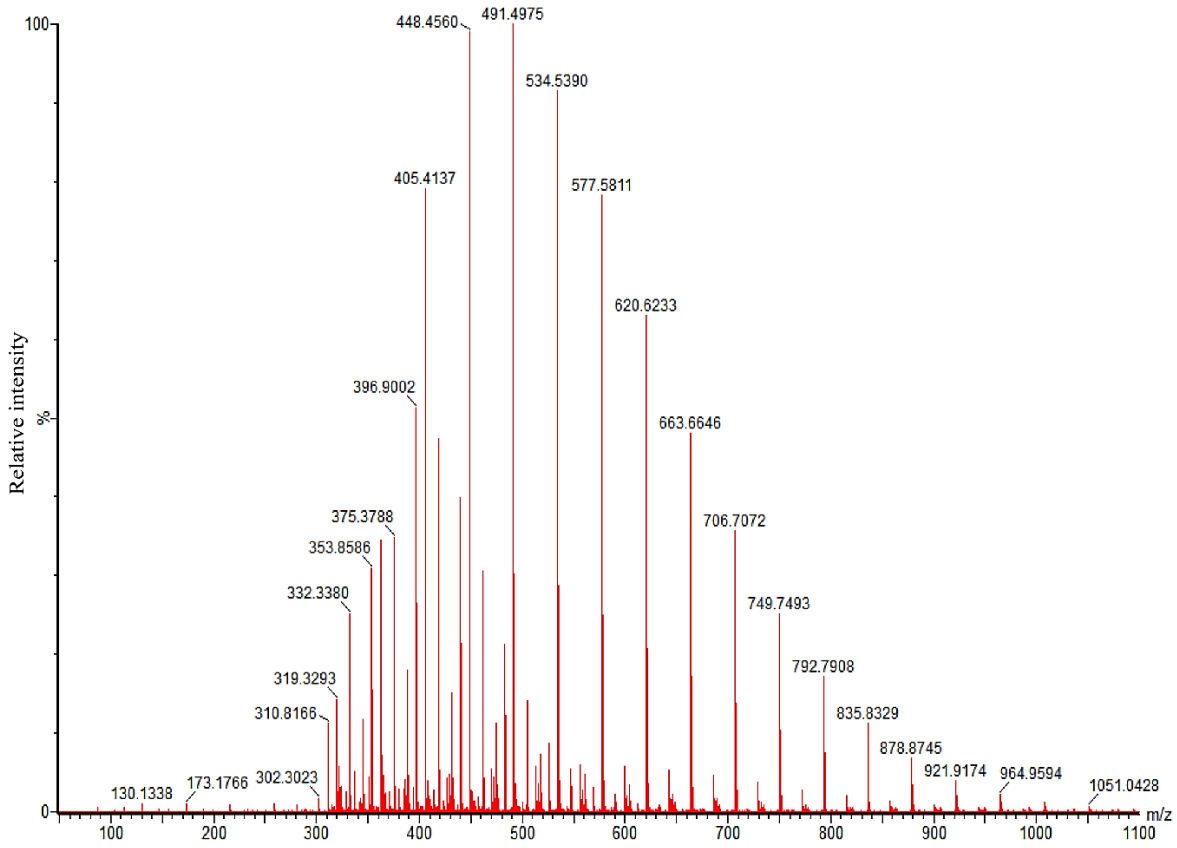


Figure 9. Mass spectrum of 600-Da BPEI. Most abundant peaks are around ~500 m/z which are the most ionized fragments of 600-Da BPEI. Most peaks have a similar difference of 43 m/z from their adjacent peaks, which is equal to the m/z ratio of one amine and an ethyl repeating unit of the polymer BPEI (i.e. 534.5 – 491.5 = 43 m/z).

Functional groups of BPEI were captured by Fourier-transform infrared spectrometry, which is a technique used to measure a transmittance of a sample over a wide spectral range. Because different functional groups have different chemical structures which absorb or transmit different frequencies. Therefore, they can be determined and analyzed by a FTIR. Figure 10 shows a FTIR spectrum of the 600-Da BPEI. The broad peak at 3300-3500 cm^{-1} indicate the N-H bond of the amines. The strong peaks at 2935, 2860, and 1467 cm^{-1} are from alkane C-H stretches of the alkyl

spacers. Carbon C-C bonds throughout the polymeric chain are indicated with the 1641 and 1566 cm^{-1}. The moderate peak at 1311 cm^{-1} confirms the C-N bond.

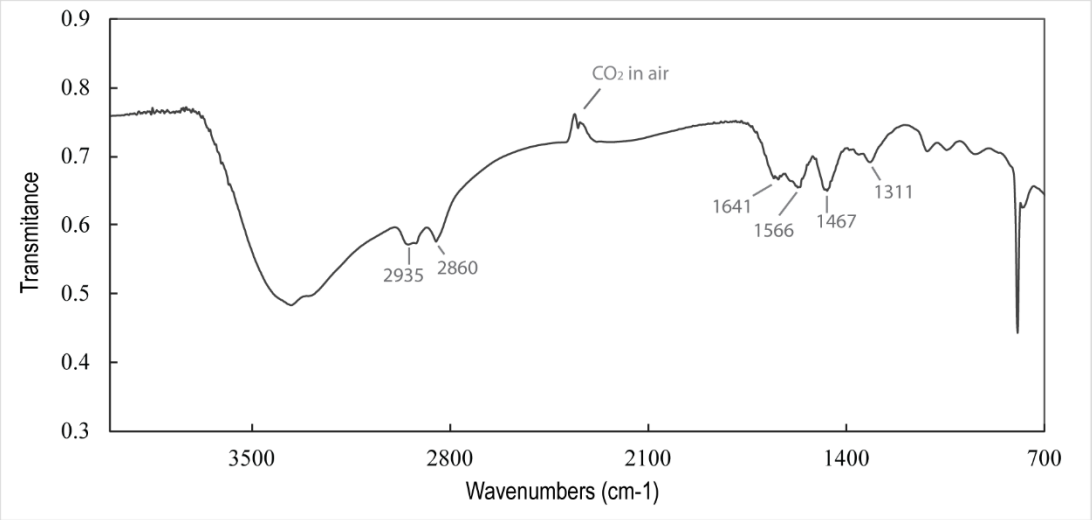


Figure 10. FTIR spectrum of 600-Da BPEI (in CCl_4)

Overall, chemical properties of our lead potentiator BPEI have been instrumentally characterized: purity, polarity, ionized fragments, and functional groups. These data are reported for future use as a helpful foundation knowledge to modify or synthesize BPEI-derivatives.

Inflammatory Response of Human Epithelial Keratinocytes exposed to BPEI

The innate immune system is one of the first-line defense mechanisms in the human body, especially in wound healing. As one of the most complex biological events, wound healing involves many interactive processes mediated by local resident cells (keratinocytes, fibroblasts, nerve cells) and infiltration of neutrophils, mast cells, macrophages, and lymphocytes to trigger production of growth factors and cytokines.[49] Cytokines are chemical messengers produced by all immune cells for their communication. Interleukins (ILs) are those serve for leukocyte communication. The activation and suppression of immune system or cell division are closely related to

interleukins. For example, interleukin IL-6 functions in proliferative phase of healing. IL-6 was found with significantly elevated amount in chronic wounds compared to acute wounds,[50] suggesting the inflammatory phase is likely stuck in chronic wound healing process. Chemokines are a group of cytokines that are responsible for leukocyte recruitment into sites of infection or injury and for maintenance of inflammatory reaction, with the best known is IL-8 (or CXCL-8).[51] Peak levels of IL-8 are often caused by neutrophils and found under a wound surface. Another subgroup of cytokines is tumor necrosis factors (TNFs), which mainly activate immune cells to sites of infection and to tumor cells to destroy them. TNFs are cytotoxic specifically to tumor cells, with TNF-α is the most outstanding member in having many physiologic functions including the survival and death of other cells. Expression of proinflammatory cytokine TNF-α also induces the production of other cytokines (IL-1, IL-6, and IL-8) that increase the inflammatory responses of leukocytes.[11, 52]

Bacterial products, such as cell wall component lipopolysaccharides (LPS) or peptidoglycan (PG), also stimulate recruitment and activation of phagocytes. These foreign products are grouped into pathogen-associated molecular patterns (PAMPs). PAMPs are recognized by toll-like receptors (TLRs) which eventually leads to secretion of cytokines IL-6, IL-8, and TNF-α in response to inflammation reactions. Large scales of these inappropriate cytokine productions may cause even more diseases: autoimmune diseases (i.e. rheumatoid arthritis and systemic lupus erythematosus), chronic wound infections, and autoinflammatory diseases (asthma and arthritis).[53-54] Therefore, a good topical anti-bacterial agent must not induce inflammation itself. Here, inflammatory responses of human epithelial keratinocytes (IL-8, IL-6, and TNF-α) after being

exposed to 600-Da BPEI for 24 hours were collected and measured using ELISA assays. Standard curve of each cytokine was graphed and is shown below (Figure 11). Standard fitted equations were found with strong correlation coefficient, R-squared values (all 3 R-squared are > 0.99). These equations were then used to calculate the amounts of cytokines released by HEKa cells. For IL-8, cell culture supernates were diluted 10x before added to the ELISA kit. For IL-6 and TNF-α, no dilutions were made to ensure the measurements fall within the dynamic range of the standard curves.

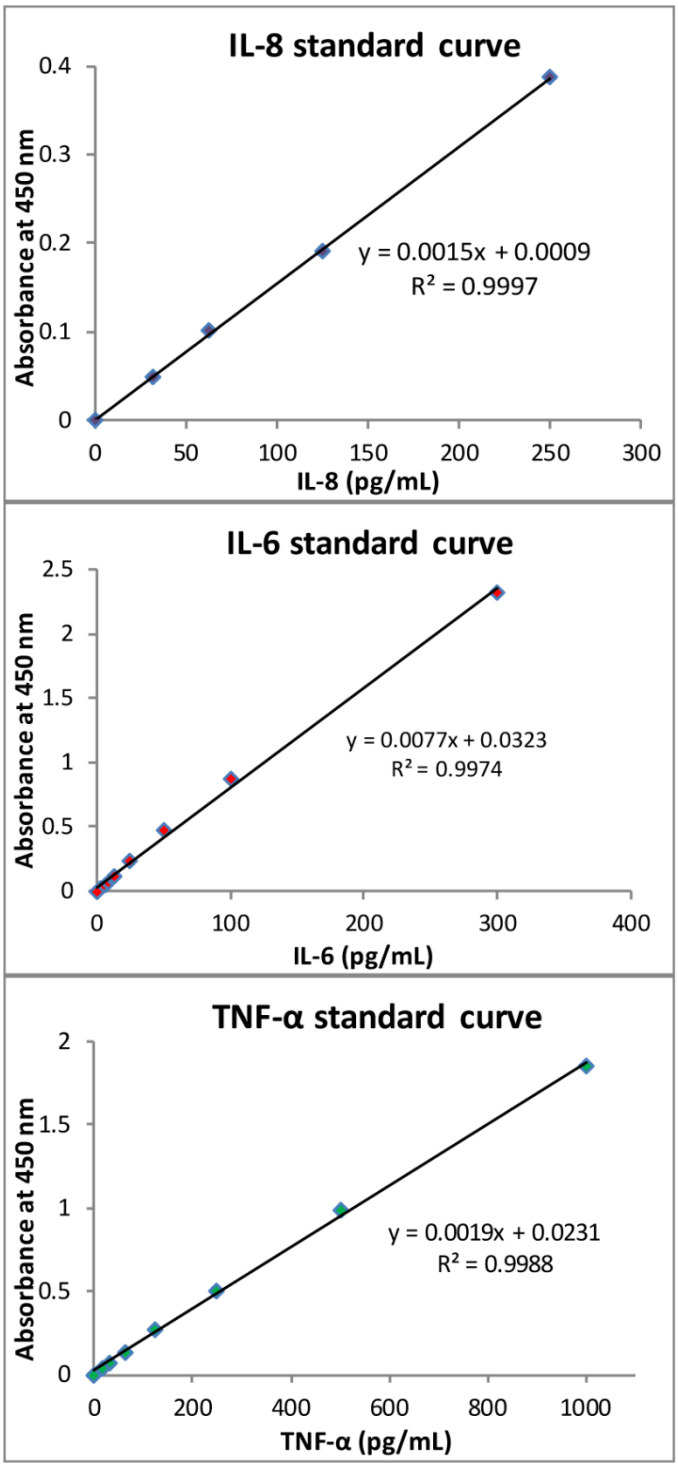


Figure 11. Standard curves of the three cytokines tested (IL-8, IL-6, and TNF-α). Linear fitted equations are shown with their corresponding R-squared values. These equations were used to calculate the amount of the cytokines released by HEKa cells.

As a result, 600-Da BPEI caused a minimal release of all three cytokines tested by HEKa cells. As shown in Figure 12, the amount of each cytokine produced is reported in picograms pg/mL. The only significant difference in responses compared to the untreated control is by peptidoglycan (PG) from *S. aureus* and by lipopolysaccharide (LPS) from *E. coli*. Variety of BPEI concentrations (64 – 1024 µg/mL) showed no significant changes in the three cytokine responses. Interleukin IL-8 was found to be the highest concentrations released (>1500 pg/mL by PG/LPS and ~200 pg/mL in untreated control). IL-6 was found to be in smaller amounts (~350 pg/mL by PG/LPS and <50 pg/mL in untreated control). The lowest-concentration cytokine found was TNF-α (~30 pg/mL by PG/LPS and <10 pg/mL in untreated control). Larger error bars in the IL-6 and TNF-α graphs were due to the smaller in absorbance intensity that was close to a detection limit. Nevertheless, statistical analyses using *t-test* (95% confidence) indicate significant differences of these cytokines' release by only the bacterial cell wall components (PG and LPS), and not by 600-Da BPEI.

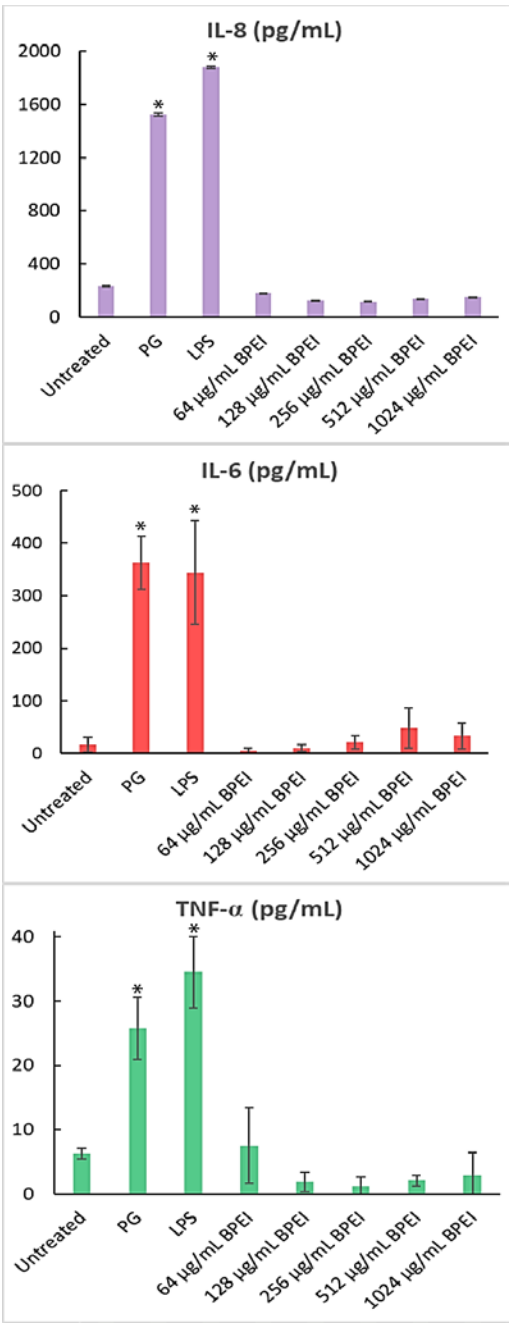


Figure 12. Cytokines released (picograms - pg/mL) by human epithelial keratinocytes (HEKa cells) in responses to peptidoglycan (PG), lipopolysaccharides (LPS), and 600-Da BPEI. Data shown the average of triplicate trials. Error bars denote standard deviation. (*) indicates significant difference found between that sample and the untreated control (t-test, p-value < 0.05).

Therapeutic Potentials of 600-Da BPEI

Staphylococci are notorious for their skin and soft-tissue infections that often lead to more complicated diseases. Each year, millions of acute skin and soft tissue infections (SSTIs) become chronic wound infections.[55-58] Instead of taking 3-6 weeks to heal, chronic wounds persist for 3-6 months. Delays in healing acute SSTIs are often due to a prolonged inflammatory phase of healing caused by bacterial debris, such as peptidoglycan from *S. aureus*, which is a PAMPs molecule. Inappropriate expression of cytokines caused by PAMPs can trigger toxic shock and blood poisoning or sepsis. Over production of these chemical messengers provokes the immune system to "panic", and destructive self-harm will be the consequence of an autoinflammation and prolonged chronic wound healing. Therefore, stopping PAMPs from triggering the release of inflammatory cytokines can theoretically restore optimal immune response. However, bacterial metabolic products including exotoxins and endotoxins are inevitably difficult to prevent. Not many successful antibacterial drugs are anti-inflammation. Fortunately, 600-Da BPEI can meet both criteria (more details in Chapter 6).

In short, BPEI is considerably safe with low *in vitro* toxicity,[45] doesn't cause cytokine release (Figure 12), prevents cytokine triggering by PAMPs, and has antibacterial and antibiofilm-potentiation potentials against MRSE, MRSA, and *P. aeruginosa* (the following chapters). Additionally, BPEI electrostatically binds Gram-positive *and* Gram-negative cell wall components (teichoic acid/PG and LPS). Thus, this interaction with BPEI can possibly decrease the inflammatory cytokine release

caused by these pathogens, which highlights excellent therapeutic potentials of BPEI for antibiotic-resistant treatment as well as for acute and chronic wound care.

Conclusions

Characterization of BPEI using instrumental analyses has been documented, laying a background foundation for future BPEI-analogs' synthesis and characteristic comparison. Inflammatory responses by human epithelial keratinocytes exposed to BPEI shows significantly lower amount than those exposed to bacterial debris PG and LPS. Therefore, more therapeutic potentials could be explored using BPEI, especially as a wound care agent due to its multifunction: antibacterial, antibiofilm, and anti-inflammation.

Chapter 3: Synergy between β-lactam antibiotics and BPEI against planktonic MRSE

Background

From a comparative epidemiology study in Belgium,[59] *S. epidermidis* isolates from catheter-related bloodstream infections (CRBSI) were found to have significant resistance to more antibiotics than the commensal isolates. More than 75% of the CRBSI isolates contained the resistance gene *mecA*, while only 3% of the *S. epidermidis* isolates from healthy individuals did. Additionally, the majority of the MRSE isolates are resistant to multiple antibiotics including oxacillin, erythromycin, and ciprofloxacin.[59] *S. epidermidis* is involved in hospital-acquired infections[60] which pose a great danger to public health. We were motivated to better understand the pathogenesis of MRSE as well as the pharmacology of antibiotics in combination with 600-Da branched polyethylenimine (BPEI) against *S. epidermidis* laboratory strains and clinical isolates. Our lab previous research started to use BPEI to restore susceptibility to methicillin-resistant *S. aureus* (MRSA) after an accidental experiment happened in 2014. At the time, a former student was examining how metal binding/blocking by BPEI affects bacteria. Unexpectedly, chloramphenicol-resistant *Bacillus subtilis* treated with chloramphenicol and BPEI resulted in death, therefore laying the foundation for subsequent projects with antibiotic potentiation against drug-resistant pathogens.[41]

β-lactam antibiotics (i.e. amoxicillin) are first-line drugs that inhibit bacterial cell wall synthesis by irreversibly binding to the penicillin-binding proteins (PBPs), a subgroup of enzyme transpeptidases. β-lactam binding to PBPs prevents them from crosslinking the cell wall peptidoglycan. Without cell wall synthesis, bacteria are unable

to replicate and consequently die. However, MRSE has the staphylococcal cassette chromosome mec (SCCmec), which contains the gene *mecA*. *MecA* is ultimately translated to create PBP2a, a unique penicillin-binding protein that has a low affinity for β-lactam antibiotics relative to other PBPs, thereby making these first-choice antibiotics ineffective.[3] In our study, we disabled this resistance factor using 600-Da BPEI, a low-molecular-weight cationic polymer. Data show that a combination of BPEI and β-lactam antibiotics kills MRSE. The proposed mechanism of action is that BPEI electrostatically binds to wall teichoic acid (WTA), which is an anionic polymer in the cell wall of *S. epidermidis* and other Gram-positive bacteria (Figure 13).

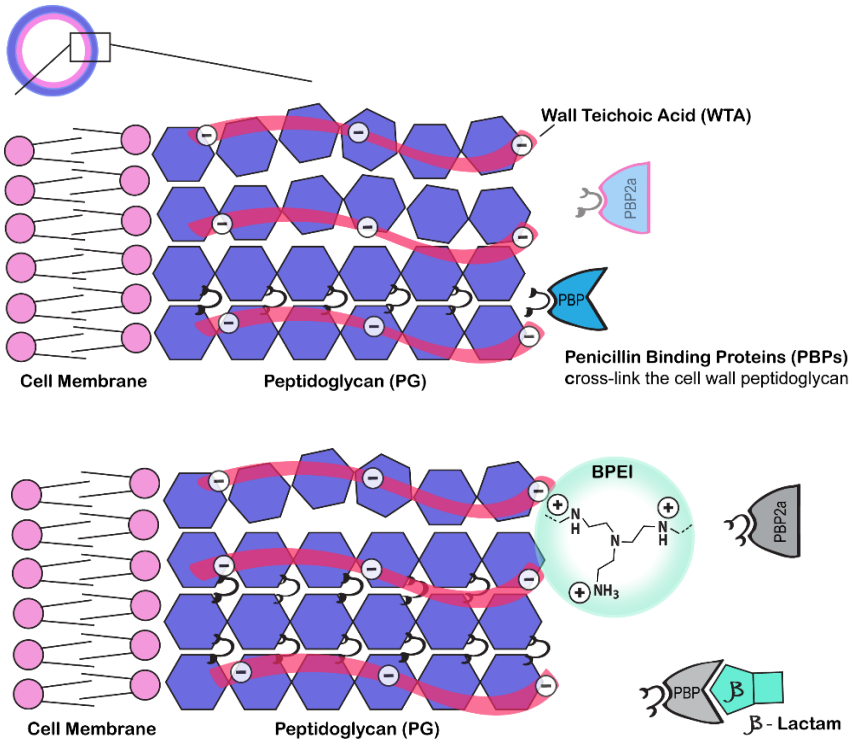


Figure 13. Illustrations of cell wall peptidoglycan in MRSE. PBPs crosslink the peptidoglycan subunits finishing the last stage of cell wall synthesis unless inhibited by β-lactams. MRSE's methicillin-resistant factor is the extra PBP2a, which is not affected by β-lactams. 600-Da BPEI binds WTA and blocks PBP2a's localization, thereby disabling the resistance.

WTA has been suggested to play an important role in the localization of penicillin binding proteins, especially PBP2a.[61] Foxley et al. successfully potentiated β-lactams against MRSA by targeting WTA with BPEI.[45] A similar mechanism of action is hypothetically believed to exist between BPEI and β-lactams against MRSE. Thus, when BPEI binds to WTA, PBP2a loses its ability to function, and MRSE's susceptibility to β-lactams is restored.

Purpose of Experiment

The purpose of this experiment is to determine the efficacy of BPEI in potentiating β-lactam antibiotics against planktonic methicillin-resistant *S. epidermidis* (MRSE).

Experimental Procedures

Materials

Staphylococcus epidermidis bacteria were purchased from the American Type Culture Collection (MRSE ATCC 29887: methicillin-resistant, MRSE ATCC 35984: methicillin-resistant, and MSSE ATCC 12228: methicillin-susceptible). Two clinical isolates of MRSE were provided by Cindy McCloskey, M.D. from the University of Oklahoma College of Medicine. Chemicals were purchased from Sigma–Aldrich (DMSO, growth media, and electron microscopy fixatives). Antibiotics were purchased from Gold Biotechnology. 600-Da BPEI was purchased from Polysciences.

In vitro Checkerboard Assays

Checkerboard assays were conducted to identify synergy between 2 drugs combined (BPEI and antibiotics) against bacteria. Briefly, stock solutions of oxacillin, ampicillin, amoxicillin, linezolid, and vancomycin were made in DMSO. Antibiotic

solutions were serial diluted and added to pre-sterilized 96-well plates so that the final DMSO concentration was less than 1%. A stock culture was made of one colony per 1 mL and added 1% v/v to cation-adjusted Mueller–Hinton broth (MHB) in the 96-well plates. Optical density readings at 600 nm (OD600) were made using a Tecan Infinite M20 plate reader immediately after inoculation. The plates were incubated for 24 hr at 35°C, and a final OD600 reading was measured. The change in OD600 was found by subtracting the initial OD600 from the final OD600 reading. A change in OD600 greater than 0.05 indicated positive growth. The minimum inhibitory concentration (MIC) was assigned as the lowest concentration of antibiotic or BPEI that inhibited bacterial growth. The fractional inhibitory concentration index (FICI) was calculated using the previously established equation: $FICI = \frac{MIC_{AB}}{MIC_A} + \frac{MIC_{BA}}{MIC_B}$ (where A represents one drug and B represents the other). Synergistic effects are determined as by EUCAST guidelines: synergy (FICI $\leq$ 0.5), additivity (0.5 < FICI < 1), and indifference (FICI > 1).[62] Each trial was done in triplicate.

Growth Curves

Tryptic Soy Broth (TSB) growth media augmented with various amounts of BPEI and/or oxacillin was inoculated at 0.5% from overnight cultures of MRSE 29887 and MRSE 35984. Cells were grown at 35°C with shaking. The OD600 was recorded every hour for each sample. Each study was done in triplicate.

Scanning Electron Microscopy (SEM)

MRSE 35984 and MSSE 12228 cells were inoculated 0.5%from an overnight culture and grown at 35C with shaking. Each strain of bacteria was grown in four separate conditions: BPEI, oxacillin, combination (BPEI+oxacillin), and control. The OD600 was

monitored, and growth was stopped at late-lag phase (OD600= 0.20–0.25). Samples were fixed with Karnovsky fixative (2% glutaraldehyde and 2% paraformaldehyde in 0.1M cacodylate buffer) for 30 min. The cells were then fixed with 1% OsO_4 for 30 min in the dark. The cells were washed with water three times. A couple drops of each sample were placed on clean, poly-l-lysine coated coverslips and air-dried for 30 min. To dehydrate, the samples went through a series of ethanol solutions (20%, 35%, 50%, 70%, and 95%), spending 15 min in each solution. Afterward, the samples were dried with hexamethyldisilazane (HMDS) and sputter-coated with AuPd. A Zeiss NEON SEM was used to image the samples at 5kV accelerating voltage. Size analysis was performed on ImageJ.

Transmission Electron Microscopy (TEM)

MRSE 35984 cells were inoculated 0.5% from an overnight culture and grown at 358Cwith shaking in four separate conditions: BPEI, oxacillin, combination (BPEI+oxacillin), and control. The OD600 was monitored, and growth was stopped at late-lag phase (OD600 = 0.20–0.25). Samples were fixed with Karnovsky fixative (2% glutaraldehyde and 2% paraformaldehyde in 0.1M cacodylate buffer) for 2 hr. The cells were washed three times with 0.2M cacodylate buffer and then stained with 1% OsO_4 in 1.5%potassium ferrocyanide for 2 hr in the dark. Samples were washed three times with water and stained with 1% uranyl acetate for 30 min. After three more washes with water, the cells were dehydrated with 50%, 70%, 95%, 95%, and 100% ethanol (20 min in each solution). The samples were immersed in propylene oxide (PO) for 1 hr to remove residual ethanol. The cell samples were then infiltrated with 2:1ofPO: Epon for 1h,1:1 of PO: Epon for 1hr, 2:1 of PO: Epon for 2hr, and pure Epon overnight. The cells were

transferred into embedding molds with fresh Epon and allowed to sink to the bottom for 24–48 hat6 0 8C. The sample blocks were ultra-thin-sectioned by an ultramicrotome to 80–100 nm thickness. The thin sections were placed on TEM copper grids and then stained with 1% uranyl acetate for 30 min. A JEOL2000FX TEM was used to image the samples at 200 kV accelerating voltage. Size analysis was performed on ImageJ.

Results and Discussion

Checkerboard assays indicate synergistic effects between BPEI and β-lactams

To investigate the synergy between 600-Da BPEI and antibiotics against MRSE, checkerboard assays were conducted. Synergistic effects were observed between BPEI and b-lactam antibiotics (oxacillin, ampicillin, and amoxicillin), but not between BPEI and vancomycin (Table). Synergy occurred when their FICI was less than 0.5, while additivity was indicated by an FICI between 0.5 to 1.[62] The MICs of BPEI and several antibiotics were tested against two laboratory strains of methicillin-resistant *Staphylococcus epidermidis*, MRSE ATCCS 29887 and MRSE ATCCS 35984, and one methicillin-susceptible strain, MSSE ATCCS 12228. As a result, the BPEI MICs for both MRSE 35984 (Figure 14A,B) and MRSE 29887 (Figure 14C–E) were 8 μg/mL, while the BPEI MIC for MSSE 12228 (Figure 14F) was 2 μg/mL. The oxacillin MICs for MRSE 35984, MRSE 29887, and MSSE 12228 were 32 μg/mL,8 μg/mL, and 0.1 μg/mL, respectively. Checkerboard assays showed synergy between BPEI and oxacillin against both MRSE 35984 (FICI= 0.5) and MRSE 29887 (FICI=0.375). In the presence of 4 mgmL@1 600-Da BPEI, the oxacillin MICs for MRSE 35984 and MRSE 29887 were reduced from 32 to 4 μg/mL and from 8 to 0.5 μg/mL, respectively. Additionally, BPEI had synergy with amoxicillin (FICI=0.5) against MRSE 35984 and ampicillin

(FICI=0.31) against MRSE 29887. Linezolid was also found to have synergy or additivity with BPEI (FICI=0.38/0.75 against MRSE 35984/MRSE29887). No synergy was seen between BPEI and vancomycin (FICI=1, Figure 14E). BPEI did not potentiate β-lactam activity against the susceptible strain, MSSE 12228, which lacks PBP2a (FICI=1, Figure 14F). The MIC of each antibiotic was lowered by a factor ranging from 4-fold (linezolid from 1 to 0.25 μg/mL) to 256-fold (amoxicillin from 64 to 0.25 μg/mL) when combined with 4 μg/mL BPEI (Table 3). To evaluate our approach further, two clinical MRSE isolates from patients at the University of Oklahoma College of Medicine were also tested. In Table , both clinical isolates had strong antibiotic resistance with high oxacillin MICs (64 and 128 μg/mL). When combined with 4 μg/mL BPEI, the MIC of oxacillin in both cases dramatically dropped to 2 μg/mL, making the bacteria no longer resistant. These data show that BPEI can effectively potentiate traditional antibiotics against MRSE.

Table 3. Synergy of 600-Da BPEI and antibiotics against MRSE

Strain	**Antibiotic**	**MIC (μg/ml)**		***MIC Antibiotic***	**FICI**	**Outcome**
		BPEI	Antibiotic	*+ 4μg/ml BPEI*		
MRSE 35984	Oxacillin	8	32	*4*	0.5	Synergy
	Amoxicillin	8	64	*0.25*	0.5	Synergy
	Linezolid	8	1	*0.25*	0.38	Synergy
	Vancomycin	8	2	*2*	1	No synergy
MRSE 29887	Oxacillin	8	4	*0.5*	0.38	Synergy
	Ampicillin	8	32	*0.5*	0.31	Synergy
	Linezolid	8	1	*0.25*	0.75	Additivity
	Vancomycin	8	2	*2*	1	No synergy
MRSE OU 26	Oxacillin	64	32	*2*	0.17	Synergy
MRSE OU 29	Oxacillin	128	16	*2*	0.27	Synergy

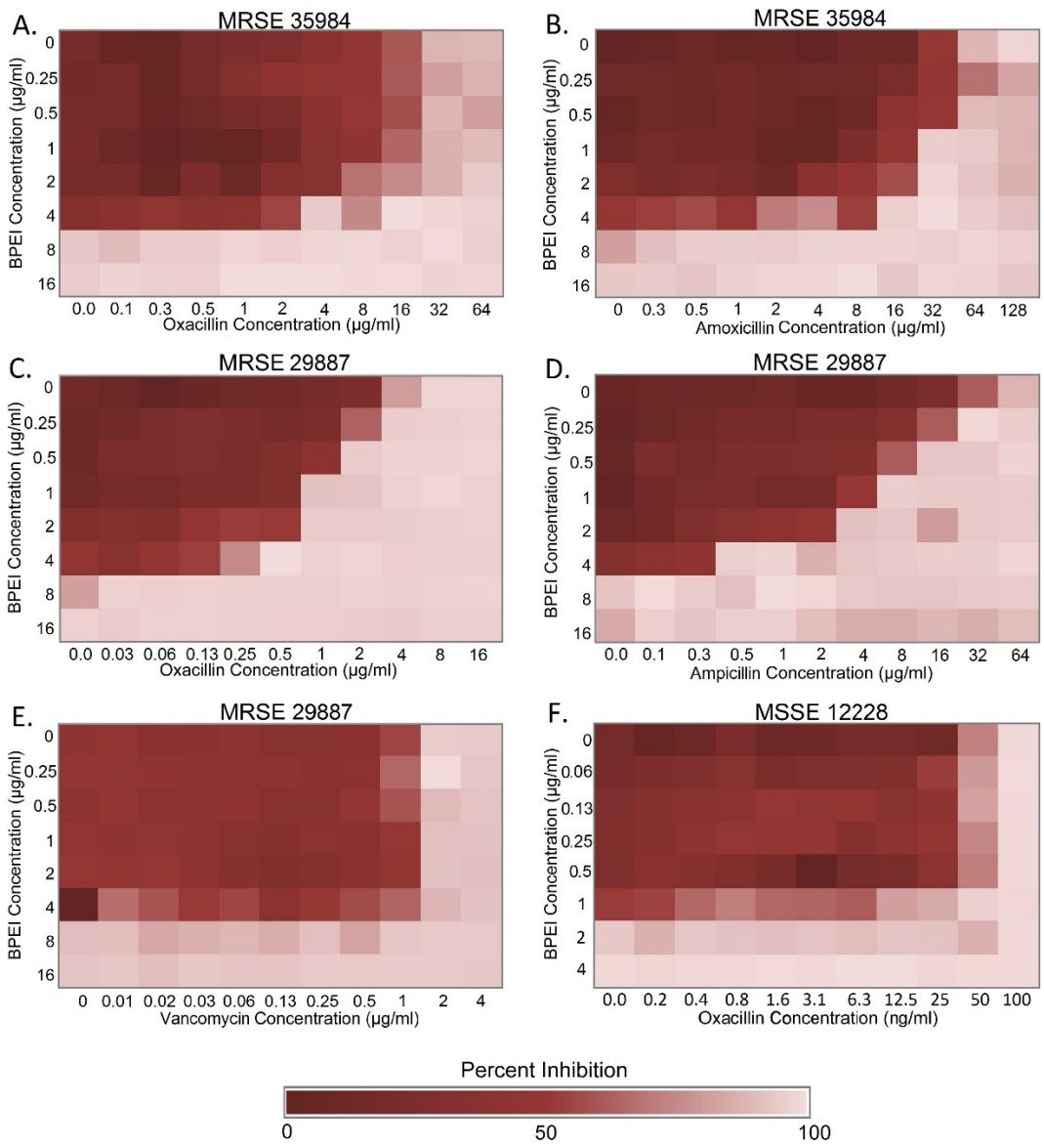


Figure 14. Checkerboard assays testing the synergy of BPEI and antibiotics on MRSE 35984, MRSE 29887, and MSSE 12228. Synergy between BPEI and β-lactams was observed on MRSE 35984 (A, B) and MRSE 29887 (C, D), but not on MSSE 12228 (F). No synergy was found between BPEI and vancomycin on MRSE 29887 (E). Each heat map is the average of three trials in the change of OD_{600}.

Synergistic effects were observed between BPEI and β-lactams but not vancomycin because the targets of b-lactams and vancomycin are distinctly different. Vancomycin binds to the D-Ala-D-Ala stems of bacterial cell wall peptidoglycan, whereas β-lactams bind to PBPs.[63] BPEI binds to WTA, a cofactor of PBP2a, while WTA

is not connected with vancomycin activity. BPEI and β-lactams target the PBPs resulting in synergy: BPEI-WTA interaction inhibits PBP2a, while β-lactams inhibit the other PBPs. A similar explanation can be used to explain the data with methicillin-susceptible S. epidermidis (MSSE) that does not have PBP2a. Likewise, WTA is not involved in the regulation of other PBPs in MSSE. Therefore, disabling WTA does not potentiate antibiotics against MSSE. Wall teichoic acid (WTA) plays an important role in BPEI potentiation of β-lactams against the Gram-positive MRSE. Studies have shown that WTA is required for antibiotic resistance and biofilm formation in MRSE.[64-67] By using NMR spectroscopy, Foxley et al. demonstrated that BPEI and WTA interacted via electrostatic binding of positively charged amine groups on BPEI and negatively charged phosphate groups on WTA.[68] We believe a similar mechanism explains the results obtained in this study. Our hypothesis is that the BPEI-WTA attractions cause steric hindrance to prevent WTA-PBP2a interaction, thereby disabling the resistance factor PBP2a. The β-lactams prevent the other PBPs from cross-linking the cell wall; consequently, the MRSE cells are killed. Synergistic and additive effects of the BPEI+ antibiotic combinations signify enormous potential benefits for patient health because these first-line antibiotics are FDA-approved. Also, the low molecular weight 600-Da BPEI has been tested to have very low cytotoxicity and nephrotoxicity.[45] Thus, BPEI could be a drug-candidate to treat MRSE infections.

Growth curves confirm antimicrobial activity of oxacillin was restored

Antimicrobial activity of oxacillin against MRSE 35984 and MRSE 29887 was restored by 600-Da BPEI. However, by comparing data in Figure 14, it is harder to disable resistance in MRSE 35984. This was confirmed by evaluating the time-dependence of

antimicrobial activity. Growth curves of the two resistant strains were monitored by recording their OD600 for 24 hours and are shown as the averages of three separate trials (Figure 15). The bacteria exposed to either BPEI alone or oxacillin alone reached stationary phase. However, each strain failed to do so in the combination treatment of BPEI+oxacillin. The OD600 increased for all of the samples except for those treated with the BPEI+oxacillin. In the BPEI+oxacillin treated samples, the OD600 dropped after 4hours for MRSE 29887 and after 8hours for MRSE 35984. This indicates a strong antimicrobial activity and also suggests bactericidal activity of our BPEI+β-lactam combination.

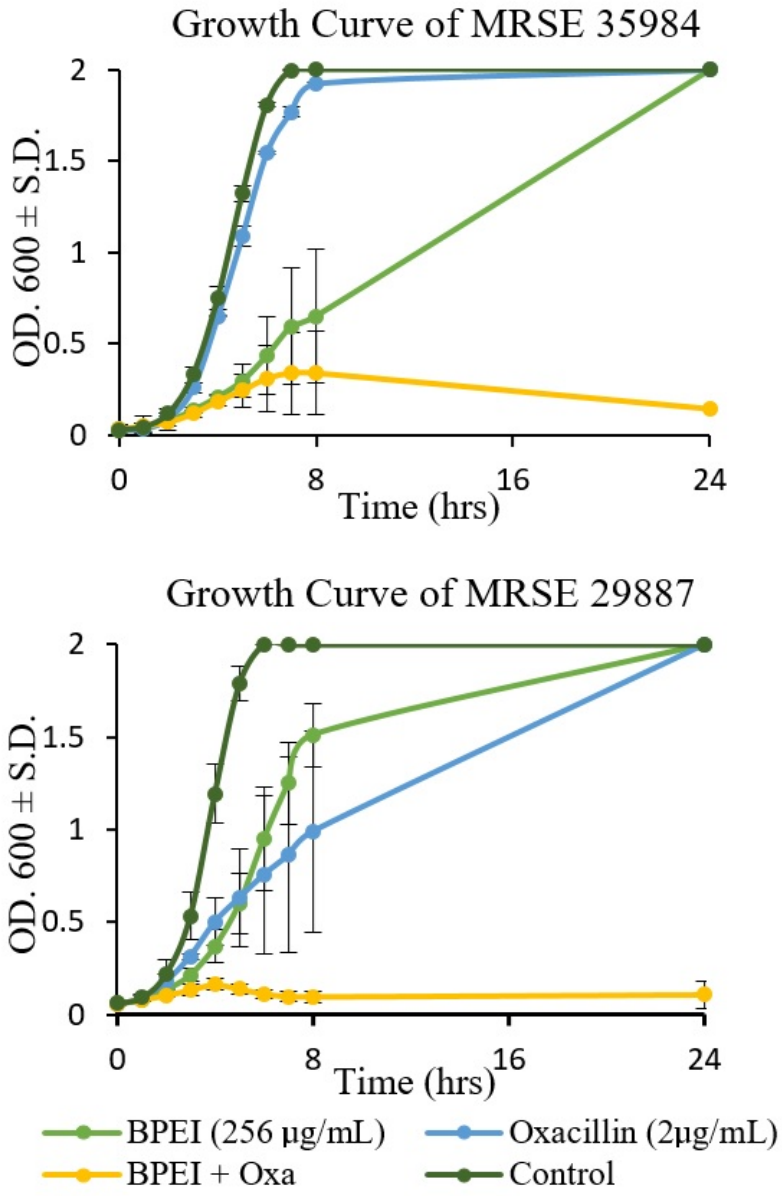


Figure 15. BPEI restores bactericidal activity of oxacillin in the combination treatment (yellow curve) against both MRSE 29887 and MRSE 35984. Each growth curve is the average of three separate trials. Error bars denote standard deviation (n=3).

Scanning and transmission electron microscopies confirm BPEI's mechanism of action

To better understand and confirm BPEI's mechanism of action against MRSE, electron microscopy was used to examine treated samples of MRSE 35984 and MSSE 12228. Bacterial cells were collected at mid-log phase. SEM images of MRSE 35984 include the

untreated control, BPEI-treated, oxacillin treated, and combination BPEI+oxacillin-treated samples (Figure 16).

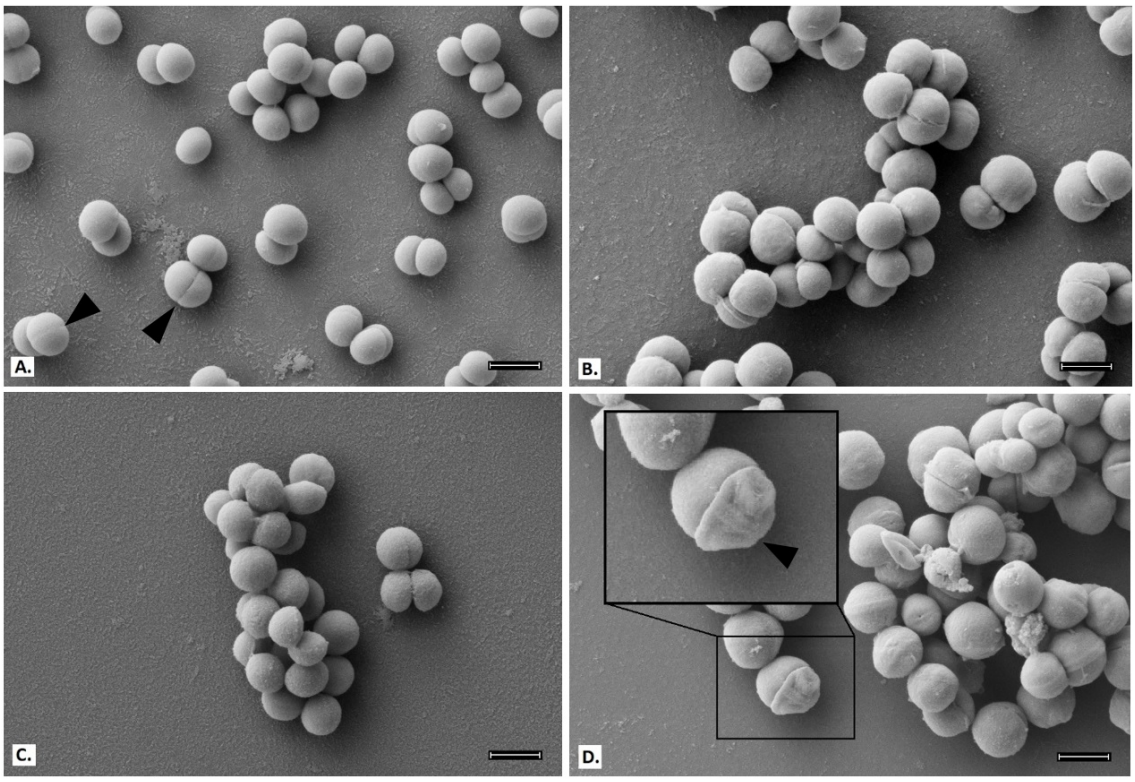


Figure 16. Scanning electron micrographs of MRSE 35984; scale bar = 1 µm. Untreated control cells appear smooth and rounded with clear division septa (arrows) (A). BPEI (256 µg/ml) treated cells (B) and oxacillin (2 µg/ml) treated cells (C) show no significant difference. Combination of BPEI+oxacillin (256 µg/ml + 2 µg/ml) treated cells (D) show extreme distortions and thicker division septa (inset).

The cells in the control sample have smooth, rounded shapes with very clear division septa (Figure 16A). BPEI-treated (Figure 16B) and oxacillin-treated (Figure 16C) cells show no noticeable differences in appearance. However, many of the cells exposed to the BPEI+ oxacillin combination have an abnormal appearance, including concave distortion and thicker division septa (Figure 16D). These cellular morphology changes were not observed on the susceptible strain, MSSE 12228 (Figure 17).

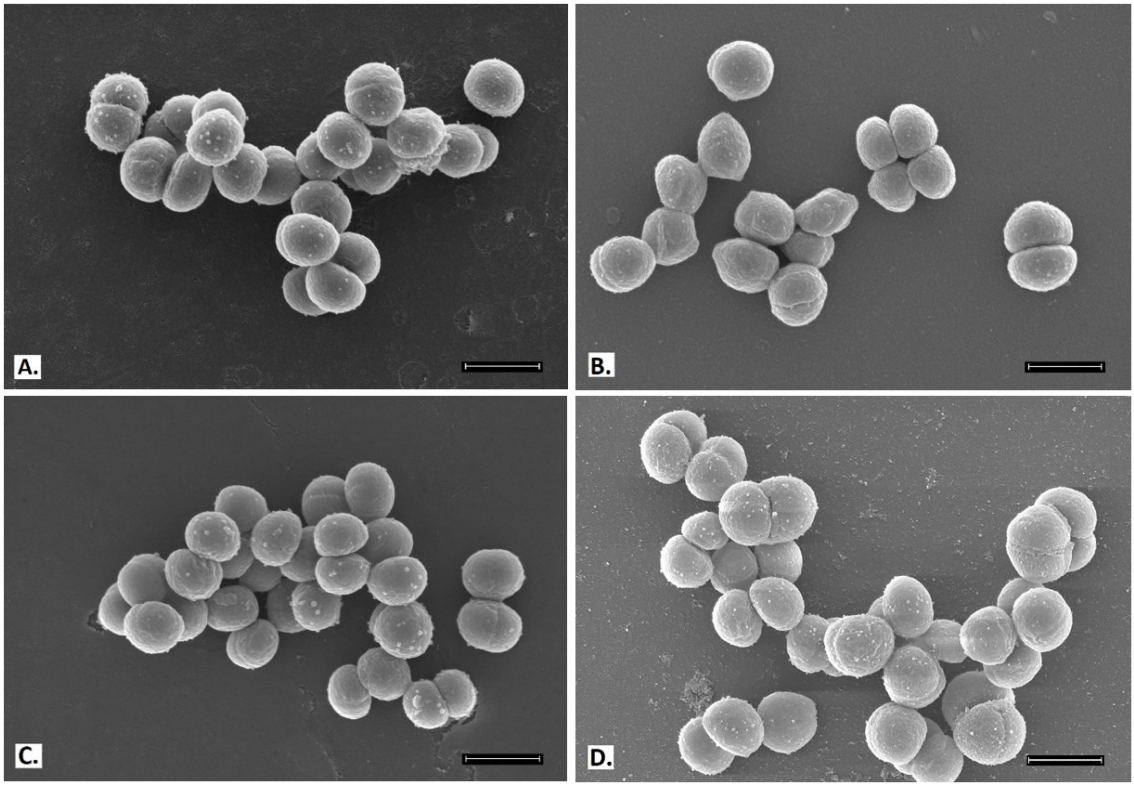


Figure 17. Scanning electron micrographs of MSSE 12228; scale bar = 1 µm. Untreated control (A), BPEI (32 µg/ml) treated (B), oxacillin (0.003 µg/ml) treated (C), and combination of BPEI+oxacillin (32 µg/ml + 0.003 µg/ml) treated cells (D) show no noticeable differences.

The majority of cells from BPEI-treated and the BPEI+ oxacillin treated samples (Figure 16B,D) appear qualitatively larger than the control sample. To confirm the difference in cell size, cell diameters were measured for both MSSE 12228 and MRSE 35984. As shown in Figure 18A, MSSE 12228 did not show a statistically significant difference (ANOVA, p-value > 0.001) in cell size among the four treated groups: control (0.79 ± 0.06 µm), BPEI-treated (0.81± 0.09 µm), oxacillin-treated (0.79 ± 0.08 µm), and combination BPEI+oxacillin-treated (0.82 ± 0.07 µm). The cell sizes of MRSE 35984 (Figure 18B) were found to be significantly different (ANOVA, p-value < 0.001) among the four treated groups: control (0.82 ± 0.07 µm), BPEI-treated (1.00 ± 0.10 µm),

oxacillin-treated (0.89 ± 0.07 µm), and combination BPEI+ oxacillin-treated (1.08 ± 0.15 µm).

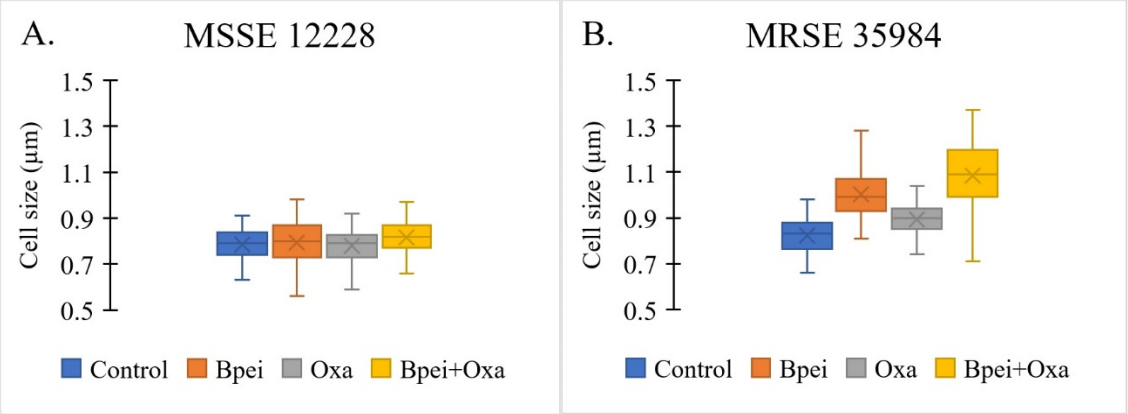


Figure 18. Cell size measurements of MSSE 12228 and MRSE 35984 from SEM images among four treated groups: untreated control, BPEI (256 µg/ml) treated, oxacillin (2 µg/ml) treated, and combination BPEI + oxacillin treated. N=100 cells/group. Mean value, X-marker; median value, center line; lower quartile and upper quartile, lower and upper ends of the box; minimum and maximum values, whiskers outside the box. No significant difference in cell size among treated groups in MSSE 12228 (ANOVA, *p-value* > 0.001) (A). Significant difference in cell size among treated groups in MRSE 35984 (ANOVA, *p-value* < 0.001) (B).

To further elucidate the mechanism of action for our BPEI+ β-lactam treatment against MRSE 35984, cross-sections of the four treated groups were imaged with TEM. TEM allows higher magnification and observation of intracellular structures of the cells. The untreated control cells (Figure 19A) have well-rounded morphologies and complete division septa, while BPEI-treated (Figure 19B) and oxacillin-treated (Figure 19C) samples display many incomplete division septa. The combination BPEI+ oxacillin-treated cells (Figure 19D) have the largest sizes, abnormal multi-division septa, and unrounded shapes that the other treated groups do not possess. Each division septum appears thicker than in the other groups, supporting the SEM data (Figure 16D). Exposure to the BPEI+oxacillin combination makes MRSE cells unable to divide and ultimately causes them to burst, resulting in cell death.

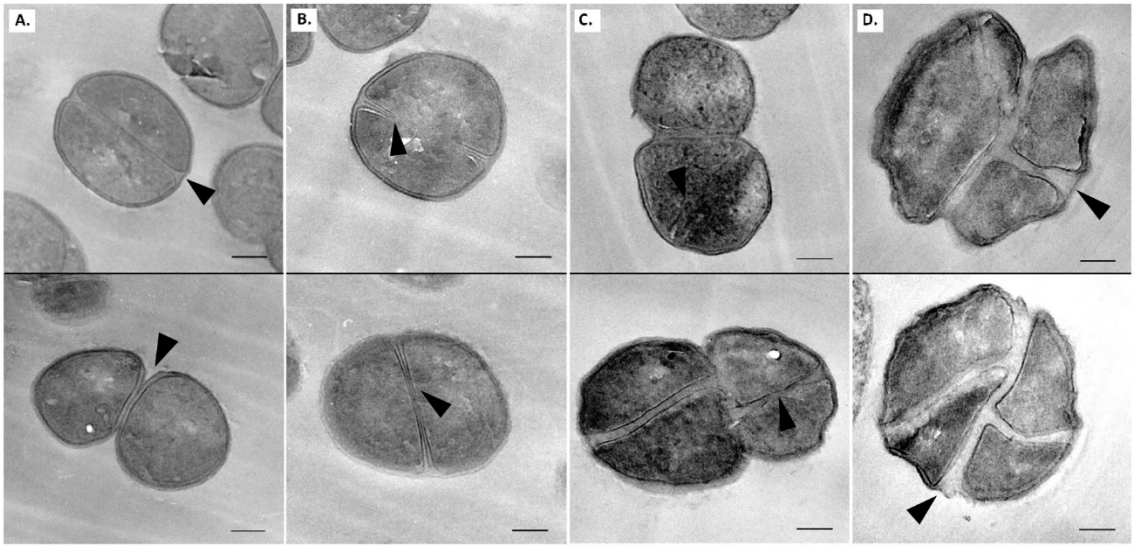


Figure 19. Transmission electron micrographs of MRSE 35984; scale bar = 200nm; arrows show division septa. Untreated control cells appear rounded with complete division septa (A). BPEI (256µg/ml) treated cells (B) and oxacillin treated (2 µg/ml) cells (C) show incomplete division septa. Combination of BPEI + oxacillin (256 µg/ml + 2 µg/ml) treated cells (D) appear to be the largest with abnormal division septa and concave morphology.

The cell envelope of Gram-positive bacteria is a strong framework whose masonry-like architecture protects against internal turgor pressure and external attack by antimicrobial agents. The cell wall is maintained in a robust state by dynamic turnover that removes weakened portions while constructing new cell wall layers. Autolysins break down the cell wall by hydrolyzing the bond between N-acetyl muramic acid and N-acetylglucosamine groups of the peptidoglycan. Synthesis of new cell wall layers involves assembly of precursors in the cytoplasm prior to transport across the membrane. Next, transglycosylase and transpeptidase enzymes assemble the new components in their proper configuration. These processes establish the current strategy of interrupting cell wall construction as a target for many antibacterial drugs. β-lactam antibiotics bind to transpeptidase penicillin binding proteins (PBPs) to prevent cross-linking of nascent peptidoglycan. Degradation by autolysins coupled with the inability to replace

peptidoglycan leads to thinning of the cell wall, loss of integrity, and rupture from internal pressure. However, MRSE endures by expressing PBP2a, whose enzymatic functions proceed in the presence of b-lactams. Cationic BPEI binds to anionic WTA to prevent WTA function, one of which is to serve as a scaffold for PBP2a enzymatic activity. In this manner, BPEI disables resistance from PBP2a.

Conclusions

Antimicrobial resistance is a critical and increasing world-wide threat to the public health. The CDC estimates that at least 2 million people in the U.S. alone are infected by antibiotic-resistant bacteria annually, leading to 23,000 deaths and $20 billion/year in US healthcare costs.[69] The threat from MRSE appears lower than MRSA because of reduced virulence and fewer toxins. However, with its ubiquitous niche on the human skin, MRSE cannot be overlooked. *S. epidermidis* bacteria can be found on nearly every medical device.[70] Fortunately, WTA in these bacteria is a weakness in antimicrobial resistance mechanisms.[71-73] Previous attempts to disable PBP2a by stopping WTA biosynthesis have not survived preclinical trials. Both MRSA and MRSE employ PBP2a, whose functionality requires the presence of WTA. Their resistance can be overcome by disabling WTA, as demonstrated with WTA-deficient strains of MRSA (*ΔtarO* mutants),[71] by inhibiting the WTA synthesis protein TarO with tunicamycin,[74] or by inhibiting another biosynthesis protein, TarG, with Targocil®.[72, 75-77] The work in these reports is strong. Targocil® and related compounds suffer from protein binding that reduces *in vivo* efficacy,[78] but new compounds have mitigated this drawback.[79] Compounds that inhibit WTA and potentiate β-lactams against MRSA also lead to potentiation against MRSE.[72]

Nevertheless, WTA remains an under exploited weakness, and our data show that cationic 600-Da BPEI targets this weakness.[80-81] We depart from the *status quo* of stopping WTA biosynthesis[72, 74] and instead target mature WTA. WTA is an anionic phosphodiester, and cationic 600-Da BPEI disables WTA via an electrostatic interaction. This, in turn, disables PBP2a. In combination, 600-Da BPEI and β-lactam antibiotics inhibit MRSE growth (this work) and MRSA growth.[80-81] The effect is characterized as synergistic from the FICI. Measuring MRSE growth reveals that bacteria exposed to sub-lethal concentrations of BPEI and oxacillin fail to reach exponential phase when the two compounds are combined. This data indicates that the mechanism by which BPEI + oxacillin prevents growth of MRSE is bactericidal. Additional checkerboard assays demonstrate anti-MRSE potency of amoxicillin and ampicillin mixed with 600-Da BPEI. Likewise, higher 600-Da BPEI concentrations decrease further the antibiotic MIC values. Yet, potentiation of linezolid challenges the premise that our discovery applies to WTA-based resistance mechanisms, such as the function of PBP2a. From calculation of the FICI, the effect is a characterized as additive rather than synergy, and thus BPEI and linezolid affect different bacterial components. We know that BPEI binds to anionic sites of the cell wall envelope[80-81] whereas linezolid acts in the cytoplasm to interfere with protein synthesis via the ribosomal 50S subunit. The potentiation of linezolid is most likely to occur by increasing its permeation into the cytoplasm. Therefore, BPEI reduces barriers from the cell membrane and/or the extracellular slime of MRSE. Yet, 600-Da BPEI does not alter the MIC of vancomycin, whose mode-of-action is constrained to the cell wall peptidoglycan. Work to evaluate increased cross-membrane permeation of antibiotics due to the presence of 600-Da BPEI is underway.

The overuse of antibiotics is reflected in the pervasiveness of MRSE. From previous studies, the staphylococcal cassette chromosome *mec*, which codes for methicillin resistance, is suggested to be a one-way horizontal gene transfer from *S. epidermidis* to the well-known super-bug, MRSA.[82-84] As a ubiquitous commensal species of human microflora, *S. epidermidis* contains an optimum reservoir for antibiotic resistance genes, making it an implicit danger. Catheter-related bloodstream infections (CRBSI) are caused primarily by coagulase-negative *Staphylococci*, which include *S. epidermidis*, and they can usually be treated with glycopeptides (such as vancomycin) without catheter removal. However, the chances of bacteremia recurring could be as high as 20%,[85] and the effectiveness of the last-resort antibiotics (linezolid, vancomycin, and daptomycin) has been reduced significantly against MRSE.[86-87] Some MRSE clinical isolates have intermediate resistance to vancomycin and caused complications in patients with sepsis and peritonitis.[88-89] Thus, a need exists to evaluate methods of combating these infections. Our strategy of combining traditional β-lactams with BPEI holds promise in the ongoing battle against MRSE.

Chapter 4: BPEI potentiates β-lactam antibiotics against MRSE biofilms

Background

Staphylococcus epidermidis belongs to the Gram-positive *Staphylococcus* genus. It has emerged as one of the most common causes of healthcare-associated infections due to the increasing use of medical implant devices.[17, 90] Unlike the coagulase-positive *Staphylococcus aureus*, *S. epidermidis* does not produce coagulase and therefore is classified under coagulase-negative staphylococci (CoNS). Accounting for about 70% of all CoNS on human skin, *S. epidermidis* is a leading cause of severe bloodstream infections. Approximately 80,000 cases of central venous catheter infections per year in the US are caused by *S. epidermidis*.[91] *S. epidermidis* is an opportunistic pathogen, like most of the CoNS, because they lack aggressive virulence factors (like those in *S. aureus*) and instead owe their pathogenic success to the ability to form biofilms.

Biofilms and Multidrug Resistance

Biofilms are multicellular agglomerations of microorganisms enclosed in a matrix of extracellular polymeric substances (EPS). Containing polysaccharides, proteins, and extracellular DNA, the EPS matrix acts as a shield that protects the organisms from host defenses and antibiotics. Biofilms can adhere to either biotic or abiotic surfaces—such as cardiac pacemakers and catheters—and have a highly regulated defense mechanism that grants intrinsic resistance against antimicrobial agents.[92] Biofilm development starts with an initial attachment of planktonic cells to a surface, which then grow into clusters of multicellular colonies. Subsequent cell-cell adhesions, divisions, and secretion of EPS create a three-dimensional architecture

designed to channel water and supply nutrients to the inner layers, thereby allowing for biofilm maturation. While the outer-layer cells remain metabolically active, the inner-layer cells are persister bacteria that often stay in a dormant state, and thus are the most difficult to eradicate with antimicrobial treatments, that only target growing organisms.[93] During biofilm maturation, part of the biofilm can detach and disperse planktonic cells, which spread to colonize new surfaces. Mechanisms of biofilm maturation and detachment are poorly understood, but studies suggest that dispersed cells are more virulent and heighten the risk of acute infections.[18, 93]

Biofilm defense mechanisms reduce antibiotic efficacy. The antibiotic concentrations required to eradicate biofilms are ten- to a thousand-fold higher than the concentrations required to kill planktonic bacteria, creating a burden on both public health and the economy from increased medical costs. Removal of biofilm-infected indwelling medical devices complicates treatments and interferes with the healing process.[92] Additionally, persistent biofilms are also a leading cause of chronic wound infections. Around 60% of chronic wound specimens—compared to only 6% for acute wounds—were found to contain biofilms in which the prevalent species was *Staphylococci*.[94] Thus, few publications offer information on *S. epidermidis* biofilm properties and antibiofilm testing, and the virulence and resistance factors of *S. epidermidis* biofilms are poorly understood.[93] Nevertheless, it is necessary to investigate and to find a treatment for these dangerous biofilm infections.

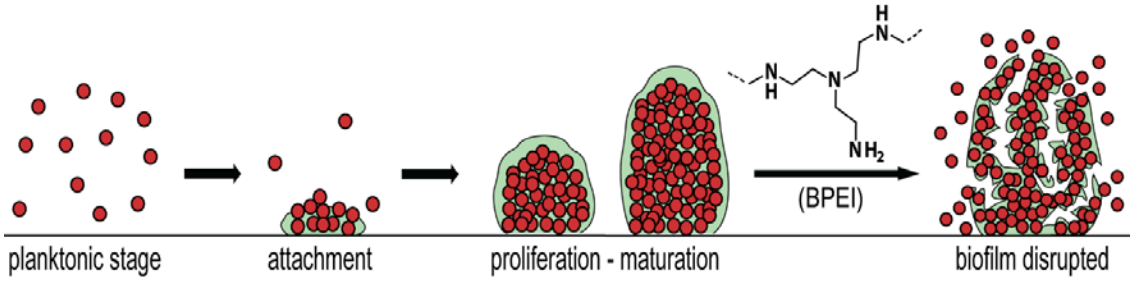


Figure 20. Biofilm formation stages and biofilm-disrupting ability of BPEI. BPEI disrupts established biofilm by collapsing the structure of EPS, releasing the cells into planktonic stage so that β-lactam antibiotics can actively target and eradicate them.

Bacterial biofilms that are impenetrable to antibiotics pose an even greater threat when they are created by drug resistant bacteria, such as methicillin-resistant *S. epidermidis* (MRSE). MRSA, MRSE, and their biofilms lead to chronic wound infections (i.e. wounds that have not proceeded through a reparative process in three months) that affect millions of Americans each year.[55-56, 58] With a dwindling arsenal of new antibiotics, existing drugs and regimens must be coupled with potentiators and re-evaluated as combination treatments for biofilms and antibiotic-resistant diseases. Our lab previously examined the efficacy of branched polyethylenimine (BPEI), a cationic polymer with a low molecular weight of 600-Da, against planktonic MRSE bacteria. Cationic BPEI, with many primary and secondary amine groups, indirectly targets the resistant factor PBP2a by electrostatically binding to anionic wall teichoic acid required for PBP2a activity. In this manner, BPEI disabled resistance in MRSE strains, restoring their susceptibility to traditional β-lactam antibiotics.[1] In this chapter, we further investigate the application of our technology to MRSE biofilms where the EPS contains numerous anionic biomacromolecules. The EPS creates a hydrophobic barrier that increases the tolerance of bacteria towards antimicrobials by reducing or preventing the

antibiotics from reaching their target(s). When BPEI binds to EPS, two changes will occur. First, the anionic character of the biofilm will be neutralized leading to a disruption of the EPS matrix. Secondly, because BPEI is a hydrophilic polymer, it will disrupt hydrophobic barriers that hinder diffusion of aqueous antibiotics (Figure 20). Thus, BPEI functions as a potentiator by inhibiting and disrupting the EPS matrix allowing antibiotics to enter and kill the bacteria. Using the MBEC (Minimum Biofilm Eradication Concentration) assay, which is represented in Figure 21 as a schematic flow, our study demonstrates that BPEI possesses antibiofilm activity itself at high concentrations. However, we also observe synergy between lower concentrations of BPEI and β-lactams against MRSE biofilms. Because it can both disable resistance mechanisms and eradicate biofilms, BPEI is a dual-function potentiator, making it a promising means of preventing and treating healthcare-associated *S. epidermidis* biofilms.

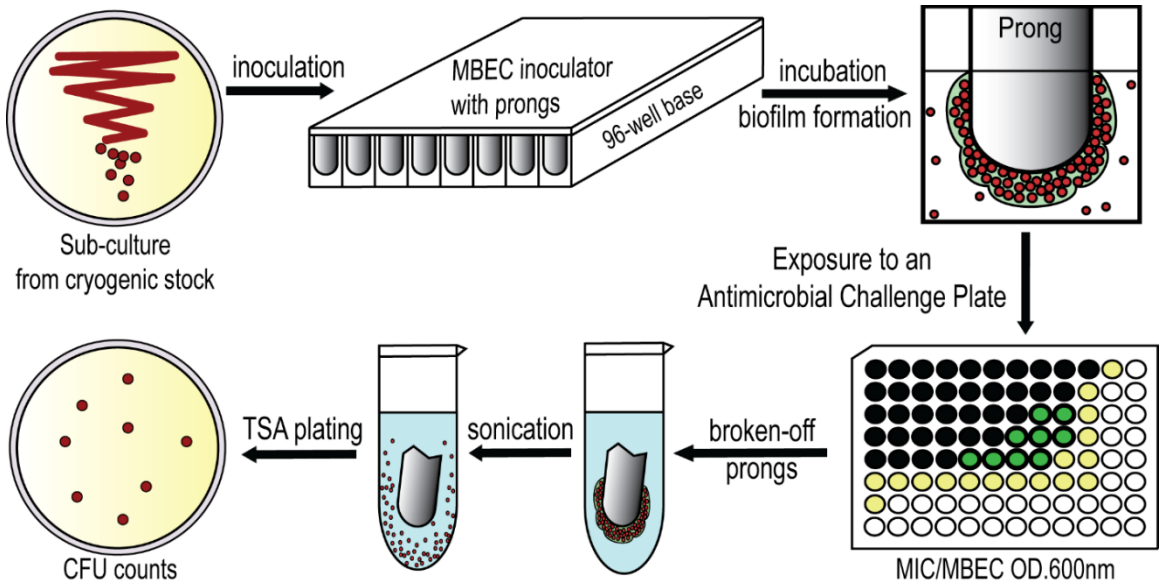


Figure 21. A schematic experimental procedure of our microtiter biofilm model for synergistic effect screening against methicillin-resistant *S. epidermidis* (MRSE) biofilms. MBEC assays were carried out using MBEC inoculator, which is a microtiter plate lid with protruding prongs attached. Each prong fits into each well and allows bacterial biofilm to form and grow. Details are given in the Experimental Procedures. The method of CFU counting is detailed in Biofilm Kill Curve.

Purpose of Experiment

The purpose of this experiment is to determine the antibiofilm synergy of BPEI and β-lactams against multidrug-resistant *Staphylococcus epidermidis*.

Experimental Procedures

Materials

In this experiment, the *Staphylococcus epidermidis* bacteria were purchased from the American Type Culture Collection (ATCC 29887: methicillin-resistant/biofilm-producer, ATCC 35984: methicillin-resistant/biofilm-producer, and

ATCC 12228: methicillin-susceptible/non-biofilm producer). Chemicals were purchased from Sigma-Aldrich (DMSO, growth media, and electron microscopy fixatives). Antibiotics were purchased from Gold Biotechnology. 600-Da BPEI was purchased from Polysciences, Inc. MBEC™ Biofilm Inoculator with 96-well base plates were purchased from Innovotech, Inc.

MBEC Assay
(The MBEC assay is adapted from previous literature reports.[95-97])

Inoculation and Biofilm Formation: A sub-culture of MRSE was grown from the cryogenic stock on an agar plate overnight at 35 °C. The MBEC plate was inoculated with 150 µL of TSB/well plus 1 µL of a stock culture made from 1 colony/mL of MRSE in TSB. The MBEC inoculator plate was sealed with Parafilm and incubated for 24 hours at 35 °C with 100 rpm shaking to facilitate biofilm formation on the prongs. Following biofilm formation, the lid of the MBEC inoculator was removed and placed in a rinse plate containing 200 µL of sterile PBS for 10 sec. Biofilm growth check (BGC) was performed by breaking a few prongs off using sterile pliers, submerging them in 1 mL PBS, and sonicating them on high for 30 minutes to dislodge the biofilm. After sonication, the biofilm solution was serial-diluted and spot-plated on agar plates for CFU counting to determine the biofilm density on the prongs.

Antimicrobial Challenge: A challenge plate was made in a new pre-sterilized 96-well plate in a checkerboard-assay pattern (followed the methods of Lam et al.[1]) to test the synergistic activity of BPEI + antibiotic combinations. Antimicrobial solutions were serial-diluted and added to the 96-well plate, which contained 200 µL of cation-adjusted Mueller-Hinton broth (MHB) per well. Following the rinsing step and biofilm

growth check, the MBEC inoculator lid was immediately transferred into the prepared antimicrobial challenge plate and incubated at 35 °C for 20-24 hours.

Recovery and Quantitative MBEC: After the challenge period, the MBEC inoculator lid was transferred into a recovery plate containing 200 µL of MHB per well, sonicated on high (Branson B-220, frequency of 40 kHz) for 30 minutes to dislodge the biofilm and then incubated at 35 °C for 20-24 hours to allow the surviving bacterial cells to grow. After incubation, the OD_{600} (optical density at 600 nm) of the recovery plate was measured using a Tecan Infinite M20 plate reader to determine the MBEC of the antimicrobial compounds tested. A change in OD_{600} greater than 0.05 indicated positive growth. Likewise, the OD_{600} for the base of the challenge plate was measured immediately after inoculation to determine the MICs of the antimicrobial compounds. The fractional inhibitory concentration index (FICI) calculated based on established equation[98] was used to determine synergy (FICI < 0.5), additivity (0.5 < FICI < 1), and no synergy (FICI = 1).

Scanning Electron Microscopy

MRSE 35984 cells were inoculated from 0.5 % of an overnight culture and grown at 35 °C with shaking in the MBEC biofilm inoculator for 24 hours to facilitate biofilm formation on the prongs. Prongs were broken off the plate using a sterile plier, submerged, treated with primary fixative (5 % glutaraldehyde in 0.1 M cacodylate buffer) in a capped vial, and incubated at 4 ± 2 °C for 2 days. The prongs were removed from the fixing solution and air-dried for 72 hours in a fume hood. They were mounted on aluminum stubs with carbon tape and sputter-coated with AuPd. A Zeiss NEON SEM was used to image the samples at 5 kV accelerating voltage.

In a different experiment, MRSE 35984 cells were inoculated from 0.5 % of an overnight culture and grown at 35 °C with shaking in the MBEC biofilm inoculator for 3 days to ensure maturation of biofilms on the prongs. Nutrient media was replaced every 24 hours. After 3 days, biofilms on the prongs were submerged into new 96-well base with BPEI (512 µg/mL) for 24 hours of treatment. Then, the prongs were broken off the plate using a sterile plier, submerged, fixed with primary fixative (5 % glutaraldehyde in 0.1 M cacodylate buffer) in a capped vial, and incubated at 4 ± 2 °C for 2 days. The prongs were removed from the fixing solution and air-dried for 72 hours in a fume hood. They were mounted on aluminum stubs with carbon tape and sputter-coated with AuPd. A Zeiss NEON SEM was used to image the samples at 5 kV accelerating voltage.

Biofilm Disrupting Assay

Two similar sets of the experiment were conducted: one used 600-Da BPEI and the other used 10,000-Da BPEI. A sub-culture of MRSE 35984 was grown from the cryogenic stock on an agar plate overnight at 35 °C. A pre-sterilized 96-well tissue-culture treated plate was inoculated with 100 µL of TSB/well plus 1 µL of a stock culture made from 1 colony/mL of MRSE in TSB. The plate was incubated at 35 °C for 24 hours to form established biofilm.[99-100] Planktonic bacteria were removed by washing 5 times with water. Crystal violet solution (0.1%) was used to stain the biofilm by adding 100 µL of the solution to each well for 15 minutes. The plate was then washed 5 times with water to remove all excess cells and dye. The plate was turned upside down and air-dried overnight.

Six separate treatments were performed on the preformed biofilm plate (total volume of 100 µL/well): untreated (negative control), BPEI-treated (32, 64, 128, and 256 µg/mL), and 30 % acetic acid-treated (positive control). The treated samples were incubated at room temperature overnight to test the biofilm-disrupting ability of BPEI. Carefully, without touching the bottom of the plate, the solubilized solution in each well was transferred to a new flat-bottom plate for an absorbance measurement of OD_{550}. The OD_{550} represents the amount of MRSE biofilm that was disrupted by BPEI, allowing for quantitative comparison of the controls and treated samples. Statistical data analysis among treated samples was performed using t-test, *n = 10*.

Minimum Biofilm Inhibitory Concentration (MBIC)

MBIC assays were conducted in a similar fashion as checkerboard assays. The full procedure for checkerboard assays are outlined in Lam et al.[1] In brief, a checkerboard assay was made in a 96-well plate to examine the synergy between BPEI and an antibiotic. After an overnight incubation, the cell suspension in the plate was discarded and washed with 100% methanol to retain only the biofilm attached on the well surface. Next, crystal violet solution (0.1%) was used to stain the bacterial biofilm for 15 minutes then washed three times with water. Stained biofilm was then dissolved with 95% ethanol for an OD_{550} (optical density at 550 nm) measurement. Data were subtracted from positive control values and reported.

Biofilm Kill Curve

Biofilm was grown in an MBEC inoculator plate for 24 hours with shaking to facilitate biofilm formation. At time zero, the prongs were sonicated in PBS for 30 minutes and then plated on agar for CFU counting. Four separate treatments were

performed in a new 96-well base: Group 1 was the untreated control, Group 2 had 64 µg/mL of BPEI, Group 3 had 16 µg/mL of oxacillin, and Group 4 had a combination of 64 µg/mL of BPEI + 16 µg/mL of oxacillin. The prongs on the MBEC inoculator were washed in PBS for 10 seconds and then transferred into the new treated base plate and incubated. Agar CFU plating was performed at 2 hours, 4 hours, 8 hours, and 24 hours for each treatment group. All the agar plating was incubated at 35 °C and counted for colony forming units the next day. Each trial was done in duplicate.

Results and Discussion

During the staphylococcal biofilm attachment stage, bacteria adhere to a surface through non-covalent interactions (e.g. electrostatic bonds) via microbial surface components recognizing adhesive matrix molecules. The next stages are biofilm proliferation and maturation, during which EPS (containing proteins, polysaccharide intercellular adhesin PIA/PNAG, teichoic acids, and eDNA) and channel architecture are produced. During the last stage—biofilm detachment and dispersal—phenol soluble modulin peptides disrupt the non-covalent interactions established in the attachment stage.[101] To survive in the human body, pathogens need to cope with the host defense mechanisms: the innate immune system, which includes neutrophils and antimicrobial peptides (AMPs) and the acquired immune system, which includes antigen-dependent T and B cells. The latter is ineffective against MRSE infections for reasons that are not well understood.[102] Since they have been colonizing human skin for millennia, perhaps *S. epidermidis* strains have evolved ways to evade the host defenses. These recalcitrant biofilms particularly threaten immunocompromised patients and those who need prosthetic limbs or artificial implant devices because biofilms can survive on abiotic

surfaces for weeks to months.[18] Motivated to join in the fight against MRSE biofilm infections, we are testing our combination treatment of BPEI and β-lactams in an MBEC microtiter biofilm model.

Confirmation of MRSE Biofilms

The MBEC plates with protruding-prong lids (shown in Figure 21) were used in our experiments to determine the antibiofilm activity of BPEI and conventional antibiotics. The prong lids with established biofilms can fit into regular 96-well microtiter plates for further antimicrobial assays. Many biofilm studies fail to confirm biofilm presence before applying treatments. In this study, scanning electron microscopy (SEM) was performed to confirm that MRSE biofilms formed on the prongs after 24 hours inoculation. Compared to the smooth surface of the control prong (Figure 22A), numerous microcolonies of MRSE were found on the inoculated prong (Figure 22B), indicating that these prongs provide surfaces for biofilm attachment and development. To better characterize the MRSE biofilm morphology, higher magnifications were obtained. Images depict spherical cocci of MRSE bacteria enfolded in a "blanket-like" coat of EPS matrix (Figure 23A). The layers of bacteria are intertwined throughout the matrix, confirming the three-dimensional architecture and the existence of EPS in biofilms (Figure 23B).Among many substances in the EPS matrix, the poly-N-acetylglucosamine (PNAG, also known as PIA) polymer in particular was suggested to have a critical impact on *S. epidermidis* biofilms both *in vitro*[103-104] and *in vivo*.[33, 35, 105] Generated from the *ica* locus, this homopolymer is believed to interact with surface proteins and protect against host defense mechanisms during biofilm formation. Another important protective exopolymer is the

pseudopeptide polymer poly-γ-DL-glutamic acid (PGA), which is encoded by the *cap* gene. Although PGA is produced in very small amounts, it plays a pivotal role in *S. epidermidis* resistance against host AMPs and leukocyte phagocytosis.[106] These biopolymers, along with teichoic acids and eDNA, comprise the slime-like EPS coat. The SEM images confirm that established MRSE biofilms have formed before treatment with BPEI and β-lactam combinations.

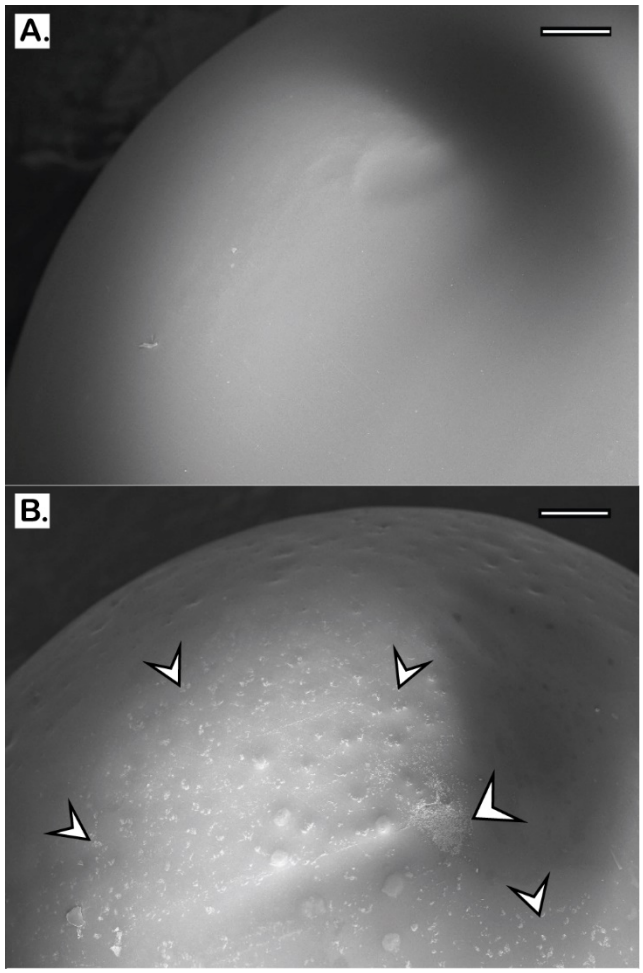


Figure 22. Scanning Electron Micrographs of the tip of MBEC prongs. A control prong with no bacteria is shown (A). MRSE 35984 biofilm colonies were formed after 24

hours of inoculation (B); the arrows highlight some of the biofilm microcolonies. Scale bars = 200 µm.

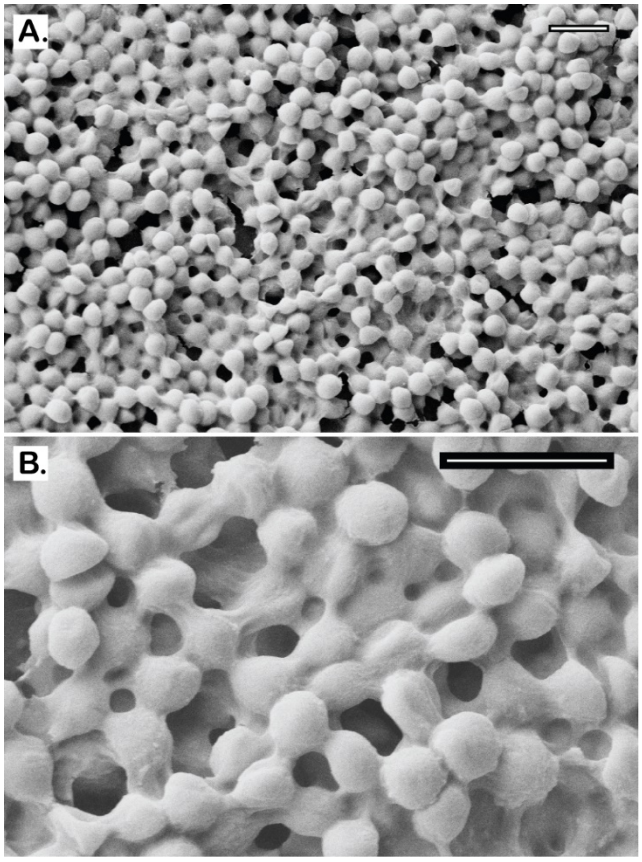


Figure 23. Scanning electron micrographs of MRSE 35984 biofilm. The intercellular matrices of EPS are captured as they wrap around every bacterium (A). At higher magnification, the EPS matrix is clearly shown to be sheltering the whole bacterial colony in an amorphous coat (B). Scale bars = 2 µm.

Efficacy of BPEI and β-lactams Against MRSE Biofilms

In our previous study, disabling PBP2a with 600-Da BPEI re-sensitizes MRSE to β-lactams.[1] Here, we investigated a combination of BPEI and β-lactam antibiotics (oxacillin and piperacillin) against biofilms formed by two MRSE strains, MRSE ATCC 35984™ and MRSE ATCC 29887™. The MICs of BPEI and the antibiotics

were found using the antimicrobial challenge plates, which measured the change in OD_{600} of planktonic bacteria. The results are consistent with our previously published study.[1] Sonication of the prongs into a recovery plate allows us to measure the MBEC values, which were found to be much higher than the corresponding MIC values. This illustrates the intrinsic resistance of biofilms. For MRSE 35984, the oxacillin MIC is 16 µg/mL, while the oxacillin MBEC is 512 µg/mL (Figure 24Aa). Likewise, for BPEI, the MIC is 8 µg/mL whereas the MBEC is 256 µg/mL (Figure 24Ab). Synergy occurs when an FICI is less than 0.5.[98] With the addition of 8 µg/mL of BPEI, a synergistic effect lowered the MBEC of oxacillin from 512 to 32 µg/mL (FICI = 0.19). Higher amounts of BPEI lowered oxacillin MBEC values further—for instance, 32 µg/mL of BPEI leads to an 8 µg/mL MBEC value for oxacillin (FICI = 0.28). For MRSE 29887, the piperacillin MIC is 512 µg/mL, and the BPEI MIC is 64 µg/mL (Figure 24Ba). Although the MBEC values for this strain were found to exceed 512 µg/mL (Figure 24Bb), synergy between 64 µg/mL piperacillin and 128 µg/mL BPEI (FICI = 0.19) eradicated the biofilms.

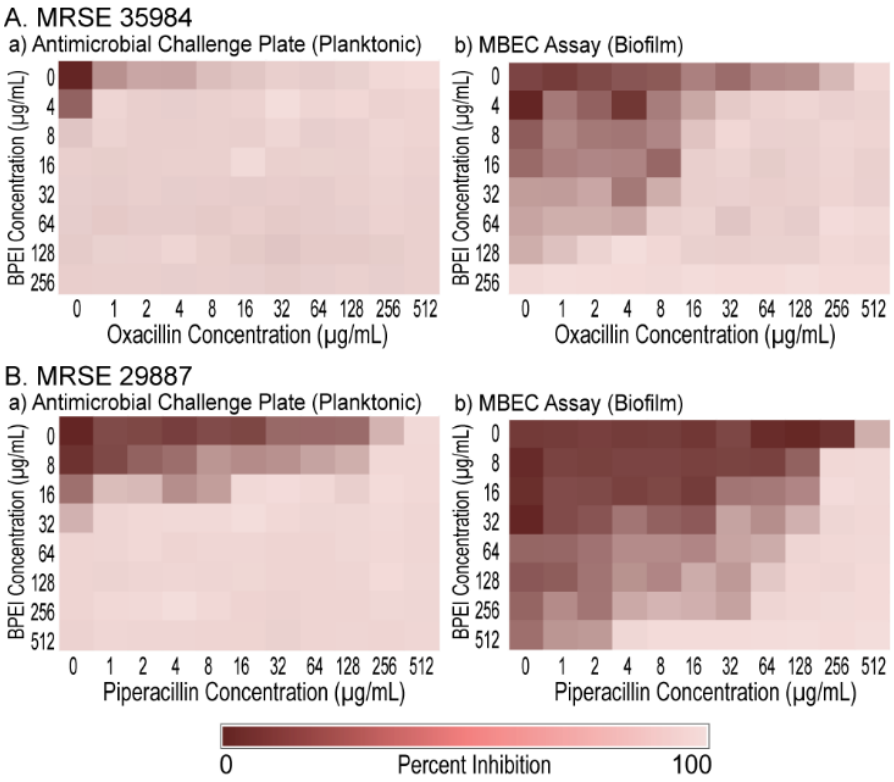


Figure 24. Synergistic effects of BPEI and antibiotics against MRSE 35984 (A) and MRSE 29887 (B) on a 96-well checkerboard pattern. The synergy was seen both on the planktonic challenge plates (A,a and B,a) and the biofilm MBEC assays (A,b and B,b).

BPEI Possesses Biofilm-Disrupting Potential

Antibiofilm activity of BPEI was supported by the biofilm disrupting assay (Figure 25). Established biofilms of MRSE 35984 were stained with crystal violet and then treated with 32, 64, 128, and 256 µg/mL of 600-Da BPEI. A negative control (0 µg/mL BPEI) and a positive control (acetic acid) were also performed. After 20 hours of treatment, BPEI-treated data was compared with the negative control using Student's t-test, and the results indicated that the MRSE biofilms were significantly dissolved by 600-Da BPEI ($n = 10$, *p-value* < 0.01). The dissolved biofilm solutions were carefully transferred to a new plate (without touching the bottom of the wells) for OD_{550}

measurement. As shown in Figure 25A, MRSE biofilm remained intact in the bottom of the negative control well, while the biofilm in the 32 and 64 µg/mL BPEI-treated wells were partially dissolved into solution. Biofilms treated with 128 and 256 µg/mL BPEI were completely dissolved, as was the biofilm treated with the positive control of acetic acid. Figure 25B shows the OD_{550} values of the crystal violet absorbance, which represent the amount of biofilm dissolved in each treatment.

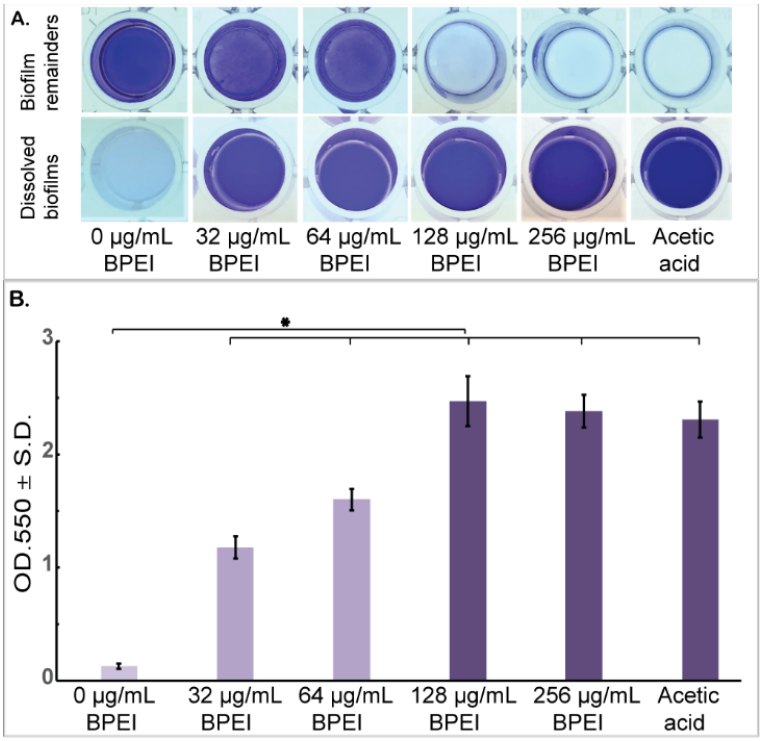


Figure 25. Established MRSE 35984 biofilms stained with crystal violet were treated with 600-Da BPEI for 20 hours, as well as the negative and positive controls. The dissolved biofilm solutions were transferred to a new plate, and the biofilm remainders are shown as top-down view, (A). The mean OD_{550} of the dissolved biofilms was measured, (B). Error bars denote standard deviation (*n = 10*). The MRSE biofilms were

significantly dissolved by 600-Da BPEI (*t-Test*, *p-value* < 0.01, significant difference between the negative control and each treatment is indicated with an asterisk).

A similar experiment was conducted using 10,000-Da BPEI (Figure 26). As with 600-Da BPEI, the t-test indicated that 10,000-Da BPEI dissolved MRSE biofilms (n = 10, *p-value* < 0.01). Greater biofilm disruption effects were seen at 64 µg/mL of 10,000-Da BPEI-treated samples (OD_{550} = 2.60, Figure 26B) than at 64 µg/mL of 600-Da BPEI treated samples (OD_{550} = 1.59, Figure 25B). According to Wiegand et al., even though high molecular weight BPEIs (over 25 000 Da) are toxic, 600 Da BPEI has high biocompatibility and a low likelihood for mutagenesis.[107] We have been able to confirm these observations using *in vitro* nephrotoxicity assay. Furthermore, 600 Da BPEI is not toxic toward colon, kidney, and HeLa cells unless the concentration is orders-of-magnitude higher than the amount required for potentiation.[45, 68] These factors suggest that a combination treatment for biofilms of bacteria with or without antibiotic resistance could be accomplished with antibiotics given topically, orally, or intravenously while BPEI potentiators are administered topically. Using BPEI in this manner would disable biofilms and resistance mechanisms while lowering concerns of BPEI toxicity. Additional work is required to measure the transdermal flux and determine if toxic levels of 600 Da BPEI can reach the dermal and subcutaneous skin layers and thereby conceivably reach the bloodstream.

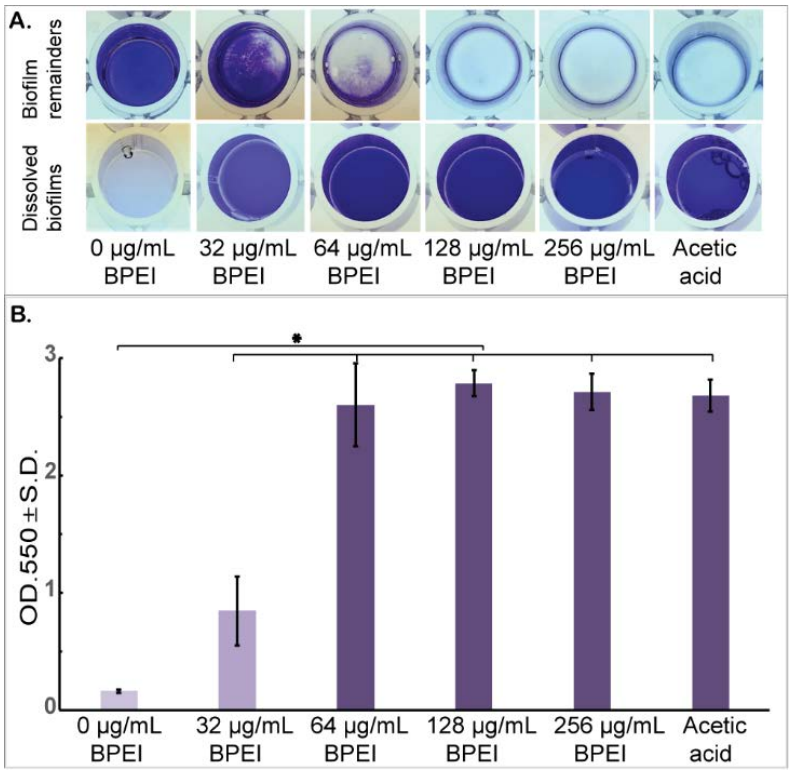


Figure 26. Established MRSE 35984 biofilms stained with crystal violet were treated with 10,000-Da BPEI for 20 hours, as well as the negative and positive controls. The dissolved biofilm solutions were transferred to a new plate, and the biofilm remainders are shown as top-down view, (A). The mean OD_{550} of the dissolved biofilms was measured, (B). Error bars denote standard deviation (*n = 10*). The MRSE biofilms were significantly dissolved by 10,000-Da BPEI (*t-Test*, *p-value* < 0.01, significant difference between the negative control and each treatment is indicated with an asterisk).

Biofilm Inhibition and Eradication Using Combination of BPEI + β-Lactams

Crystal violet assays were used to demonstrate that BPEI synergizes with piperacillin to inhibit MRSE biofilm formation. This assay is similar to the checkerboard assay used in our previous study.[1] However, we tested the antibiofilm activity instead of the MICs, so a modified procedure was used. Twenty-four hours after

inoculation in a 96-well checkerboard plate containing combinations of 600-Da BPEI and piperacillin, the cell suspension supernatant was discarded, leaving the attached biofilms, which were then stained with crystal violet for measurement at OD_{550} to quantify the remaining biomass. The Minimum Biofilm Inhibitory Concentration (MBIC) of BPEI was found to be 64 µg/mL, and the MBIC of piperacillin was 64 µg/mL. As shown in Figure 27, less biofilm formed in BPEI + piperacillin combination wells than in the piperacillin wells. Additionally, higher concentrations of BPEI corresponded to greater inhibition of biofilm formation. For example, 8 µg/mL of BPEI and 16 µg/mL of piperacillin prevented biofilm growth, however 16 µg/mL of BPEI also prevented biofilm growth when combined with 8 µg/mL of piperacillin. These results confirm that 600-Da BPEI possesses inhibitory activity against MRSE biofilms.

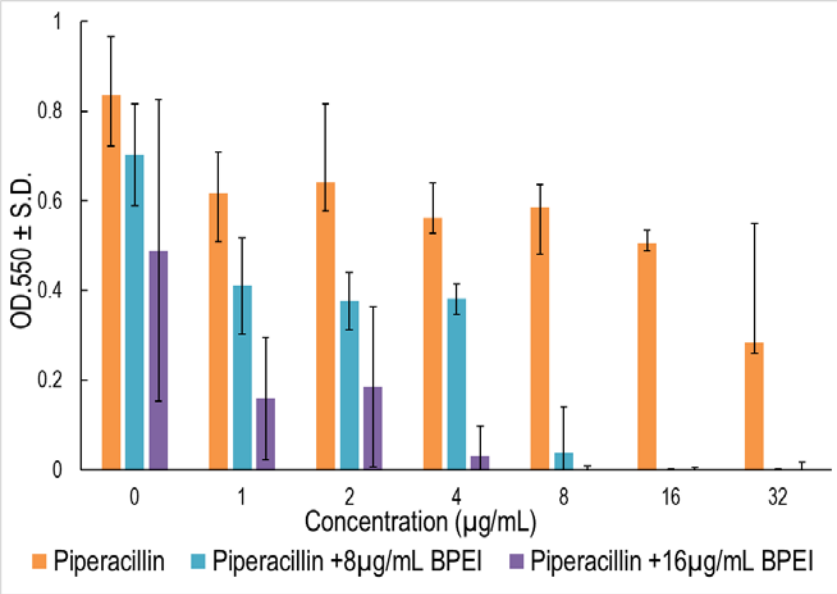


Figure 27. Crystal violet absorbance represents MRSE 35984 biofilm biomass. Strong antibiofilm formation synergy between BPEI and piperacillin was observed, compared

to individual piperacillin or BPEI treated samples. Error bars denote standard deviation (*n = 3*). PIP, piperacillin.

No antibiotic currently on the market can eradicate pathogenic biofilms, but the combination treatment of BPEI + oxacillin showed promise. Established biofilms of MRSE 35984 were treated in four different groups: Untreated control, BPEI-treated, oxacillin-treated, and combination (BPEI + oxacillin)-treated. A kill curve was generated to compare the antibiofilm activities of the treatments (Figure 28). Before treatment, all four groups had the same cell density of approximately 10^5 CFU/mL of bacteria. After treatments, the cell densities of each treated group were monitored by serial-diluting and agar-plating the sonicated prongs. Neither BPEI-treated nor oxacillin-treated groups could eradicate the biofilms, though they did inhibit the rate of the bacterial growth compared to the untreated control. At time 24 hours, cell densities were ~10^7 CFU/mL in the control group, ~10^5 CFU/mL in the BPEI-treated group, and ~10^3 CFU/mL in the oxacillin-treated groups. Since implantable medical devices have ample surface area for bacterial colonization, even a low bacterial inoculum (~10^2 CFU/mL *S. aureus*[108]) can provoke an infection. Oxacillin did eradicate some biofilm—as indicated by its declining kill curve in Figure 28—but the remaining persister bacteria within the biofilm on the treated prongs (>10^3 CFU/mL at 24 hours) are sufficient to grow and spread to new niches. Compared to the control group at time 24 hours (~10^7 CFU/mL), the combination treatment of BPEI + oxacillin reduced the cell density of the biofilms by 100,000-fold (<10^1 CFU/mL), illustrating the combination's potential to eradicate biofilms.

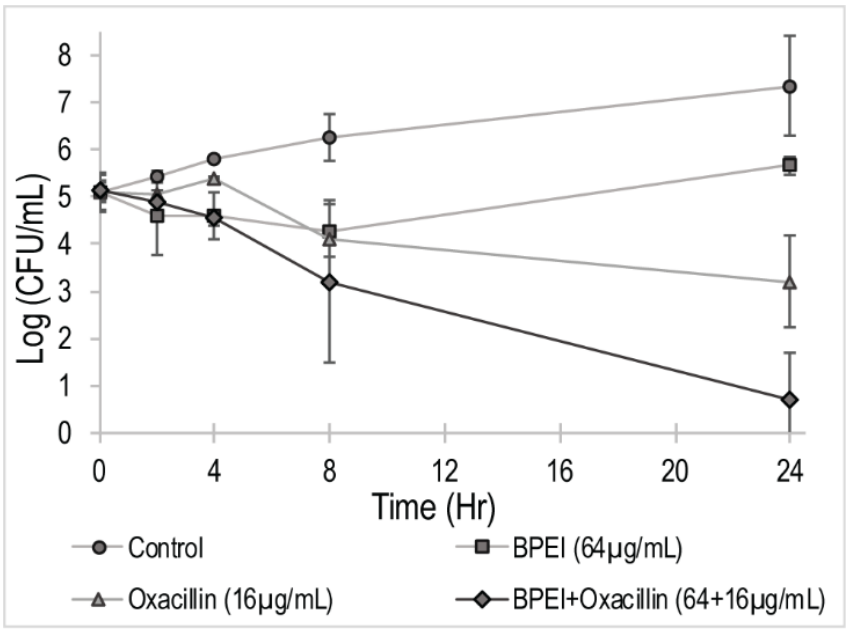


Figure 28. Biofilm kill curve of MRSE 35984. Only the combination treatment of BPEI+oxacillin (64 µg/mL + 16 µg/mL) – the diamond-curve – could eradicate MRSE 35984 biofilms. Error bars denote standard deviation (*n = 2*). CFU, colonies forming units.

Efficacy of BPEI on 3-Day-Old Biofilms

To test our technology against a more realistic chronic wound model, we qualitatively investigated BPEI's effects on a 3-day-old MRSE biofilm. MRSE 35984 was grown on the MBEC device for 3 days prior to treatment. Then, the untreated control and the BPEI-treated (512 µg/mL) samples were fixed and imaged for microscopic analysis. As shown in Figure 29, the untreated MRSE biofilms were thick, and encased in EPS (Figure 29A), and they densely occupied the entire prong surface (Figure 29C). In contrast, after BPEI treatment, the EPS coat was visibly disrupted which reveal the bacterial cells with a thin or non-existent EPS coating (Figure 29B), and a greater proportion of the prong surface was exposed (Figure 29D). These results

indicate that BPEI not only can effectively potentiate antibiotics against planktonic cells, but also against the established biofilms through an EPS-disruption mechanism. The exposure of the individual cells without the EPS protection would make them more vulnerable to antimicrobial agents, increasing the likelihood of clinical treatment success against persistent pathogenic biofilms.

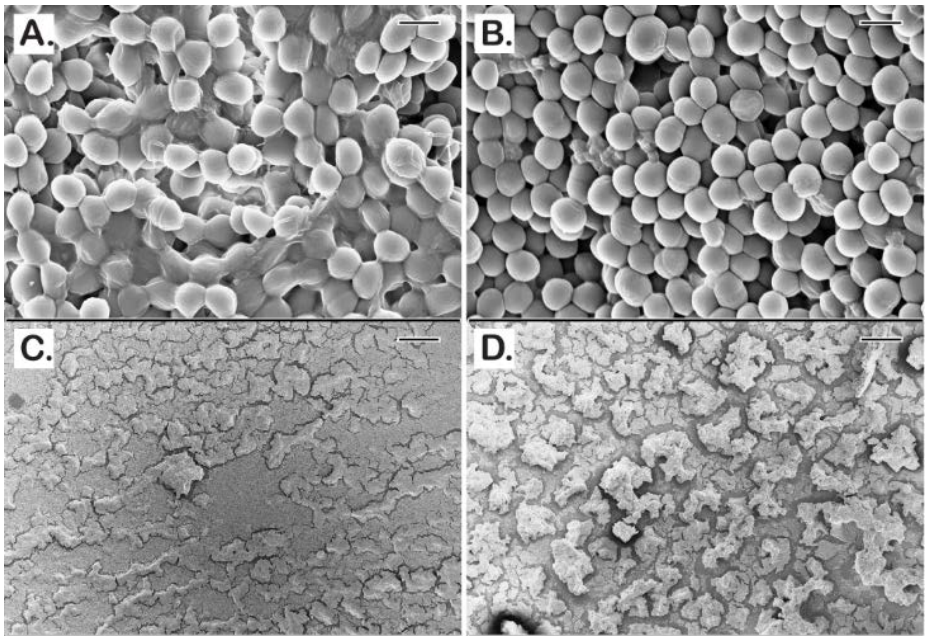


Figure 29. Scanning electron micrographs of established MRSE 35984 biofilms (3-day old). The untreated control sample shows thick EPS enfolding every bacterial cell (A). BPEI-treated sample shows disrupted EPS and significant number of exposed cells without the EPS (B). At lower magnification, the untreated control (C) biofilms appear with full and tightly occupied biofilms, while the BPEI-treated sample (D) shows disjointed biofilms by many revealed surfaces. Scale bars (A and B) = 1 μm. Scale bars (C and D) = 100 μm.

Many studies have tested cationic agents against pathogenic biofilms. In one study, Bottcher *et al*. used norspermidine, a natural trigger for *Bacillus subtilis* biofilm

disassembly, to synthesize mimetic cationic compounds. Their compounds were able to disrupt established biofilms of *B. subtilis* and *S. aureus.* A library of synthetic guanidine and biguanidine polyamines were shown to inhibit biofilm formation although few were able to disrupt established biofilms.[109] Our approach to biofilm treatment is unique because BPEI, a small macromolecule, can be a biofilm inhibitor and disruptor against not only the susceptible strains but also the resistant staphylococcal strains with the added benefit of disabling antimicrobial resistance mechanisms of planktonic cells. As a dual-function potentiator, 600-Da BPEI is a more powerful and versatile therapeutic agent than other cationic polymers.

Conclusions

According to the Centers for Disease Control and Prevention, most human bacterial infections involve biofilm-producing pathogens from common diseases (such as periodontitis, chronic prostatitis, and cystic fibrosis), which can infect artificial protheses.[110] *Staphylococcus epidermidis* is the most prevalent microorganism isolated from CoNS infections of chronic wounds, medical device-related infections, and postoperative endophthalmitis.[91, 111] Eradicating established microbial biofilms remains a difficult endeavor in both research and clinical settings. EPS frustrates the therapeutic efficacy of almost every available antibiotic. High dosages of antibiotics can be toxic to the human body and often cause adverse side effects. Therefore, drug developers need to stock the arsenal with alternative approaches that eliminate biofilm infections without harming the body's natural defenses. Bacteria within a biofilm differ from their planktonic counterparts in a number of ways, including using the matrix of EPS, extracellular DNA, and extracellular WTA as barriers against antimicrobial agents.[31, 65-

[67, 112-118] By targeting WTA-mediated resistance in MRSA/MRSE, 600-Da BPEI acts as a dual-function potentiator that can improve wound care outcomes by restoring potency to existing antibiotics. Overall, the strong synergy between BPEI and β-lactam antibiotics make this combination a promising treatment for *S. epidermidis* biofilms because 600-Da BPEI's *in vitro* cytotoxicity is low,[45, 68] and lower antibiotic concentrations reduce adverse side effects. Future experiments will be conducted to elucidate the antibiofilm mechanism of our combination therapy and to test our technology against more virulent superbugs. With the evolution of microorganisms outpacing our development of new drugs, it is imperative that different strategies are developed and implemented quickly. Hopefully, our approach will mark a turning point in the ongoing battle against MRSE biofilms.

Chapter 5: BPEI potentiates ampicillin against MRSA biofilms

Background

Methicillin-resistant *Staphylococcus aureus* (MRSA) infections pose a serious threat worldwide. MRSA is the predominant species isolated from medical-device-related biofilm infections and chronic wounds. Its ability to form biofilms grants it resistance to almost all antibiotics on the market. Answering the call for alternative treatments, our lab has been investigating the efficacy of 600 Da branched polyethylenimine (BPEI) as a β-lactam potentiator against bacterial biofilms. Our previous study showed promise against methicillin-resistant *Staphylococcus epidermidis* biofilms. This study extends our previous findings to eradicate a more virulent pathogen – MRSA biofilms. Microtiter minimum biofilm eradication concentration models, crystal violet assays, and electron microscopy images show synergistic effects between BPEI and ampicillin as a two-step mechanism: step one is the removal of the extracellular polymeric substances (EPS) to expose individual bacteria targets, and step two involves electrostatic interaction of BPEI with anionic teichoic acid in the cell wall to potentiate the antibiotic.

Prevalence and Pathogeneses

The threat posed by antimicrobial resistance (AMR) on human health is well known. We recently reported that 600-Da BPEI eliminates β-lactam resistance in methicillin-resistance *Staphylococcus aureus* (MRSA) by preventing the essential localization of PBP4 enzymes.[119] However, the sinister nature of AMR infections is amplified when the pathogens are sequestered in biofilms that shield them from effective antimicrobials and/or the innate immune system. According to a systematic review and

meta-analysis,[120] the prevalence of biofilms in chronic wounds is almost 80%. Many of the predominant species found in chronic wounds are from the genus *Staphylococcus* (~60%).[94] In addition to compromising wound healing,[121] *Staphylococcus aureus* contributes a high percentage to biomedical device infections.[65] Bacterial biofilms are resilient because their self-produced matrix of extracellular polymetric substances (EPS) grants them protection against host defenses and antibiotics.[92, 110, 117] The EPS matrix contains hydrated carbohydrate polymers, proteins, and extracellular DNA (eDNA) in a complex architecture to provide nutrients, promote the transfer of genetic material, and protect the biofilm against harsh conditions. Only the outer-most layers of cells in a biofilm are metabolically active, while the persistent inner-layer cells remain dormant, thereby evading antibiotics.[117] First-line β-lactam antibiotics , such as ampicillin, are the most commonly prescribed drugs for bacterial infections. In many developing countries, these antibiotics are sold over the counter, and their use in livestock is poorly regulated. Lack of regulation can lead to overexposure, thereby encouraging acquired antimicrobial resistance. As the most common agricultural pathogens in developing countries, AMR has a convenient means of spreading to humans.[13] According to the CDC, MRSA infections pose a grave threat to the society and economy.[122] One out of seven severe cases of MRSA results in death.[123] Its resistance has been documented within all available antibiotic classes, including the last-resort antibiotics.[15] With a dwindling collection of new antibiotics and in the absence of antibiofilm drugs on the market, alternative treatments that combine existing drugs with potentiators have become a central line of research. Here, we demonstrate the ability of 600 Da branched polyethylenimine (BPEI) to eradicate MRSA biofilms. Our previous studies have shown that this low-molecular-

weight BPEI exhibits low *in vitro* cytotoxicity on human cells,[45] and strong potentiation with β-lactam antibiotics against planktonic MRSA cells.[45, 68] Strong synergy was also found against methicillin-resistant *Staphylococcus epidermidis* (MRSE) and its biofilms.[1-2] Thus, we hypothesize that BPEI would potentiate ampicillin against MRSA biofilms using similar biochemical mechanisms.

Gram-positive bacteria, such as *S. aureus* and *S. epidermidis*, have a thick peptidoglycan layer in their cell walls. For each division cycle, penicillin-binding proteins (PBPs) are responsible for one of the last stages of cell wall synthesis: cross-linking the subunits of the peptidoglycan. β-lactam antibiotics irreversibly bind to PBPs, preventing them from performing this vital function. Consequently, the bacteria are unable to divide and eventually burst from excessive cytoplasmic pressure. However, in MRSA/MRSE, the enzymes PBP2a and PBP4 with low binding affinity to β-lactams allow the bacteria to withstand the antibiotic attack. An important regulator of PBP2a/4 is wall teichoic acid (WTA) that is decorated with *N*-acetylglucosamine, *D*-alanine, and hydroxyl on a phosphodiester backbone.[61, 124] The phosphates impart strong anionic properties to WTA and consequently WTA attracts essential metal ions to the cell wall environment.[40, 125-128] However, we have shown that the anionic nature of WTA can be exploited to circumvent the PBP2a/4 enzymes responsible for β-lactam resistance in MRSA. 600-Da BPEI, a small cationic polymer, electrostatically binds to anionic WTA in the bacterial cell wall, thus prohibiting WTA from properly localizing PBP2a/4 enzymes. This process effectively potentiates β-lactams against planktonic MRSA[45, 68, 119] and MRSE.[1-2] As described below, we extend the investigation of 600-Da BPEI potentiators to MRSA biofilms and demonstrate strong efficacy against two biofilm-forming MRSA clinical

isolates (MRSA OU6 and OU11) that are strongly resistant to antibiotics. (clinical data are shown in Table 4)

Table 4: MRSA clinical isolates susceptibility data

MRSA Clinical Isolate Data Collected at OUHSC Clinical Microbiology Laboratory								
			Clindamycn		Daptomycin		Erythromycin	
Isolate	Species	Methicillin Resistant	MIC	Interp	MIC	Interp	MIC	Interp
6	S. aureus	Y	R	>4	S	≤0.5	R	>4
11	S. aureus	Y	R	>4	S	≤0.5	R	>4
Isolate	Species	Methicillin Resistant	Gentamicin		Linezolid		Oxacillin	
6	S. aureus	Y	MIC	Interp	MIC	Interp	MIC	Interp
11	S. aureus	Y	S	≤4	S	2	R	>2
			S	≤4	S	2	R	>2
Isolate	Species	Methicillin Resistant	Tetracycline		Trimeth/Sulfa		Vancomycin	
6	S. aureus	Y	MIC	Interp	MIC	Interp	MIC	Interp
11	S. aureus	Y	S	≤4	S	≤0.5/9.5	S	2
			S	≤4	S	≤0.5/9.5	S	1
Unless otherwise indicated, identificaiton and susceptibility performed by								
	the Beckman Coulter MicroScan Walkaway 96plus using the PC33 gram positive panel							
*Presumed resistant/D test (inducible clindamycin resistance) positive								
^Species identification and oxacillin/methicillin Susceptibility/Resistance determined								
	by Verigene Gram Positive Blood Culture assay (probes for Genus/species and mecA)							

Purpose of Experiment

The purpose of this experiment is to determine the synergy of 600-Da BPEI and ampicillin against MRSA lab strains and MDR-*S. aureus* clinical isolates' biofilms.

Experimental Procedures

Materials:

In this experiment, the *Staphylococcus aureus* (MRSA 43300) was purchased from the American Type Culture Collection. Two MRSA clinical isolates (MRSA OU6 & OU11) from patient swabs were kindly provided by Dr. McCloskey from the University of Health Sciences Center with an institutional review board (IRB) approval. Chemicals (DMSO, growth media, and electron microscopy fixatives) were purchased from Sigma-Aldrich. Antibiotics (ampicillin and polymyxin B) were purchased from Gold Biotechnology. 600 Da BPEI was purchased from Polysciences. MBEC™ Biofilm Inoculators were purchased from Innovotech. Isopore polycarbonate membrane filters (0.1 μm pore size, hydrophilic, 13 mm diameter) were purchased from MilliporeSigma.

MBEC Assay

This method is adapted from our previous study.[2] In brief, bacterial culture was inoculated in an MBEC pronged-inoculator and incubated for 24 hr to allow *biofilm formation*. Then, the preformed biofilm prong lid was washed and treated in a separate *challenge plate* which was prepared as a checkerboard assay:[1] serial dilutions of BPEI and antibiotic solutions were added to a 96-well base plate with a total volume of 200 μL cation-adjusted Muller Hinton broth (MHB) per well. The change in optical density at 600 nm (Δ OD_{600}) was measured. Minimum inhibitory concentration (MIC) of each drug is determined as the lowest concentration that inhibited cell growth ($\Delta OD_{600} < 0.05$). Fractional inhibitory concentration index (FICI) was calculated as: $FICI = \frac{MIC_{AB}}{MIC_A} + \frac{MIC_{BA}}{MIC_B}$. Synergistic effects are determined using EUCAST guidelines: synergy (FICI ≤ 0.5), additivity (0.5 < FICI < 1), and indifference (FICI > 1).[62] The treated pronged-

inoculator was then washed and transferred to a *recovery plate* with 200 µL MHB/well to sonicate and recover any remaining biofilm bacteria. The recovery plate was then incubated overnight before measuring ΔOD_{600} to determine MBECs and FICIs of the drugs tested on the biofilms.

Biofilm Disrupting Assay

This method is also described in details by Lam et al.[2] This experiment was parallelly conducted with polymyxin B (PmB, a cationic polypeptide antibiotic) and BPEI. In short, an overnight MRSA OU 6 culture was inoculated in a tissue-culture treated 96-well plate (100 µL of tryptic soy broth or TSB/well) with an inoculation size of 1 µL/well (~5 x 10^5 CFU/mL). The plate was incubated at 35 ^oC for 24 hr to allow the bacteria to form biofilm. It was then washed with water to remove planktonic bacteria and stained with 100 µL of crystal violet solution (0.1%) per well for 15 min. The stained plate was washed excessively with water 5 times to remove any unbound stain and air-dried overnight. Vary concentrations of PmB (64 and 128 µg/mL) and 600 Da BPEI (64 and 128 µg/mL) were added to the stained-biofilm plate with a total volume of 100 µL/well. A negative control (water only) and positive control (30% acetic acid) were also conducted at the same time of treatment. After 20 hr, without touching the biofilm layer in the bottom of the plate, solubilized solution in each treated well was carefully transferred to a new 96-well plate for an OD_{550} measurement, which represents the corresponding amount of biofilm disrupted by each treatment.

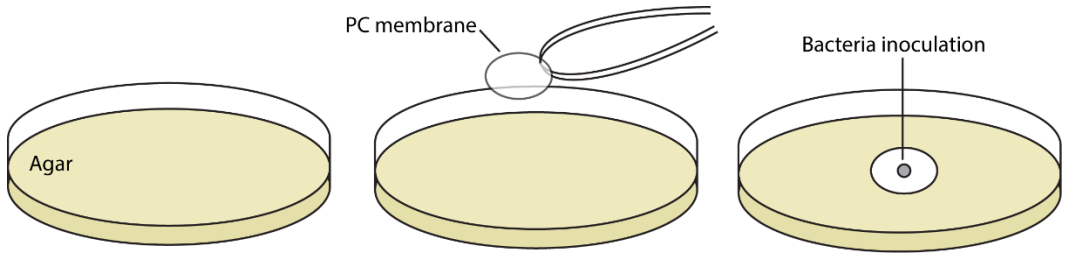
Scanning Electron Microscopy (SEM)

MRSA OU6 were inoculated from 0.5% of an overnight culture on glass coverslips and grown at 35 °C. After 24 hr. the biofilm-formed on glass coverslips were

carefully removed and washed in water for 10 s. Then each sample was submerged in different treated solution (untreated control, 128 µg/mL BPEI-treated, and bleach-positive control) for another 24 hr. Next, they were removed, washed in water for 10 s, and submerged in primary fixative (5% glutaraldehyde in 0.1 M cacodylate buffer) and incubated at 4 ± 2 °C for 2 days. The glass coverslips were removed from the fixing solution and air-dried for 72 hr. They were mounted on aluminum stubs with carbon tape and sputter-coated with AuPd. A Zeiss NEON SEM was used to image the samples at 5 kV accelerating voltage.

SEM of Biofilms on Polycarbonate Membrane Filters

Pre-sterilized polycarbonate (PC) membranes were gently adhered to a tryptic soy agar plate using sterilized forceps. A volume of 2 µL of the stock MRSA OU6 solution (~5 x 10^5 CFU/mL) was pipetted on top of each PC membrane and incubated at 35 °C for 7-8 hr, when the MRSA biofilm colony on the PC membranes became visible to the naked eye.



The PC membranes with preformed biofilm was then carefully removed off the agar, transferred into a treatment solution of 256 µg/mL BPEI, and incubated for another 20 hr. Untreated and treated PC samples were removed and washed in water for 10 s. They were submerged in primary fixative (5% glutaraldehyde in 0.1 M cacodylate buffer) and incubated at 4 ± 2 °C for 2 days. The PC samples were air-dried slowly for 3 more days.

They were mounted on aluminum stubs with double-side carbon tape, sputter-coated with AuPd, and imaged at 5 kV accelerating voltage by a Zeiss Neon SEM.

Results and Discussion

Minimum biofilm eradication concentration (MBEC) assays were utilized on the two clinical isolates of MRSA (OU6 and OU11) and a lab strain MRSA ATCC 43300. The MRSA bacteria are used to inoculate a 96-well inoculation plate, where MRSA biofilms were grown on prongs protruding from the plate lid, known as the MBEC inoculator lid and based on the Calgary biofilm device. The inoculator lid was washed to remove unattached MRSA cells and transferred into a separate 96-well base for treatment with BPEI and ampicillin combinations arranged in a checkerboard assay pattern, the so-called the challenge plate. The final step is moving the treated inoculation lid to a third plate (the recovery plate) containing growth-media only and using sonication to dislodge the biofilm and recover cells remaining in the biofilm. In this manner, we are able to evaluate the synergy of BPEI and ampicillin against MRSA biofilms. Standard CLSI (Clinical & Laboratory Standards Institute) guidelines describe a standard MIC assay using 96-well plates inoculated with a standard cell density, usually ~10^6 CFU/mL. However, the MIC data reported here is non-standard because, rather than inoculation via micropipette transfer from an overnight culture, inoculation of the challenge plate occurs from the biofilm-coated inoculation lid where treatment challenge disrupts the protective biofilm EPS matrix. MRSA cells are dislodged and dispersed into the challenge plate media. These cells in the challenge plate media are susceptible to killing by the 600-Da BPEI, ampicillin, or their combinations and a minimum inhibitory concentration can be determined. We refer to this value as MIC_{CP} to differentiate it from MIC measurements

made with standard methods. The MBEC is determined from cell growth in the recovery plate and reflects the ability of 600-Da BPEI, ampicillin, or its combinations to kill the biofilm remaining attached to the prongs of the inoculation lid. The MIC_{CP} and MBEC data are shown for comparison (Table 5).

Table 5. Synergistic effects between BPEI and ampicillin against MRSA biofilms

Strain	BPEI (μg/mL)		Ampicillin (μg/mL)			FICI	Synergy?
	MIC_{CP}	MBEC	MIC_{CP}	MBEC	MBEC + 64 μg/mL BPEI		
MRSA 43300	64	>256	128	>256	2	0.13	yes
MRSA OU6	>256	>256	256	>256	64	0.25	yes
MRSA OU11	>256	>256	128	>256	32	0.19	yes

As shown in Table 5, MRSA 43300s BPEI MBEC (>256 μg/mL) is much larger than its MIC_{CP} (64 μg/mL). Similarly, the ampicillin MBEC (>256 μg/mL) is higher than the corresponding MIC_{CP} (128 μg/mL). The MBECs for BPEI and ampicillin against the two clinical isolates, MRSA OU6 and OU11, are greater than the highest amount tested, 256 μg/mL. Although the MBECs exceeded the tested concentrations, strong synergy (FICI < 0.5) was found between BPEI and ampicillin against the biofilms of MRSA 43300, OU11, and OU6 with an FICI of 0.13, 0.25, and 0.19, respectively. For example, when combined with 64 μg/mL of BPEI, the ampicillin MBECs for MRSA 43300, OU6, and OU11 were reduced to 2, 64, and 32 μg/mL, respectively. For these strains, the MIC_{CP} is higher than previously reported values for planktonic MRSA cells evaluated with CLSI methods,[119] which showed that 600-Da BPEI lowers the MIC for the planktonic cells and renders them susceptible to oxacillin. As described above, the disparity arises from different methods of inoculation and the cell density in the challenge plate media is

unknown and likely varies between wells. Nevertheless, the MIC_{CP} can be used to show that BPEI and ampicillin combinations can be used to kill antibiotic-resistant cells dislodged from the inoculation lid.

Heatmaps of the average checkerboard results are shown in Figure 30. Data used to determine MIC_{CP} in the challenge plate containing MRSA planktonic data are shown on the left (Figure 30Ai, Bi, and Ci) and the corresponding biofilm data are on the right (Figure 30Aii, Bii, and Cii). As expected, the MBECs are larger than the respective MIC_{CP} values. This demonstrates the intrinsic protective nature of biofilms against antimicrobial agents. The stair-case pattern found in the heatmaps indicate synergy of BPEI and ampicillin against both planktonic and biofilm forms of MRSA 43300, OU6, and OU11 strains. As BPEI concentration increases, the required MIC_{CP} and MBEC values of ampicillin decrease to achieve high inhibition percentage, highlighting the potentiating ability of BPEI against pathogenic biofilms.

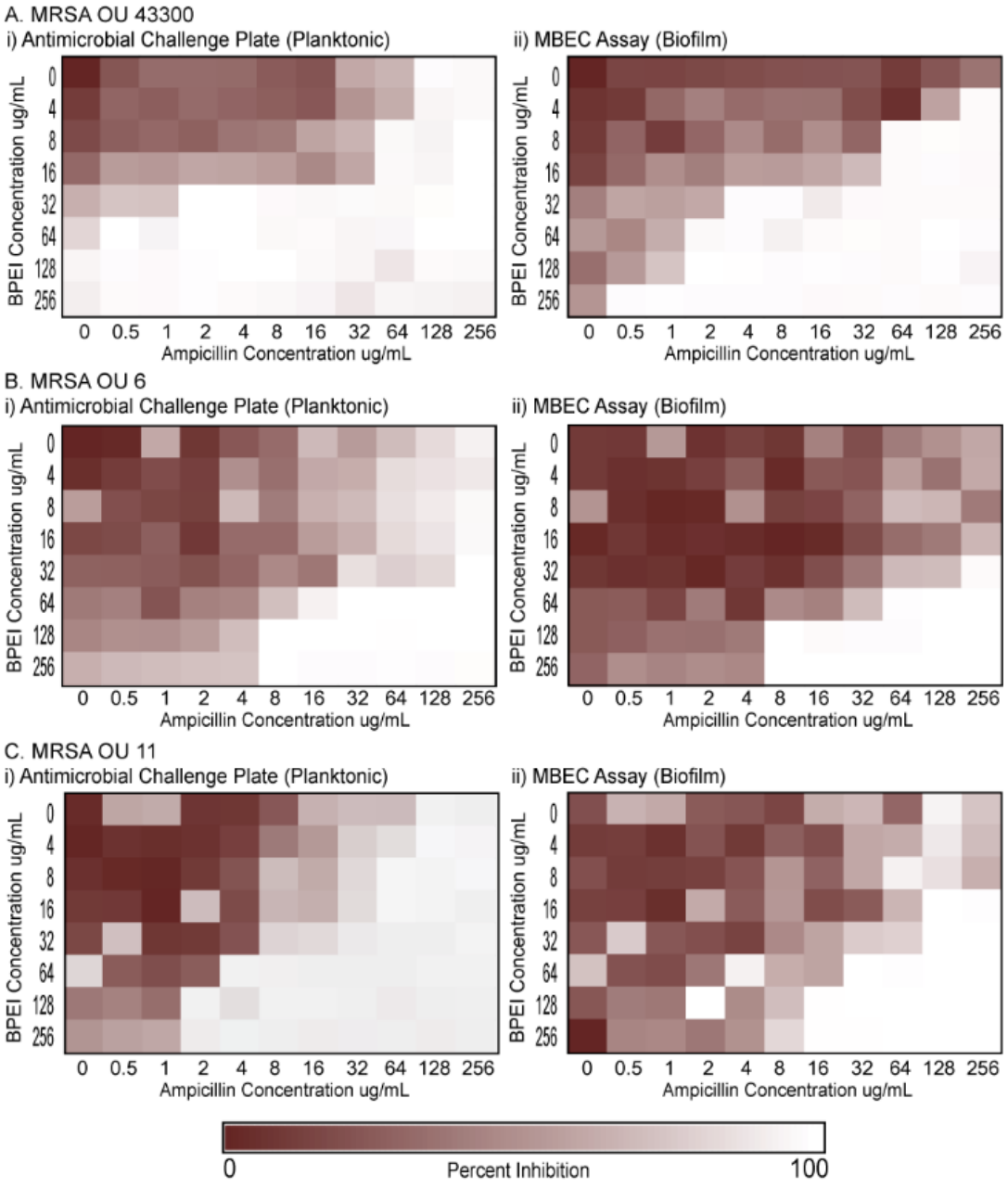


Figure 30. Synergy between BPEI and ampicillin against MRSA 43300 (A), MRSA OU6 (B), and MRSA OU11 (C). Checkerboard assay data on planktonic bacteria are shown on the left (Ai, Bi, and Ci), and corresponding biofilm data are shown on the right (Aii, Bii, and Cii).

To better elucidate the antibiofilm activity of BPEI, biofilm disruption assays were conducted along with a comparison study using the common cationic antibiotic polymyxin B. Briefly, MRSA OU6 biofilms were grown on the bottom of a 96-well plate for 24 h. After repeated washing, the biofilms were stained with crystal violet for semiquantitative analysis. The biofilms were then treated to investigate the ability of BPEI or polymyxin-B to disrupt the biofilm. As shown in Figure 31, the negative control of water only had no impact on disrupting the MRSA biofilms because the biofilm layer remained intact in the bottom (top-down photographic image in Figure 31A). On the other hand, 600 Da BPEI (64 and 128 μg/mL) completely dispersed the MRSA biofilms into its solution in a manner similar to that of the positive control, acetic acid. However, exposure to polymyxin B, a U.S. Food and Drug Administration (FDA)-approved cationic polypeptide antibiotic, resulted in a slight dissolution in biomass, although 128 μg/mL was more effective than 64 μg/mL. The biofilm-disrupting properties are quantitatively reported as OD550 measurements of the amount of biofilm dislodged (Figure 31B). This demonstrates BPEI's ability to eradicate MRSA biofilms by forcing them to detach and disperse its bacterial cells into planktonic culture, where they transition from a persistent quiescent state into a metabolically active realm and thus become vulnerable to antibiotics.

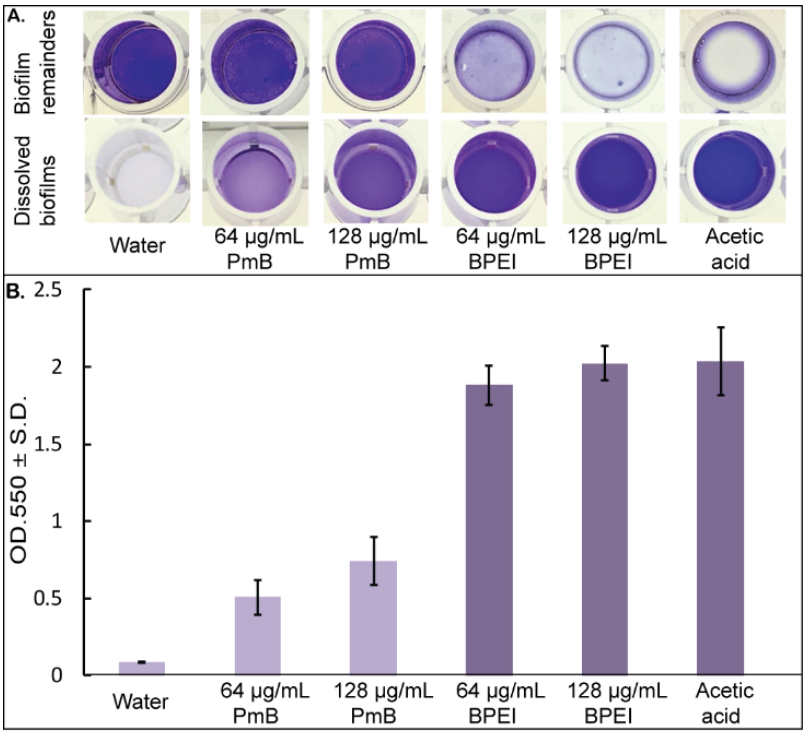


Figure 31. Established MRSA OU6 biofilms stained with crystal violet were treated with polymyxin B (PmB) and 600 Da BPEI for 20 hours, as well as the negative control (water only) and positive control (30% acetic acid). The dissolved biofilm solutions were transferred to a new plate, and the biofilm remainders are shown as top-down view, (A). The mean OD_{550} of the dissolved biofilm solution was measured, (B). Error bars denote standard deviation (*n = 10*).

To better characterize the effect of BPEI on MRSA biofilms, morphological analysis was performed using scanning electron microscopy (SEM). Twenty-four hr-established MRSA biofilms on glass coverslips were treated with 128 µg/mL of BPEI. An untreated control and the BPEI-treated samples were then fixed and imaged with SEM. As shown in Figure 32A and 32C, the untreated control MRSA biofilm is enclosed in a thick coat of EPS. Like all biofilm-forming bacteria, the EPS is their self-made protection against harsh environments and antibiotics. With BPEI treatment, the

preformed MRSA biofilm lost most of its EPS coat (Figure 32B). At higher magnification (Figure 32D), the lack of EPS in the treated sample rendered the inner layers of the bacteria—which were hidden in the untreated control—visible. To mimic a wound environment, MRSA biofilms were grown on polycarbonate (PC) membrane filters (0.1 µm pore size) placed directly only tryptic soy agar. The membrane pores allow for nutrient absorption and we found that these biofilms are more robust than those grown on glass slides. In the untreated control sample (Figure 33A), the EPS is so thick that the SEM scan cannot locate the bottom of the PC membrane filter. In BPEI-treated sample (Figure 33B), many areas are exposed from the absence of EPS, including the bottom surface of the membrane filter whose nano-size pores (tiny white dots through the crack in Figure 33B) are clearly visible.

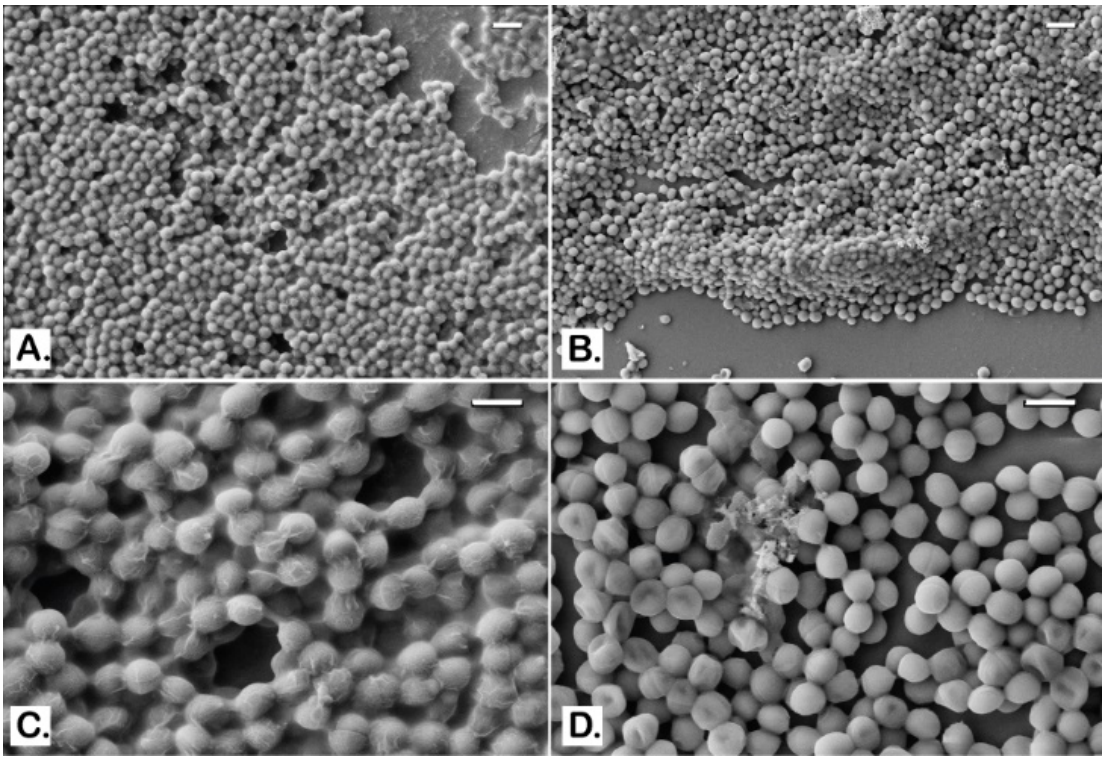


Figure 32. SEM images of MRSA OU11 biofilms on glass coverslips. Untreated control biofilms are shown to be covered and wrapped around in the matrix of EPS (A and C).

BPEI-treated samples have much less EPS with many cells being exposed (B and D). Scale bars in A and B = 2 μm. Scale bars in C and D = 1 μm.

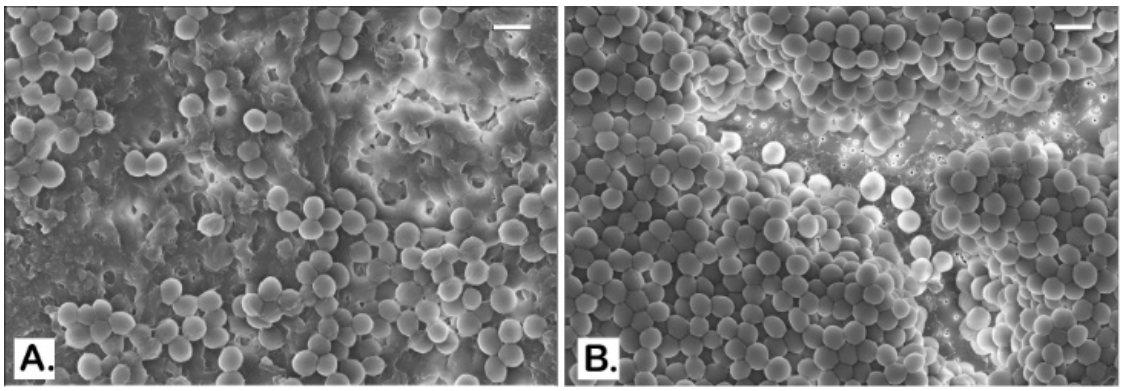


Figure 33. SEM images of established MRSA OU6 biofilms on PC membranes. Very thick coat of the EPS matrix is present in the untreated control biofilm on the PC membrane which also blocks the bacterial cells from being captured in the microscope (A). BPEI-treated sample has a much clearer view as the EPS removed and even the membrane surface is exposed as many nano-size pores are seen at the bottom (B). Scale bars in A and B = 1 μm.

The biofilm EPS of *S. aureus* contains a high fraction of polysaccharide intracellular adhesin (PIA) and anionic species that are prime targets for 600 Da BPEI binding, such as eDNA and extracellular teichoic acid (TA). The latter is a key component in the biofilm EPS matrix of *S. epidermidis*[31] and *S. aureus*.[117, 129] It enhances bacterial adhesion to biotic and artificial surfaces, which is the first step of biofilm formation. TA has a negative net charge at neutral pH because it contains more negatively-charged phosphates than positively-charged D-alanine residues.[129] Using nuclear magnetic resonance spectroscopy, we found that 600-Da BPEI electrostatically binds wall teichoic acid, which indirectly hinders the resistance factor PBP2a/4.[68] Similarly, BPEI most likely binds extracellular TA in the EPS matrix, and also eDNA, to disrupt biofilm

structural integrity, as seen in Figure 32 and 33. The exposure of individual bacteria could enhance their contact with various drugs and components of the immune system.

Conclusion

Skin or soft-tissue infections (SSTIs) arise from abrasions, nonsurgical wounds, burns, or chronic health problems.[130] For chronic wound infections associated with MRSA and its biofilm, treatment options are scarce. Patients afflicted with these chronic wounds suffer from physical pain and disabilities in addition to psychological and emotional stresses and poor quality of life. Current inpatient treatments include cleansing, debridement, maintaining a moist tissue environment, and, when possible, eliminating the underlying pathology or factors that contribute to poor wound healing.[131] In advanced cases, amputation may become necessary. Death, especially in elderly patients, may result from sepsis that can be associated with chronic wounds. Antibiotics can be used effectively against susceptible infections. For drug-resistant infections, the best practices for effective inpatient intervention are strict sanitary guidelines and antibiotics, such as intravenous vancomycin plus piperacillin/tazobactam or IV treatment with new antibiotics of last resort.[131] Nevertheless, biofilms and antimicrobial resistance create substantial technological barriers to treating chronic wound infections. This presents a significant and critical need for a way to counteract biofilms and antimicrobial resistance. The 600 Da BPEI is a dual-function potentiator because it disrupts biofilms that are otherwise impenetrable to antibiotics, and also it counteracts β-lactam resistance mechanisms in MRSA However, success requires that 600 Da BPEI have low toxicity. In dermal applications, low-molecular-weight BPEI was shown to have high biocompatibility and low genotoxic potential.[107] We also confirmed the non-cytotoxicity

of 600 Da BPEI toward human kidney, colon, and HeLa cells by using in vitro nephrotoxicity assays.[45, 68] Additional experiments are planned to determine 600 Da BPEI's toxicity levels in dermal and subcutaneous layers. With bacterial evolution outpacing the discovery of antimicrobial agents, it is imperative to seek alternative treatments options, such as coupling existing drugs with potentiators. With a dual-function mechanism that eliminates antibiotic efficacy barriers in both planktonic and biofilm-encased bacteria, 600 Da BPEI has promise as a therapeutic agent for improving wound care and combating medical device infections. Potency of first-line antibiotics such as ampicillin can now be restored by the addition of BPEI against drug-resistant MRSA, as seen by their strong synergistic effects. Combinations of BPEI and antibiotics could be administered to diagnosed or suspected staph-biofilm infections, which would improve the efficacy of treatment of resistant, biofilm-forming pathogens.

Chapter 6: Broadening the spectrum of antibiotics capable of killing multidrug-resistant *Staphylococcus aureus* and *Pseudomonas aeruginosa*

Background

Infections from drug-resistant superbugs, such as methicillin-resistant *Staphylococcus aureus* (MRSA) and *Pseudomonas aeruginosa* are a serious threat because reduced antibiotic efficacy complicates treatment decisions and prolongs the disease state in many patients. To expand the arsenal of treatments against antimicrobial resistance (AR) pathogens, 600-Da branched polyethylenimine (BPEI) can overcome antibiotic resistance mechanisms and potentiate β-lactam antibiotics against Gram-positive bacteria. BPEI binds cell wall teichoic acids and disables resistance factors from penicillin binding proteins PBP2a and PBP4. The present study describes a new mechanism of action for BPEI potentiation of antibiotics generally regarded as agents effective against Gram-positive pathogens but not Gram-negative bacteria. 600-Da BPEI is able to reduce the barriers to drug influx and facilitate the uptake of a non-β-lactam co-drug, erythromycin, that targets the intracellular machinery. Also, BPEI can suppress cytokine interleukin IL-8 release from human epithelial keratinocytes. This enables BPEI to function as a broad-spectrum antibiotic potentiator which expands the opportunities to improve drug design, antibiotic development, and therapeutic approaches against pathogenic bacteria, especially for wound care. This study was published in ChemMedChem Journal.[3]

Bacterial Membranes and The Non-β-Lactam Antibiotics

Crossing the bacterial membrane is a difficult task for many antimicrobial drugs that must reach their intracellular targets of Gram-positive and Gram-negative bacteria. Improving antibiotic efficacy can be accomplished with potentiation adjuvants comprising a vast array of different compounds and targets.[132-140] A common theme is weakening the cell envelope framework. The outermost portions of the cell envelope of Gram-negative and Gram-positive bacterial pathogens are under exploited weaknesses in antimicrobial resistance mechanisms.[61, 141-144] Many efforts are focused on inhibitors to the cytoplasmic expression and/or the membrane translocation of essential proteins, enzymes, and precursors required for the assembly of molecules required for the cell-envelope machinery and architecture. These approaches may suffer from deleterious protein binding effects or have low solubility from hydrophobic properties necessary to cross the membrane barriers. Likewise, methods to overcome resistance are different depending on whether the pathogen is a Gram-positive or Gram-negative bacterium.

The divergent approaches to overcome resistance arise from the intrinsic nature of bacterial cell walls and their differing mechanisms of antibiotic resistance. The cytoplasm of Gram-positive bacterial cells is surrounded by a single phospholipid bilayer and this membrane is surrounded by a thick layer of peptidoglycan interlaced with anionic teichoic acids. However, the phospholipid membrane of Gram-negative bacteria is encased by a periplasm region that contains a thin peptidoglycan layer attached to an asymmetric outer membrane bilayer (Figure 34). The inner leaflet of the outer member contains phospholipids, but the outer leaflet contains lipopolysaccharides. Together, these layers comprise a formidable barrier to the influx and/or diffusion of

antibiotics into the periplasm and cytoplasm to reach their drug targets. Approaches to disable resistance from β-lactamase enzymes and efflux pumps, such as using inhibitors, are often tailored for Gram-negative bacteria, such as multi-drug resistant *Pseudomonas aeruginosa* (MDR-PA), and rarely work against Gram-positive bacteria that lack these primary resistance mechanisms. Resistance in Gram-positive bacteria, for example methicillin-resistant *Staphylococcus aureus* (MRSA), is dominated by alternative means to continue the assembly and synthesis of peptidoglycan; thereby bypassing the activity of β-lactams.

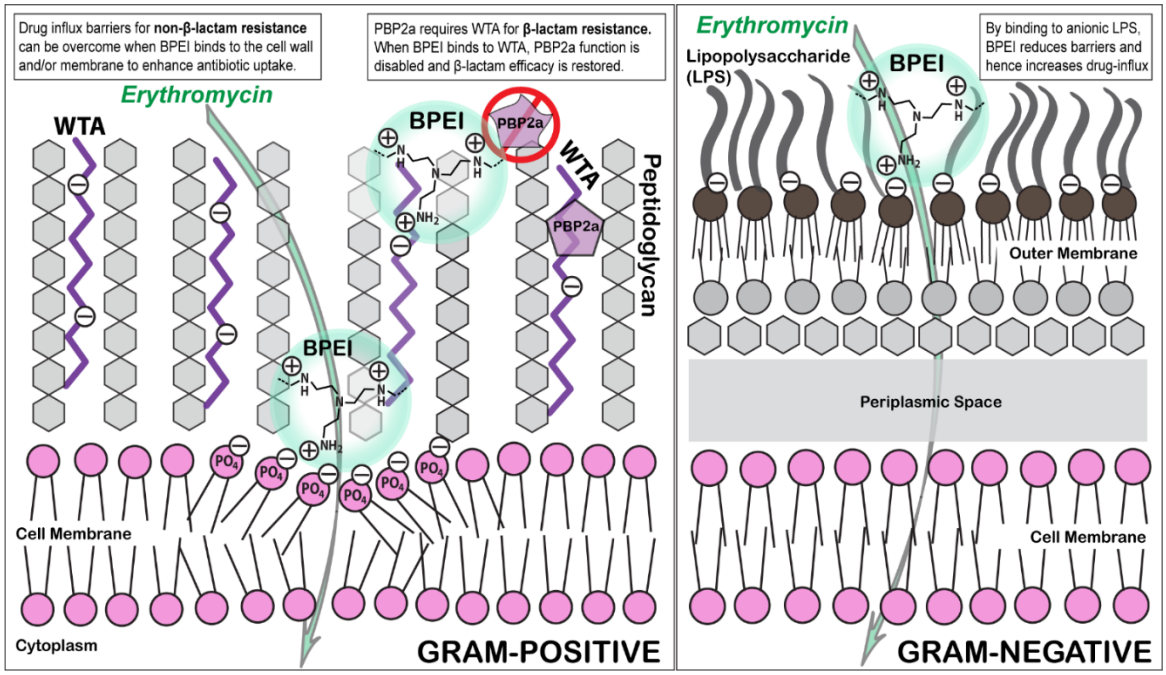


Figure 34. Graphical presentation of 600-Da BPEI's mechanisms of action on Gram-positive and Gram-negative cell wall and membrane. Cationic BPEI not only binds anionic wall teichoic acid (WTA) to indirectly disable penicillin binding proteins PBP2a/4 (which only function properly by localization of WTA), it also electrostatically binds the phosphate heads of the lipid membrane, causing a partial loss of the permeability barrier. Consequently, BPEI can potentiate both β-lactams and non-β-lactams (those target intracellular machinery) against MRSA (Gram-positive). In *Pseudomonas* (Gram-negative), BPEI binds anionic LPS, creating new hydrophilic conduits to enhance drug-influx

First-line antibiotics include the β-lactam class of antibiotics, considered among the safest antibiotics to use.[145-148] In 2015, the US had 269.3 million antibiotic prescriptions given by healthcare providers, which is equivalent to 838 prescriptions per 1000 people. Among them, β-lactams (i.e. penicillin, oxacillin, and amoxicillin) were the most popular prescribed antibiotics with amoxicillin at the top of the chart at 171 prescriptions per 1000 people.[28] Although MRSA is β-lactam resistant, disabling penicillin binding protein PBP2a and PBP4 renders MRSA susceptible. We reported that cationic 600-Da branched polyethylenimine (600-Da BPEI) accomplishes this objective by interacting with wall teichoic acid (WTA) that is essential for PBP2a/4 functionality.[1, 45, 68, 119] For those with penicillin allergies, erythromycin and other broad-spectrum macrolides are prescribed as standard of care antibiotics, but clinical isolates of MRSA do not respond to erythromycin treatment. Here, we show that MRSA clinical isolates with erythromycin resistance can be rendered drug-susceptible when 600-Da BPEI is used to reduce the barriers to drug-influx. Importantly, we also show that 600-Da BPEI potentiates erythromycin against clinical isolates of MDR-PA. This is noteworthy because erythromycin is regarded as an antibiotic without efficacy against Gram-negative bacteria, including those without antimicrobial resistance. The mechanism of action (MOA) involves binding with anionic sites of the bacterial cell envelope (lipopolysaccharide (LPS), wall teichoic acid (WTA), lipoteichoic acid (LTA)) to create new hydrophilic conduits for erythromycin to reach the cytoplasm (Figure 34). 600-Da BPEI is hydrophilic and targets anionic sites on the cell envelope away from the alkyl chains of membrane bilayers. It reduces diffusion barriers to increase drug uptake and enables broad-spectrum efficacy against different bacterial

species. Instead of acting as an antimicrobial agent itself, low concentrations of 600-Da BPEI potentiate the efficacy of erythromycin against clinical isolates of MRSA and MDR-PA. Additionally, BPEI reduces interleukin-8 (IL-8) cytokine's release from primary human epithelial keratinocytes (HEKa) cells, suggesting another therapeutic application for wound care. These data also show that improving the efficacy of standard of care antibiotics, such as β-lactams and macrolides, against AMR Gram-positive and Gram-negative, bacteria creates new opportunities to improve patient health and well-being.

Purpose of Experiment

The purpose of this experiment is: to investigate a new mechanism of action of 600-Da BPEI in broadening the spectrum of erythromycin antibiotic against multidrug-resistant (MDR) *Staphylococcus aureus* and MDR-*Pseudomonas aeruginosa;* and to examine the ability of BPEI in reducing interleukin-8 (IL-8) cytokine's release from *S. aureus* peptidoglycan on primary human epithelial keratinocytes (HEKa) cells.

Experimental Procedures

Materials

Two MRSA clinical isolates (MRSA OU6 and MRSA OU11) and *P. aeruginosa* (PA OU19) from patient swabs were kindly provided by Dr. McCloskey from the University of Health Sciences Center with an institutional review board (IRB) approval. Chemicals (DMSO, growth media, erythromycin, polymyxin B, H33342 dye, and peptidoglycan from *Staphylococcus aureus* (product number 77140) were purchased from Sigma-Aldrich. 600-Da BPEI was purchased from Polysciences. HEKa cells (primary human epithelial keratinocytes), Epilife Medium, and growth supplement were

purchased from Invitrogen. Human IL-8/CXCL8 Quantikine ELISA Kit was purchased from R&D.

In Vitro Checkerboard Assay

Checkerboard assays were conducted to identify synergy between BPEI and antibiotics against bacteria. Serial dilutions of antimicrobial agents (BPEI and antibiotic solutions) were added to a 96-well microtiter plate with 100 µL cation-adjusted Muller Hinton broth (CAMHB) per well. Untreated control and positive control (5% bleach) were also conducted. Bacterial inoculation (5×10^5 CFU/mL) from an overnight culture was added to the plate (1 µL/well) and incubated at 37°C for 20 hr. The change in optical density at 600 nm (ΔOD_{600}) was measured using a Tecan Infinite M20 plate reader immediately after inoculation. Minimum inhibitory concentration (MIC) of each drug is determined as the lowest concentration that inhibited cell growth ($\Delta OD_{600} < 0.05$). Fractional inhibitory concentration index (FICI) and synergistic effects are determined using EUCAST guidelines: synergy ($FICI \leq 0.5$), additivity ($0.5 < FICI < 1$), and indifference ($FICI > 1$).[62] Each assay was done in triplicate.

Cell-permeation Assay / bisBenzimide H33342 Intracellular Accumulation

Cryogenic stock of bacteria (MRSA OU6, OU11, MRSE 35984, or PA OU19) was inoculated overnight on tryptic soy agar. The culture was sub-inoculated in fresh tryptic soy broth (TSB) media for another 5-6 hours with shaking (100 rpm/min). Cells were pelleted by centrifugation at 7000 rpm for 40 min. The supernatant was discarded. The cells were resuspended in PBS and readjusted to $OD_{600} = 1.0$. (which had a density of ~7×10^9 CFU/mL). Aliquots of the cell suspension were transferred to a 96-well flat-bottom black plate (180 µL/well) including the controls of the solvent (PBS blank), the

untreated cells, and treated samples (either BPEI treated or polymyxin-B treated). Five technical replicates of each group were conducted. Hoechst 33342 bisbenzimide (H33342) was added (20 µL) to each well (final concentration of 5 µM). Fluorescence was read right after adding the H33342 by a Tecan Infinite M20 plate reader with the excitation and emission filters of 355 and 460 nm, respectively. Fluorescence data were normalized to the emission before cells were added in the PBS control, and they were plotted against time to show the cellular uptake of H33342 over 10 min.

Cell viability assays

with resazurin were performed with MRSA OU11 cells were grown in TSB as similar to the procedure of cell-permeation assays until they reach a density of ~7 x 10^9 CFU/mL. Then the cell culture was transferred into a 96-well plate (100 µL/well) for BPEI or polymyxin B (PmB) treatments at varied concentrations from 64 - 512 µg/mL. Controls of untreated and positive control of 5% bleach were also conducted. The plate was incubated at 37°C overnight. Resazurin (50 µL; final concentration of 50 µg/mL) was then added and, after 1 hour of incubation, the fluorescence intensity was measured (λ_{ex} = 560 nm; λ_{em} = 590 nm).

IL-8 responses

HEKa cells were seeded in T-75 tissue culture flasks with Epilife media supplemented with human keratinocyte growth supplement 100ug/mL and 100 U/mL of pen/strep and incubated at 37°C in a CO_2 incubator. Fresh media was replaced every 2 days. Until the cell confluence reach 80-90%, they were split into a new passage. To avoid cell senescent, all experiments were performed with cells at passage 3-7. HEKa cells were cultured in a new 24-well plate until 80-90% confluence (total volume = 1 mL/

well). Then treatments of 600-Da BPEI (64, 128, 256, 512, and 1024 μg/mL) or *S. aureus* peptidoglycan (5 μg/mL) were added in triplicate cultures for 24 hr. The cell media was collected in 1.5 mL Eppendorf microtubes and stored at -20°C until ELISA assays were performed. Concentrations of IL-8 cytokine released into the media were quantified followed the instructions of Quantikine Colorimetric ELISA assay kits (R&D Systems). Absorbance was measured at 450 nm and 570 nm. Final corrected absorbance was the subtraction at 450 nm from the one at 570 nm.

Results and Discussion

Since the 1950s, erythromycin—a macrolide antibiotic—has been widely used as a substitute for β-lactams for penicillin-allergic patients. It is a first-line treatment for many pediatric infections.[149] Because erythromycin targets protein synthesis instead of the cell wall, it could be effective against methicillin-resistant staphylococci if the drug was able to reach the cytoplasm. The ability of 600-Da BPEI to increase erythromycin susceptibility was determined with *in vitro* checkerboard assays in 96-well microtiter plates. For two clinical MRSA isolates, their erythromycin MICs were over 2000 μg/mL (Figure 35).

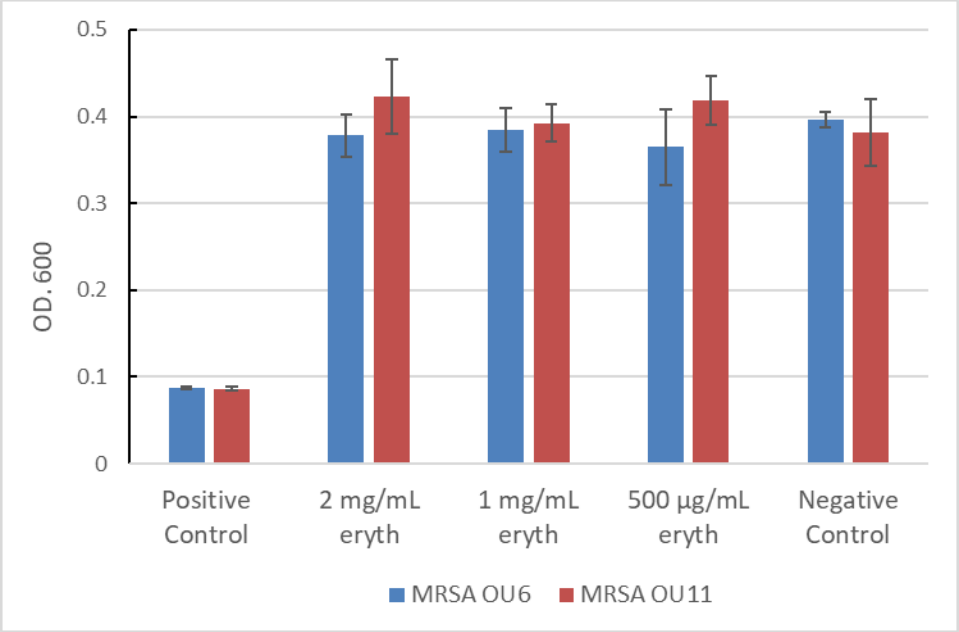


Figure 35. Absorbance (OD.600) of erythromycin (eryth) MIC scan on MRSA OU6 and OU11 shows that the two bacterial strains had high resistance to erythromycin (both MICs are over 2000 µg/mL since no inhibitory effect was found; n = 3).

This demonstrates the strong resistance of MRSA, likely imposed by cell wall peptidoglycan and teichoic acids that hinder drug influx. However, 600-Da BPEI binds to these sites[1, 45, 68, 119] and improves the MRSA susceptibility to erythromycin. The MIC is reduced by 2-3 orders of magnitude in the presence of 16 µg/mL of 600-Da BEPI (Figure 36 and Table 6). This broadens the spectrum of potential anti-MRSA drugs because, as previously reported,[4, 119] 600-Da BPEI was able to eliminate only β-lactam resistance in these MRSA isolates and their biofilms. Against the MDR-PA clinical isolate OU19, 16 µg/mL BPEI lowers the erythromycin MIC from 256 to 2 µg/mL (Figure 36 and Table 6). This demonstrates antibiotic potentiation against a formidable Gram-negative pathogen. As shown in Figure 35, potentiation by 600-Da BPEI relies on its interaction with different bacterial targets due to the different cell envelope architecture

of MRSA and MDR-PA. Nevertheless, 600-Da BPEI can overcome both resistance barriers, and erythromycin potentiation by 600-Da BPEI is characterized as synergistic (Table 6). According to the EUCAST guidelines, a fractional inhibitory concentration index (FICI) is used to identify synergistic effects. FICI values can indicate synergy (FICI ≤ 0.5), additivity ($0.5 < FICI < 1$), or indifference ($FICI \geq 1$).[62] Erythromycin and 600-Da BPEI have synergy against MRSA (FICI = 0.26 for OU6, 0.31 for OU11) and MDR-PA OU19 (FICI = 0.26).

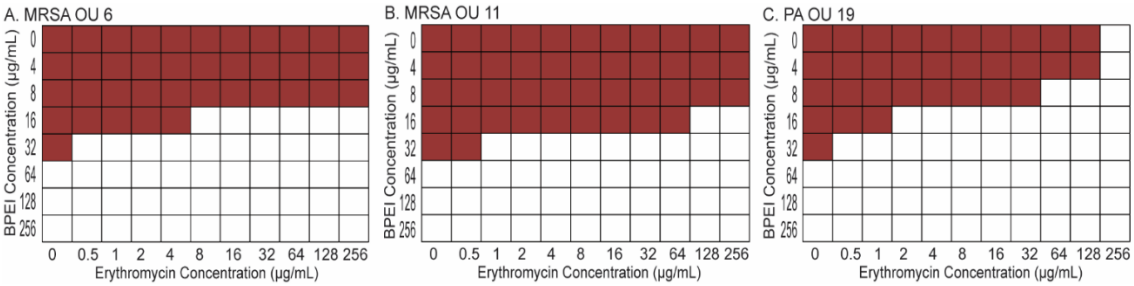


Figure 36. Checkerboard data presentation of bacterial growth inhibition from the combination of erythromycin and 600-Da BPEI. The MICs in these checkerboard assays can be used to show synergy in the clinical isolates MRSA OU6 (A), MRSA OU11 (B), and PA OU19 (C). Each assay was performed in triplicate and the data presented above are the average of these assays.

Table 6. Synergy of 600-Da BPEI and antibiotics against MRSA and MDR-PA clinical isolates

Strain	Antibiotic	MIC[a] BPEI (µg/mL)	MIC[a] Antibiotic (µg/mL)	MIC[a] Antibiotic with 16 µg/ml BPEI	FICI[b]	Outcome
MRSA OU6	Erythromycin	64	>2000	8	0.26	Synergy
MRSA OU11	Erythromycin	64	>2000	128	0.31	Synergy
PA OU19	Erythromycin	64	256	2	0.26	Synergy

[a] MIC, Minimum Inhibitory Concentration; [b] FICI, the minimum Fractional Inhibitory Concentration Index

Synergy between 600-Da BPEI and erythromycin is attributed to increase drug influx. Resistance to non-β-lactam antibiotics (such as macrolides, tetracyclines, and fluoroquinolones) involves membrane-bound efflux-pump proteins. These protein assemblies eject toxic substances (i.e. antibiotics), hindering accumulation of antibiotics in the bacterial cells.[150-152] To examine increased drug influx, we tested the ability of 600-Da BPEI to increase the intracellular concentration of a fluorescence probe molecule, Hoechst 33342 bisbenzimide (H33342). H33342 fluoresces when it penetrates the cell-membrane and binds to intracellular DNA. Greater accumulation of H33342 in the cells creates a higher fluorescence intensity. Fluorescence measurements were taken for untreated and BPEI-treated samples immediately after adding the H33342 dye**.**

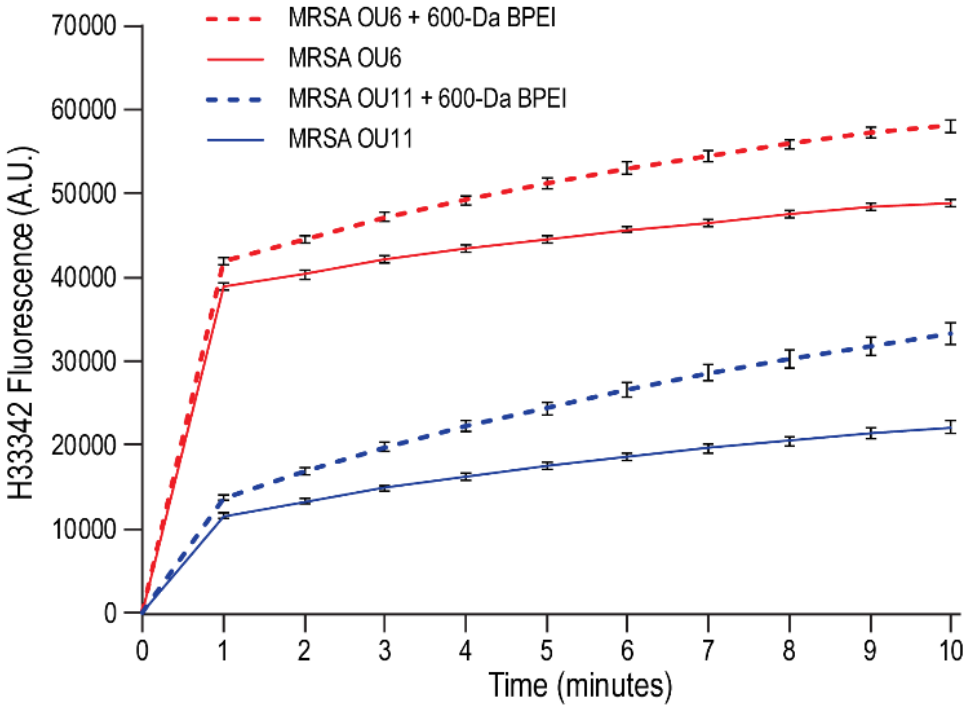


Figure 37. H33342 permeation curves show the addition of BPEI (128 μg/mL) enhances the cell-membrane permeability of MRSA OU6 and OU11 as the fluorescence of H33342 increased, compared to their untreated control. Error bars denote standard deviation (n = 5).

As shown in Figures 37, 600-Da BPEI enhanced dye uptake in MRSA OU6 and MRSA OU11. The BPEI-treated cells had much higher fluorescence intensity by approximately 10,000 fluorescence units compared to their untreated controls. Similar trends are observed for the influx of H33342 into cells of the MDR-PA clinical isolate OU19 (Figure 38). *P. aeruginosa* is well-known for a powerful drug-efflux system and thus the low accumulation of H33342, compared to Gram-positive MRSA, is not unexpected. Nonetheless, as with MRSA, 600-Da BPEI increases the uptake of H33342 in PA OU19.

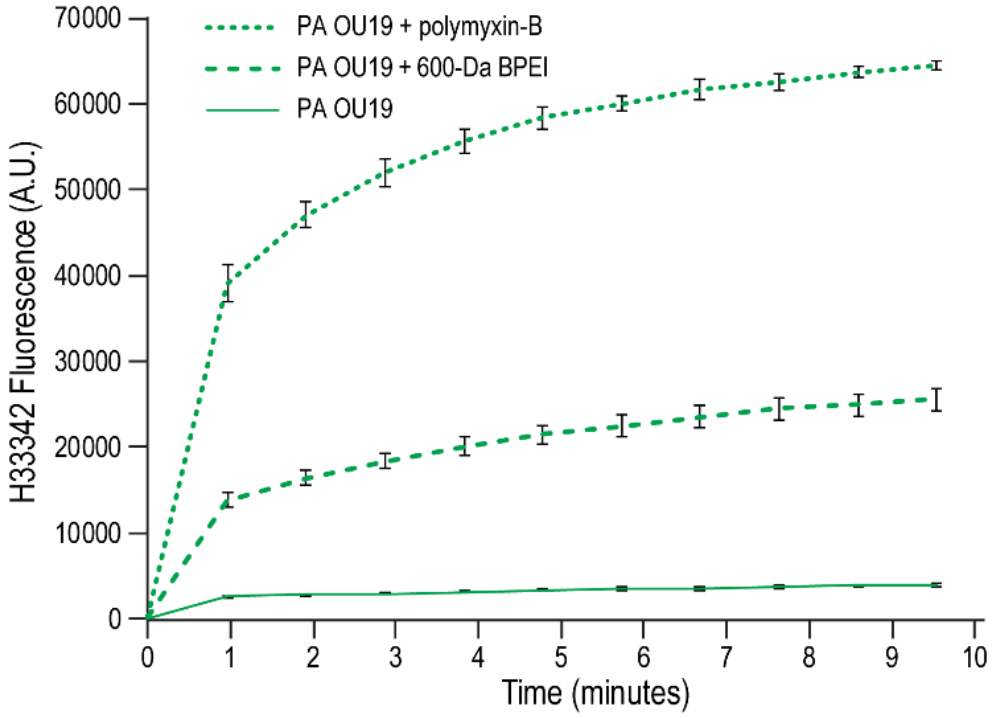


Figure 38. H33342 permeation curves show the addition of of 128 µg/mL polymyxin B (PmB) drastically increases the dye uptake more than twice of that 128 µg/mL BPEI does on P. aeruginosa PA OU19. Error bars denote standard deviation (n = 6).

The concentration of BPEI, 128 μg/mL, used in fluorescence assays would appear to be a lethal concentration as it is greater than the MIC of each isolate. However, an important consideration is that generating fluorescent signals above the detection limit requires a higher cell density (~ 7 x 10^9 CFU/mL) than in checkerboard assays (~ 5 x 10^5 CFU/mL). Thus, while 128 μg/ml of 600-Da BPEI is lethal in the checkerboard assays, is it sublethal in the fluorescence studies. This is shown by measuring cell viability using a resazurin cellular metabolism assay. MRSA OU11 was grown until it reached the same cell density in H33342 assays (~ 7 x 10^9 CFU/mL) before BPEI treatment. Resazurin was then added and, after 1 hour of incubation, the fluorescence intensity was measured. Cellular metabolic product NADH irreversibly reduces resazurin into resorufin, which emits strong fluorescence at 580-590 nm, indicating cell viability. As shown in Figure 40, MRSA cells were slightly less viable with higher concentrations of 600-Da BPEI, suggesting that the membrane remains intact. Previous studies showed that BPEI attached to the surface of MRSA cells.[68, 119] Additionally, scanning electron micrographs of MRSA show that sub-lethal amount of 600-Da BPEI altered the cell wall morphology.[1, 68, 119] These data support a MOA involving the ability of 600-Da BPEI to weaken the cell envelope rather than lysing the bacteria. This is a different MOA than that of polymyxin-B, a cationic antibiotic known to cause widespread disruption of bacterial membranes.

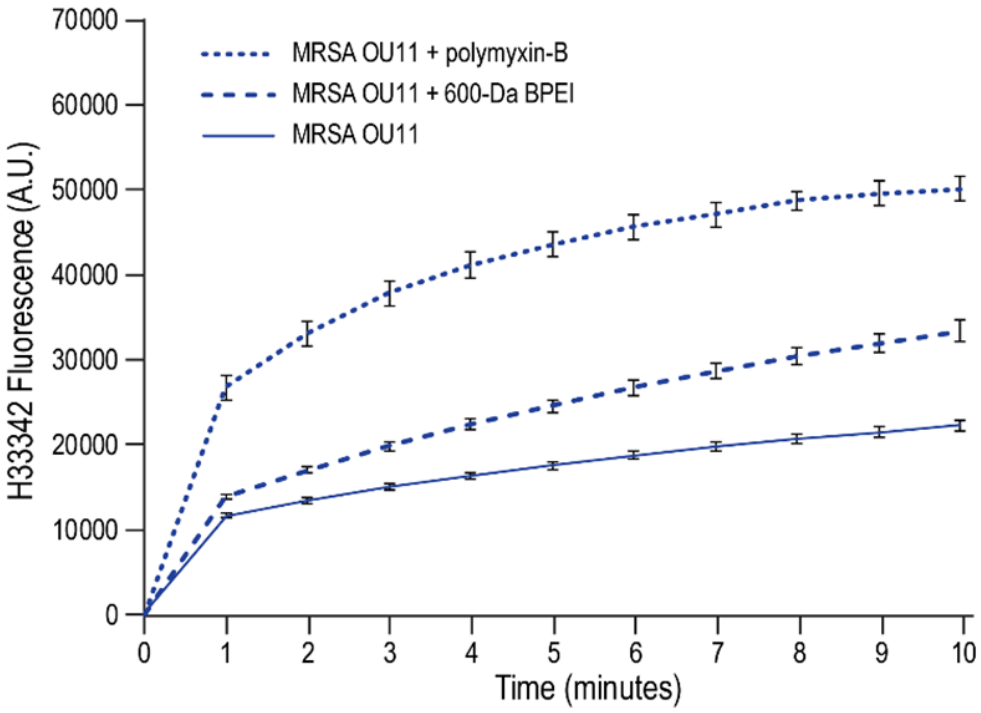


Figure 39. H33342 permeation curves show the addition of 128 μg/mL polymyxin B (PmB) drastically increases the dye uptake by MRSA OU11, more than twice of that 128 μg/mL BPEI does. Error bars denote standard deviation (n = 5).

Using the resazurin assay, corresponding concentrations of polymyxin-B were more lethal to MRSA OU11 (Figure 39) than 600-Da BPEI. In fact, 64 μg/mL of polymyxin-B (PmB) caused more cell deaths than 512 μg/mL 600-Da BPEI, and the highest concentration of PmB (512 μg/mL) killed the entire MRSA sample. These experiments highlight the low antibiotic propensity, but high potentiation ability, of 600-Da BPEI. These data also support the paradigm that PmB is considered a Gram-negative selective drug due to its low MICs (≤ 2 μg/mL), while Gram-positive bacteria require much higher concentration of PmB (≥ 32 μg/mL) due to the diffusion barrier imposed by the thick bacterial cell wall.[153]

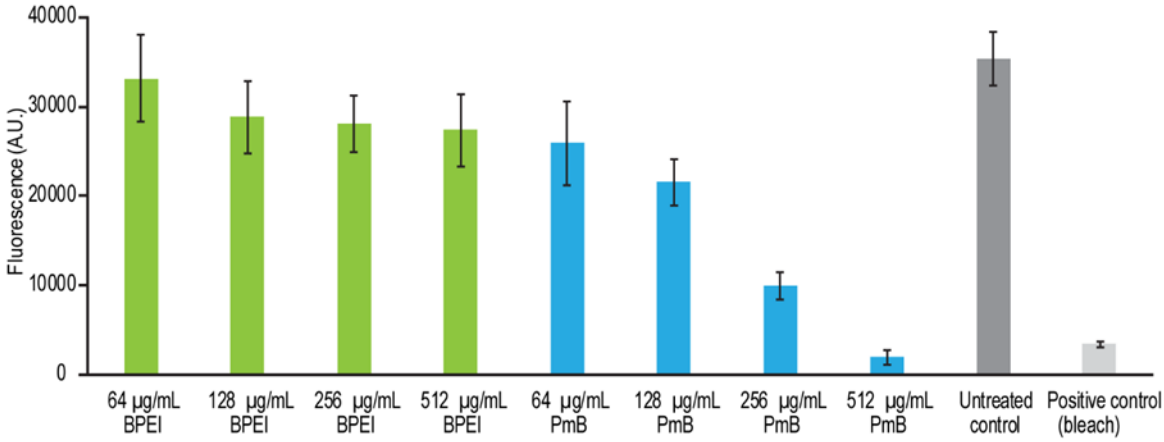


Figure 40. Resazurin assay indicates cell viability of MRSA OU11 (at the cell density of ~7*10^9 CFU/mL) treated with either BPEI or polymyxin B (PmB). Resazurin is converted to resorufin by cellular metabolism product $NADH/H^+$ and thus provide an indication of cell viability. Error bars denote standard deviation (n=8).

The different MOAs of 600-Da BPEI and PmB can be examined by gauging their effect on the influx of H33342. The clinical isolate PA OU19 (Figure 38) and MRSA OU11 (Figure 39) were exposed to similar amounts of 600-Da BPEI and PmB. As shown, PmB dramatically increased the intracellular concentration of H33342 by disrupting the membrane bilayer using its hydrophobic alkyl tail. In contrast, 600-Da BPEI is hydrophilic and lacks the energetic driving force to penetrate the membrane. Thus, BPEI reduces drug diffusion barriers within the peptidoglycan layer of MRSA and LPS of PA without damaging the membrane. This MOA also explains why the rate of H33342 influx during the first few minutes is much higher for PmB than 600-Da BPEI. The ability of PmB to disrupt membrane layers aligns with the literature precedent that PmB is nephrotoxic and neurotoxic towards human cells.[154] In contrast, 600-Da BPEI is unlikely to damage the membranes[45-46, 155] but instead reduces drug-influx barriers that allows

faster diffusion through the bacterial membrane that allows enhanced H33342 accumulation in the MRSA and PA cells.

The therapeutic potential for 600-Da BPEI is strong and has a foundation in previous work of its antibiotic[46, 155] and drug-delivery characteristics. First reported in 1995, large-molecular-weight BPEIs (> 25,000 Da) have strong interactions with lipid bilayers and high transfection activity for gene delivery both in vitro and in vivo due to high N/P ratios (polycationic nitrogen binding to anionic phosphates in DNA or RNA).[43-44, 156-158] Large BPEIs have higher transfection efficiency than small BPEIs (< 5 kDa). Although large PEIs is more beneficial than viral-vectors in gene therapy, larger molecular weights correspond to higher cytotoxicity due to more interactions with blood components.[38-39, 159] Unlike large-molecular-weight BPEIs, 600-Da BPEI is non-cytotoxic[45] and furthermore it lacks the size and high charge ratio of N/P to be an effective gene delivery candidate. Unlike polypeptide antibiotics (i.e. polymyxin-B), 600-Da BPEI lacks the hydrophobic region necessary to dissolve through the cytoplasmic membrane. However, as an antibiotic potentiator, the surface charge of 600-Da BPEI is sufficient to attach to anionic teichoic acids of the MRSA cell wall[1, 45, 68, 119] and lipid phosphate groups of the membrane to create hydrophilic regions for drug intake, which explains its antibiotic synergy with erythromycin against the clinical isolates of MRSA. In a similar attraction force, 600-Da BPEI binds anionic LPS of *P. aeruginosa* and thus opens more pathways for a co-drug to easily pass through the bacterial membrane.[5] Because of this new MOA, 600-Da BPEI may have broader applications than originally envisioned.[1, 45-46, 68, 119, 155]

Staphylococci are notorious for their skin and soft-tissue infections that often lead to more complicated diseases. Each year, millions of acute skin and soft tissue infections (SSTIs) become chronic wound infections.[55-58] Instead of taking 3-6 weeks to heal, chronic wounds persist for 3-6 months. Delays in healing acute SSTIs are often due to a prolonged inflammatory phase of healing caused by bacterial debris, such as peptidoglycan from *S. aureus*, which is a Pathogen-Associated Molecular Pattern (PAMP) molecule. Preventing *S. aureus* peptidoglycan from triggering the release of inflammatory cytokines will restore the optimal inflammatory response.[160] However, successful drugs are elusive because the cell wall debris has a large variation in size and shape, making it virtually impossible to target peptidoglycan with monoclonal antibodies that recognize specific polysaccharide units. Instead, 600-Da BPEI binds the anionic sites of peptidoglycan and prevents the release of cytokines. As shown in Figure 41, S. aureus peptidoglycan causes the release of interleukin-8 (IL-8) from primary human epithelial keratinocytes (HEKa) cells. IL-8 is a cytokine and chemokine molecule involved with neutrophil recruitment to the wound site.[161] Its release is stimulated when peptidoglycan binds to, and is mainly recognized by, toll-like receptor 2 (TLR2).[162-166] In contrast, 600-Da BPEI does not cause the HEKa cells to release IL-8. However, when 600-Da BPEI and S. aureus peptidoglycan are added to HEKa cells, the amount of IL-8 diminishes, suggesting another promising therapeutic benefit of BPEI for wound care.

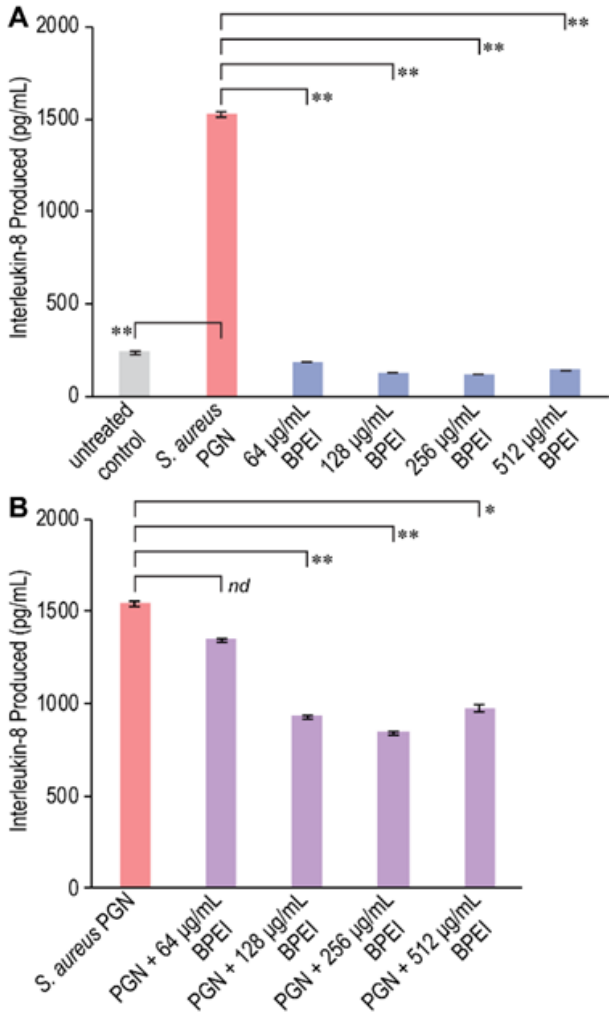


Figure 41. ELISA assays show the amount of cytokine IL-8 released by human epithelial keratinocytes (HEKa cells) in responses to: peptidoglycan (PGN) and 600-Da BPEI (A); combinations of PGN and 600-Da BPEI (B). Data are shown as average of triplicate trials. Error bars denote standard deviation. Statistical analysis with the student's t-test generates p-values of < 0.05% (95% confidence, denoted by ∗) and <0.01 (99% confidence, denoted by ∗∗). nd = no statistical difference.

Experts predict that, by 2050, antimicrobial resistance (AMR) will be the leading cause of death, claiming 10 million lives a year—a figure that exceeds the number of deaths caused by cancer today. A swift global response is required to prevent this alarming scenario,[7] but pharmaceutical companies are facing significant market pressures that hinder their ability to meet this need. The cost of bringing a drug to

market is extraordinary, up to a billion dollars, yet there are little or no incentives for clinicians to use the new drug. New antibiotics are held in reserve as drugs of last resort to prevent the emergence of resistance. Instead, the paradigm of antibiotic potentiators has emerged to overcome resistance barriers and restore efficacy to existing antibiotics; thereby providing an opportunity to kill drug-resistant and drug-susceptible bacteria with the same formulation. However, antibiotic + potentiator combinations are being developed against Gram-negative pathogens or Gram-positive pathogens rather than a broad-spectrum formulation against both.

Conclusions

The data reported demonstrate potentiation of erythromycin against Gram-positive and Gram-negative pathogens. They provide a better understanding of the 600-Da BPEI mechanisms of action against multidrug-resistant MRSA and *P. aeruginosa* that may lead to development of broad-spectrum antibiotic and potentiator combinations. Antibiotic combination therapy using existing drugs also reserves the newer last-resort antibiotics for use against the most serious cases of antibiotic-resistant infection. Yet, the need to couple 600-Da BPEI with an antibiotic for effective killing of AMR pathogens creates technical hurdles of reducing drug toxicity while matching the pharmacokinetics and pharmacodynamics (PK/PD) of the combination. These problems are mitigated when the combination is used as a topical agent against wound infections. We know that 600-Da BPEI dissolves biofilms[1] and expanding the possible classes of antibiotics for potentiation that increases therapeutic opportunities. Chronic wound infections, those that have not proceeded through a reparative process in three months, affect millions of Americans each year[55-56] and are often caused by drug resistant

bacteria, such as MRSA and MDR-PA. In the absence of a robust pipeline of new drugs, existing drugs and regimens have to be re-evaluated as combination(s) with potentiators that overcome biofilms and/or antibiotic resistance. Ideally, the potentiator should be a single compound with multi-function properties that disable biofilms and antibiotic resistance and possibly diminish inflammation. We envision wound treatment with antibiotics given topically, orally, or intravenously, and external topical application of 600-Da BPEI to disable biofilms, resistance mechanisms, and reduce inflammation. This mitigates concerns about toxicity and differences in the PK/PD of antibiotics vs. 600-Da BPEI. This may improve wound care outcomes by restoring potency to existing antibiotics with a single potentiator. Likewise, using an antibiotic potentiator, such as 600-Da BPEI, to lower the release of cytokines in response to peptidoglycan stimulation increases the therapeutic benefit of 600-Da BPEI. Efforts to evaluate the ability of 600-Da BPEI to modulate cytokine release in response to other PAMPs is currently underway. Reducing inflammation helps prevent many acute infections from becoming chronic wounds; and lowers the risk of recurrent infection and tissue necrosis.[167-168] that results in substantial morbidity, disability, hospitalization, and mortality, especially among older adults.[169]

Chapter 7: Overcoming multidrug resistance and biofilms of *Pseudomonas aeruginosa* with a single dual-function potentiator

Background

Pseudomonas aeruginosa (PA) is a Gram-negative bacterium that often causes hospital-acquired infections and cystic fibrosis. PA infections are difficult to treat due to their resistance to antibiotics and the ability to form biofilms which result in severe chronic infections. Antibiotic resistance in PA is both intrinsic and acquired through complex mechanisms and mainly involves barriers from lipopolysaccharide, efflux pumps, β-lactamase, and outer membrane porins. It becomes even more challenging for clinical management when these bacteria are sequestered in biofilms. These problems would be alleviated if, upon the initial presentation of bacterial infection symptoms, clinicians were able to administer an antibiotic that kills both susceptible and otherwise resistant bacteria; and also eradicates biofilms. As the most common class of antibiotics, β-lactams could be used in a new drug if the leading causes of β-lactam antibiotic resistance – permeation barriers from lipopolysaccharide (LPS), efflux pumps, and β-lactamase enzymes – were also defeated. Success may be possible with a discovery made in our laboratory. In this study, we demonstrate the ability of 600-Da BPEI to overcome multidrug resistance and biofilms of PA in combination with existing antibiotics. Mechanisms of action of our technology are also elucidated. *It's important to note that this is a large cooperative project that involved the entire lab workforce for both data collection and writing the research manuscript*. I'm not the sole first-author, and my main contribution leads to the data shown here in this chapter. The more

detailed and throughout research manuscript is published on ACS Infectious Diseases Journal.[5]

Pathogeneses and Virulence

Accounting for around 11-13% of all healthcare-associated infections, PA is identified as the second most common cause of hospital-acquired pneumonia. Common infections caused by PA include pneumonia, urinary tract infections (UTI), bloodstream infections, respiratory tract infections, surgical site/skin infections.[170] PA is listed as one of the eleven serious threats in the 2019 CDC's antibiotic resistance threats in the U.S.[6] In pediatric intensive care units (ICUs), PA is the most common cause of hospital-acquired pneumonia.[171] PA infections are associated with high morbidity and mortality, especially with immunocompromised patients. In children with cystic fibrosis, 97.5% of them are found to be infected with PA by 3 years old.[172] Multidrug resistance in PA isolates has been emerging in ICUs (resistant to ceftazidime, piperacillin, gentamicin, and ciprofloxacin). As a heavy concern in wound healing, PA is prevalent in burn units because their biofilms are impenetrable to antibiotics which lead to chronic wound infections.[173-174] For instance, diabetic wound infections and foot ulcers often become chronic because they stall in suboptimal inflammatory phase of healing perpetuated by biofilms.[169, 175-177] PA infections and their biofilms create serious health issues, and the threat to patient survival increases when the bacterium is multidrug resistant *P. aeruginosa* (MDR-PA).[178-181] Antibiotic resistance in PA is both intrinsic and acquired through complex mechanisms and mainly involves barriers from lipopolysaccharide (LPS), efflux pumps, β-lactamase, and outer membrane porins. Biofilms and antibiotic resistance create substantial technological hurdles to patient treatment.[182] This presents a

significant and critical need for way to counteract them. Existing drugs and regimens are coupled with potentiators that overcome antibiotic resistance *or* biofilms.[183] However, it is possible to develop a single compound that disables biofilms *and* combats antibiotic resistance. As a multi-purpose potentiator, 600-Da branched polyethylenimine (BPEI) has the ability to disable resistance and dissolve their biofilms. We have used 600-Da BPEI to confront the biofilm directly and disrupt the protective exopolymer substances (EPS) network of methicillin-resistant staphylococci while simultaneously counteracting β-lactam resistance mechanisms.[2, 45, 68, 184] In this report, we show that 600-Da BPEI also disables MDR mechanisms, and biofilms, in *P. aeruginosa* obtained from the American Type Culture Collection (ATCC) and antibiotic resistant clinical isolates.

Purpose of Experiment

The purpose of this experiment is to investigate the ability of 600-Da BPEI to overcome multidrug resistance and biofilms of *P. aeruginosa* in combination with existing antibiotics and to elucidate the treatment's mechanisms of action.

Experimental Procedures

Materials

In this experiment, the *Pseudomonas aeruginosa* bacteria were purchased from the American Type Culture Collection (ATCC BAA-47 and 27853). Additional MDR-PA strains (PA OU1, 12, 15, 19, and 22) were obtained from clinical isolates from the University of Oklahoma Health Sciences Center using appropriate IRB protocols and procedures. Wild-type *P. aeruginosa* PAO1 and its efflux pump deficient mutant, PaΔ3, were kindly provided by Prof. Helen Zgurskaya, University of Oklahoma. Chemicals were purchased from Sigma-Aldrich (DMSO, growth media, and electron microscopy

fixatives). Antibiotics were purchased from Gold Biotechnology. 600-Da BPEI was purchased from Polysciences, Inc. MBEC™ Biofilm Inoculator with 96-well base plates were purchased from Innovotech, Inc.

Checkerboard Assays and Growth Curves

Checkerboard assays were followed the methods of Lam *et al.* to determine the synergistic effect between 600-Da BPEI and antibiotics against the *P. aeruginosa* strains growing in cation-adjusted Mueller-Hinton broth (CAMHB).[1, 45] Bacterial growth curves were obtained using CAMHB media augmented with various amounts of 600-Da BPEI and/or piperacillin inoculated with *P. aeruginosa* BAA-47 cells from an overnight culture ($5x10^5$ CFU/mL). Cells were grown at 35 °C with shaking. The OD_{600} (optical density at 600nm) was monitored and recorded for each sample over 24 hr. Each checkerboard trial was done in triplicate. Each growth curve was done in duplicate.

MBEC Assay:

The MBEC assay is adapted from previous literature reports.[2, 4]

Inoculation and Biofilm Formation: A sub-culture of P. aeruginosa BAA-47 was grown from the cryogenic stock on an agar plate overnight at 35 °C. The MBEC plate was inoculated with 150 µL of MHB/well plus 1 µL of a stock culture made from 1 colony/mL of P. aeruginosa BAA-47 in MHB (~$5x10^5$ CFU/mL). The MBEC inoculator plate was sealed with Parafilm and incubated for 24 hr at 35 °C with 100 rpm shaking to facilitate biofilm formation on the prongs. Following biofilm formation, the lid of the MBEC inoculator was removed and placed in a rinse plate containing 200 µL of sterile PBS for 10 sec.

Antimicrobial Challenge: A challenge plate was made in a new pre-sterilized 96-well plate in a checkerboard-assay pattern to test the synergistic activity of 600-Da BPEI + antibiotic combinations. Antimicrobial solutions were serial-diluted and added to the 96-well plate, which contained 200 µL of MHB per well. After the rinsing step, the preformed biofilm prong lid was immediately transferred into the prepared antimicrobial challenge plate and incubated at 35 °C for 20-24 hr.

Recovery and Quantitative MBEC: After the challenge period, the MBEC inoculator lid was washed and transferred into a recovery plate containing 200 µL of MHB per well, sonicated on high (Branson B-220, frequency of 40 kHz) for 30 minutes to dislodge the biofilm and then incubated at 35 °C for 20-24 hr to allow the surviving bacterial cells to grow. After incubation, the OD_{600} of the recovery plate was measured using a Tecan Infinite M20 plate reader to determine the MBEC of the antimicrobial compounds tested. A change in OD_{600} greater than 0.05 indicated positive growth. Likewise, the OD_{600} for the base of the challenge plate was measured to determine the MICs of the antimicrobial compounds. The fractional inhibitory concentration index (FICI) calculated based on established equation[62] was used to determine synergy ($FICI \leq 0.5$), additivity ($0.5 < FICI < 1$), and no synergy ($FICI \geq 1$).

Scanning Electron Microscopy

P. aeruginosa BAA-47 cells were inoculated from an overnight culture ($5x10^5$ CFU/mL) and grown at 35 °C with shaking. The bacteria were grown in four separate sub-lethal treatments: 600-Da BPEI, piperacillin, combination (600-Da BPEI + piperacillin), and untreated control. Growth was stopped at late-lag phase. Samples were collected by centrifugation and fixed with Karnovsky fixative (2% glutaraldehyde and

2% paraformaldehyde in 0.1M cacodylate buffer) for 30 min. The cells were then fixed with 1% OsO4 for 30 min in the dark. The cells were washed with water three times. A couple drops of each sample were placed on clean, poly-L-lysine coated coverslips and air-dried for 30 min. The samples were dehydrated by going through a series of ethanol solutions (20%, 35%, 50%, 70%, and 95%), spending 15 min in each solution. Afterward, the samples were dried with hexamethyldisilazane (HMDS). They were then mounted on aluminum stubs with carbon tape and sputter-coated with AuPd. A Zeiss NEON SEM was used to image the samples at 5 kV accelerating voltage.

H33342 Bisbenzimide and NPN Accumulation Assays

Overnight culture of *P. aeruginosa* BAA-47 was used to inoculate fresh MHB media for another 5 hr at 35 °C with shaking. Bacterial cells were collected by centrifugation at 6000 rpm for 40 min and resuspended in PBS. The OD_{600} of the cell suspension was adjusted to ~ 1.0 and kept at room temperature during the experiment. Aliquots (180 µL/well) of the cell suspension were transferred to a 96-well flat-bottom black plate in the format of column 1, PBS blank; column 2, untreated control cells BAA-47; column 3, cells BAA-47 + BPEI (sub-lethal concentration). Five technical replicates of each group were conducted. Fluorescent probes Hoechst 33342 bisbenzimide (H33342) or 1-*N*-phenylnaphthylamine (NPN) was added (20 µL) to each well with a final concentration of 5 µM. Fluorescence was read immediately after the addition of H33342 or NPN by a Tecan Infinite M20 plate reader with the excitation and emission filters of 355 and 460 nm for H33342 or 350 and 420 nm for NPN, respectively. Fluorescence data were normalized to the emission before cells were added in the PBS

control, and they were plotted against time to show the cellular uptake of H33342 or NPN over 10 min.

Results and Discussion

BPEI synergizes β-lactams against multidrug-resistant Pseudomonas aeruginosa

Checkerboard assays demonstrate synergistic effects between 600-Da BPEI and β-lactam antibiotics against two laboratory strains of *Pseudomonas aeruginosa*, ATCC 27853 and ATCC BAA-47, and several multidrug-resistant (MDR) clinical isolates from patients at the University of Oklahoma College of Medicine. The minimum inhibitory concentrations (MICs) of 600-Da BPEI and piperacillin against these strains were determined and used to calculate the fractional inhibitory concentration index (FICI).[1, 68] An FICI lower than 0.5 indicates synergy while an FICI between 0.5 and 1 represents additivity. The 600-Da BPEI MICs against *P. aeruginosa* ATCC 27853, ATCC BAA-47, and 5 clinical isolates varied from 8 to 64 μg/mL (Table 7). For the β-lactam antibiotic piperacillin, resistance in *P. aeruginosa* is defined by USCAST as a minimum inhibitory concentration (MIC) ≥ 8 μg/mL.[185] As shown in Table 7, the ATCC strains were susceptible to piperacillin yet the clinical isolates exhibited strong piperacillin resistance. Using checkerboard assays (Figure 42), the presence of 600-Da BPEI lowered the MIC of piperacillin against MDR-PA isolate OU1 and the other tested strains (Supporting Information from Lam et al.[5])

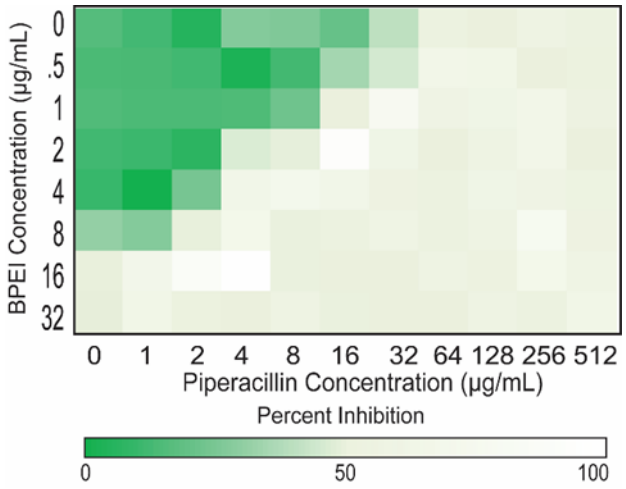


Figure 42. Checkerboard assay data demonstrating that sub-lethal amounts of 600-Da BPEI lower the piperacillin MIC against a MDR clinical isolate of *P. aeruginosa*, OU1. The MIC of piperacillin (64 µg/mL) is resistant but 2 µg/mL of 600-Da BPEI (3.3 µM) reduces the β-lactam MIC to 4 µg/mL which is interpreted as susceptibility.

Table 7 data were collected without tazobactam, a β-lactamase inhibitor, suggesting that enzymatic activity cannot maintain this form of β-lactam resistance. Perhaps the intracellular piperacillin concentration is sufficient to overcome losses from β-lactamase hydrolysis. β-lactams are bactericidal antibiotics. Yet, sublethal concentrations of piperacillin become bactericidal when combined with sub-lethal concentrations of 600-Da BPEI (Figure 43). Within 24 hours, the untreated control group grew to an OD_{600} of 2, as so did the individual treatment of either 600-Da BPEI or piperacillin alone, indicating that these concentrations are insufficient to kill the bacteria. Only the combination 600-Da BPEI + piperacillin treatment could effectively stop its growth, highlighting the restorative value of 600-Da BPEI on β-lactam antibiotic efficacy.

Table 7. MIC and FICI values for *P. aeruginosa* treated with 600-Da BPEI, piperacillin, and their combination.

Strain	MIC [µg/mL]						FICI	Outcome
	600-Da BPEI	PIP/TAZO [1,2]	PIP[1,3]	PIP[1,3]	+	600-Da BPEI		
PA 27853	16	-	4	0.25	+	4 µg/mL	0.31	Synergy
PA BAA-47	32	-	4	1	+	8 µg/mL	0.63	Additivity
PA OU1	16	64	64	4	+	2 µg/mL	0.31	Synergy
PA OU12	8	128	128	8	+	4 µg/mL	0.31	Synergy
PA OU15	32	n.d.	128	32	+	8 µg/mL	0.5	Synergy
PA OU19	64	n.d.	> 256	1	+	16 µg/mL	0.31	Synergy
PA OU22	64	n.d.	> 256	4	+	16 µg/mL	0.37	Synergy

[1]Piperacillin (PIP) susceptibility breakpoints are resistance ≥ 8 µg/mL; susceptible < 8 µg/mL
[2]Determined by the OUHSC Clinical Microbiology laboratory; TAZO = tazobactam
[3]Determined in this work; piperacillin only, no tazobactam added; n.d. = not determined

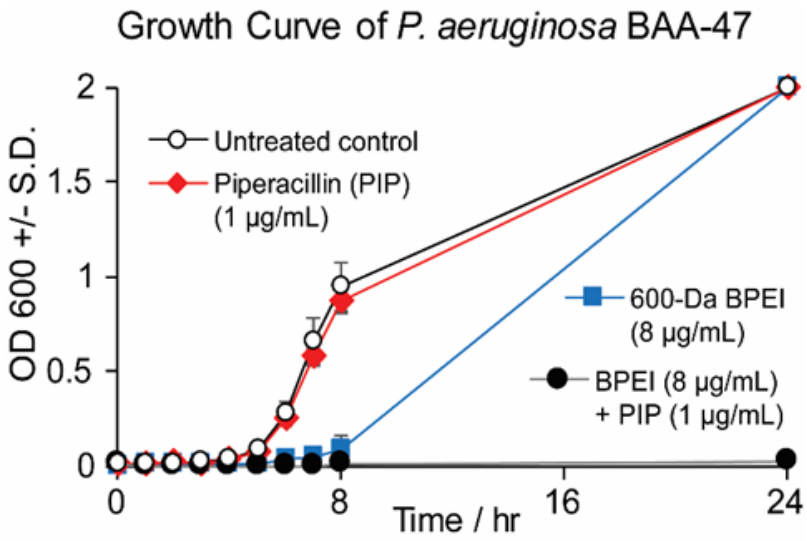


Figure 43. Growth curves of PA BAA-47 shows that sub-lethal amounts of 600-Da BPEI and piperacillin slow bacterial growth but do not kill the culture. However, treating the culture with a combination of 600-Da BPEI and piperacillin, each at sub-lethal concentrations, is. Error bars denote standard deviation (*n = 2*).

Mechanisms of action of BPEI on the influx and efflux effects

As described below, 600-Da BPEI does not inhibit efflux pumps. However, there are concentration dependent effects of 600-Da BPEI, which has antibiotic properties at high concentration. At lower concentrations used for β-lactam potentiation, the mechanism of likely involves disrupting the LPS layer to increase intracellular antibiotic concentrations and overcome β-lactamase enzymes and efflux pumps. At slightly higher concentrations need to potentiate erythromycin, 600-Da BPEI causes slight perturbations to the outer membrane. However, previous data collected with fluorescence microscopy show that sub-MIC concentrations of 600-Da BPEI do not accumulate within *E. coli* cells.[68] The ability of improve β-lactam efficacy at low concentration occurs because the cross-linked network of LPS presents a barrier to free-diffusion of antibiotics. The outer membrane of *P. aeruginosa* contains numerous beta barrel proteins amongst the alkyl chains of the phospholipid and LPS leaflets. These porins allow for the diffusion of β-lactam antibiotics[186] between the extracellular milieu and the periplasmic space.[187] However, the inner-core, outer-core, and O-antigen regions of LPS slow the uptake of β-lactams.[188] Ca^{2+} and Mg^{2+} ions stabilize these anionic regions and we posit that 600-Da BPEI also binds to these sites to cause localized reduction in the diffusion barrier. This was evaluated by determining if 600-Da BPEI binds to LPS and by performing permeation assays that monitor the intracellular concentration of probe molecules.

Isothermal Titration Calorimetry (ITC) was used to measure the enthalpy of molecular binding interactions between 600-Da BPEI and the LPS isolated from *P. aeruginosa.* An exothermic reaction was found during their titration, indicating an electrostatic binding portfolio between cationic BPEI and anionic regions of LPS.[5] This

binding would cause localized disruption of the LPS-metals network and creates new avenues of access for β-lactams to reach porin transporters imbedded in the membrane lipid tails. Although 600-Da BPEI may be increasing antibiotic influx, it may also be hindering efflux pumps. This can be tested with a fluorescence assay. Using *P. aeruginosa* PAO1 that is multi-drug resistant,[189] bacterial cells were exposed to the fluorescent probe H33342 that is also a substrate for efflux pumps. Fluorescence spectroscopy data measure its accumulation within the cells (Figure 44). The fluorescence intensity of H33342 is significantly enhanced when bound to the cell membranes and bacterial DNA, levelling off at the maximum intracellular cellular concentration of H33342. The addition of 600-Da BPEI increased its fluorescence intensity four-fold. The increase of H33342 intracellular concentration suggests that 600-Da BPEI either enhanced the passive diffusion or inactivated the active efflux system. Using PAO1's efflux-deficient mutant, PaΔ3,[189] the fluorescence intensity increases further. This shows that 600-Da BPEI is not blocking efflux processes. If BPEI was blocking efflux, the intensities would be same because the efflux pump target is absent in PaΔ3 cells and 600-Da BPEI would not influence the intracellular concentration in this mutant strain. However, the probe concentration does increase in the presence of 600-Da BPEI and thus the effect is attributed to increased drug influx that allows *Pseudomonas* cells take up more of the fluorescent molecule.

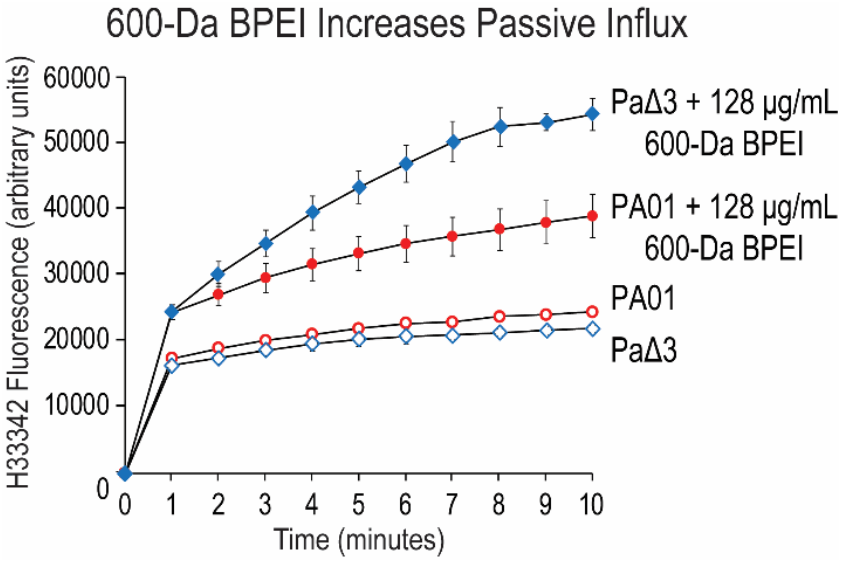


Figure 44. Effect of 600-Da BPEI on the intracellular accumulation of the DNA-binding H33342 by *P. aeruginosa* BAA-47. Real-time kinetics of H33342 uptake show that 600-Da BPEI significantly increased the H33342 accumulation (closed red circles) into the bacterial cells, compared to the untreated control (open red circles). Similar effects are seen with the efflux deficient mutant PaΔ3 (open and closed blue diamonds). The intracellular concentration of H33342 in the treated cells is higher than the wild-type cells indicating that 600-Da BPEI does not hinder efflux processes. Error bars denote standard deviation (*n = 5*).

A noteworthy consideration is that the concentration of BPEI (128 µg/mL) used in fluorescence assays is higher than those needed for potentiation or MICs because the cell density needed for a detectable fluorescence signal was much higher. All fluorescence studies used a cell density of ~$6x10^9$ CFU/mL, while checkerboard assays only inoculated a cell density of $5x10^5$ CFU/mL. Therefore, an amount of 128 µg/mL BPEI for fluorescence assays is considered sub-lethal (which is tested and confirmed by resazurin assays, Figure 45). The reduction of resazurin to resorufin occurs via cellular metabolism and thus is an excellent reporter of cell viability.[190] As shown in Figure 45,

128 μg/mL of 600-Da BPEI for this large cell density (~$6x10^9$ CFU/mL) is not lethal but causes a 12.5% reduction in cell viability. However, resazurin fluorescence values for cells treated with polymyxin-B are near background levels indicating that these cells are dead. These results have several important impacts. First, the BAA-47 cells in the H33342 fluorescence assays are viable and thus drug influx and efflux processes control the intracellular concentration rather than widespread disruption of outer membrane that leads to cell lysis. Secondly, 600-Da BPEI is less toxic to *P. aeruginosa* BAA-47 cells than polymyxin B that is also toxic toward eukaryotic cells. The biocompatibility of 600-Da BPEI has been demonstrated against mouse fibroblast cells,[68] immortal human cell lines,[45] and primary human kidney epithelial cells.[45] Finally, at sub-lethal concentration, 600-Da BPEI is not disrupting cellular energy metabolism because resazurin reduction occurs via the conversion of $NADH/H^+$ to NAD^+ and thus outer membrane energetics are also likely to be unaffected.

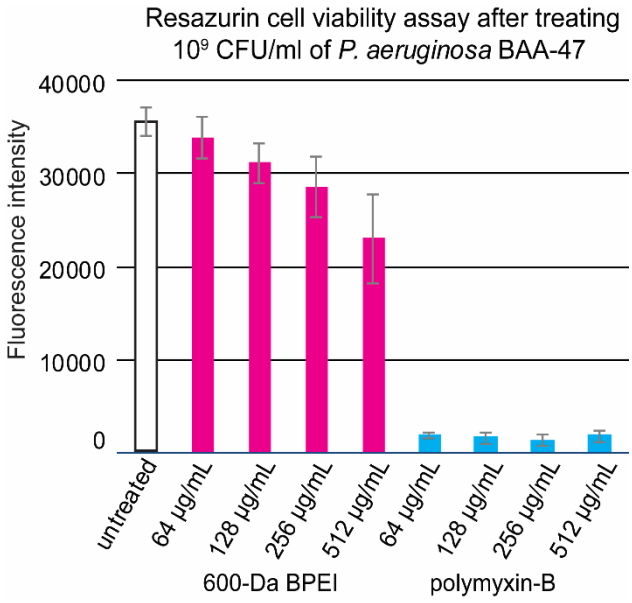


Figure 45. Incubation of PA BAA-47 cells at high cell density (~6x10^9 CFU/mL) with resazurin produces the fluorescence molecule resorufin via cellular metabolism. Treating these cells with 600-Da BPEI prior to resazurin addition results in lower emission that indicates (a) the cells are alive, (b) BPEI has affected the growth rate in a concentration-dependent manner, and (c) the cells are not depolarized. This contrasts with cells treated with polymyxin-B, which kills the cell culture at all concentrations tested. Error bar denotes standard deviation (n = 8).

The LPS leaflets are stabilized by electrostatic interactions between their anionic sites and metal ions. For instant, Mg^{2+} ions allow the formation of a stable membrane layer by binding to phosphate groups of the lipid A moiety and forming electrostatic bridges between adjacent LPS molecules. Additional phosphate and carboxylate groups are found on the core oligosaccharides.[187-188, 191-192] The o-antigen groups are decorated with hydroxyl and the occasional carboxylate groups that can also attract metal ions.[192] These anionic LPS sites are critical resistance mechanisms.[141] As Hancock found, various compounds (including cationic species), disrupt LPS's Mg^{2+} chelation and

increase *P. aeruginosa' s* susceptibility to antibacterial agents.[193-195] The primary amines on 600-Da BPEI enable it to bind with phosphate and carboxylate groups, and its flexible branches facilitate structural reorganization to reach multiple binding sites within the inner- and outer-core regions of LPS, and span adjacent LPS molecules. As a consequence, 600-Da BPEI increases the bacterial membrane permeability and allows more influx of H33342 (As shown in Figure 44).

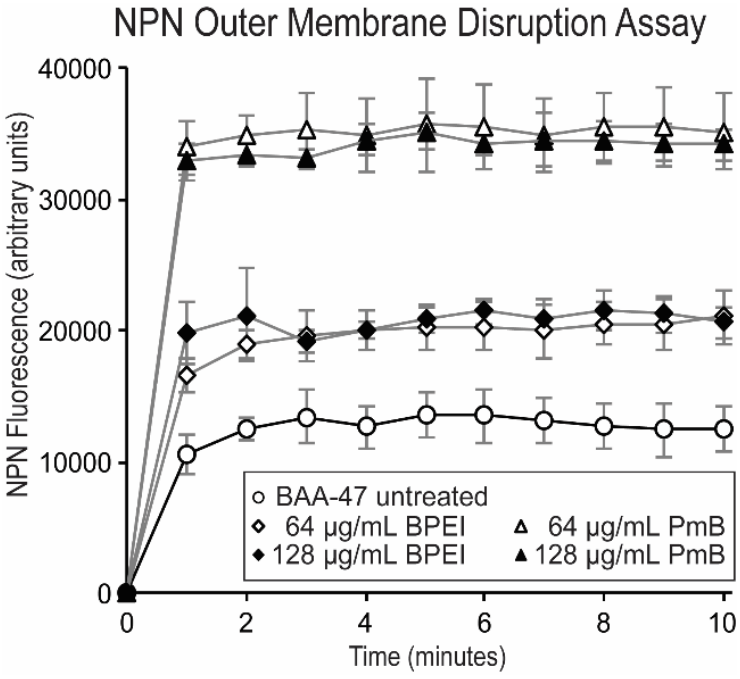


Figure 46. The dye 1-*N*-phenylnaphthylamine (NPN) accumulates in hydrophobic regions and fluoresces when bound to phosphate groups. Polymyxin-B (PmB) allows greater uptake of NPN than 600-Da BPEI. Error bars denote standard deviation.

Whether BPEI increases the permeation properties or disrupts the outer membrane lipid bilayer, H33342 and resazurin assays cannot answer the question. To better elucidate its mode of action, fluorescence probe molecule 1-*N*-phenylnaphthylamine (NPN) was used because it localizes to the lipid membrane and fluoresces when bound to phospholipids. In the absence of agents that disrupt cell

membrane, fluorescence is weak from barriers to passive diffusion. However, then the outer membrane is breached, NPN can easily reach phospholipids of the inner leaflet and fluorescence intensity increases. As shown in Figure 46, NPN fluorescence reaches value of about 13000 units in a sample of ~$6x10^9$ CFU/ml *P. aeruginosa* BAA-47 cells. Treating a similar sample with 64 µg/mL of polymyxin-B causes a 2.7 fold increase in fluorescence intensity, which occurs via insertion of polymyxin-B into the membrane via self-promoted uptake.[193] However, 64 and 128 µg/mL of 600-Da BPEI cause a 1.5 fold increase in NPN fluorescence and we know that these concentrations of 600-Da BPEI are non-lethal (Figure 45). Thus, we suggest that 600-Da BPEI is weakening the LPS diffusion barrier, but it is not intercalating into the membrane bilayer that otherwise would lead to a higher increase in NPN fluorescence intensity.

SEM images demonstrate adverse effects of 600-Da BPEI on morphology

The ability of 600-Da BPEI to weaken the LPS diffusion barrier without causing widespread membrane disruption and cell lysis is shown with scanning electron microscopy (SEM). SEM was conducted to examine morphology and the possible effects of 600-Da BPEI on bacterial cell division. *P. aeruginosa* BAA-47 cells were grown to mid-log phase and subjected to four separate treatments: untreated control, sublethal 600-Da BPEI, sub-lethal piperacillin, and combination of 600-Da BPEI and piperacillin, each at sub-lethal combinations. SEM images of the untreated control sample (Figure 47A) show that all the cells have regular rod-shape with a normal size distribution and division septa are clear. BPEI treated cells (Figure 47B) are longer and cell-division septa show a gradual narrowing rather than a sharper interface. The piperacillin treated cells (Figure 47C) are longer, do have signs of a well-form division septum, and exhibit signs of cell

wall weakening without bursting. Combination of BPEI + piperacillin caused the treated cells (Figure 47D) to rupture (Figure 47E) and show extreme distortions in shape (Figure 47F). The extreme distortions both in size (~20 times longer than untreated control cells) and shape without obvious division septa suggests that the cell envelope is damaged and that recruiting, activity, and/or competence of bacterial divisome[196-197] components is hindered. These cellular morphological changes and cell wall weakening aid in explaining the bactericidal properties of the BPEI + piperacillin combination when the concentration of each of the compounds is sub-lethal on their own.

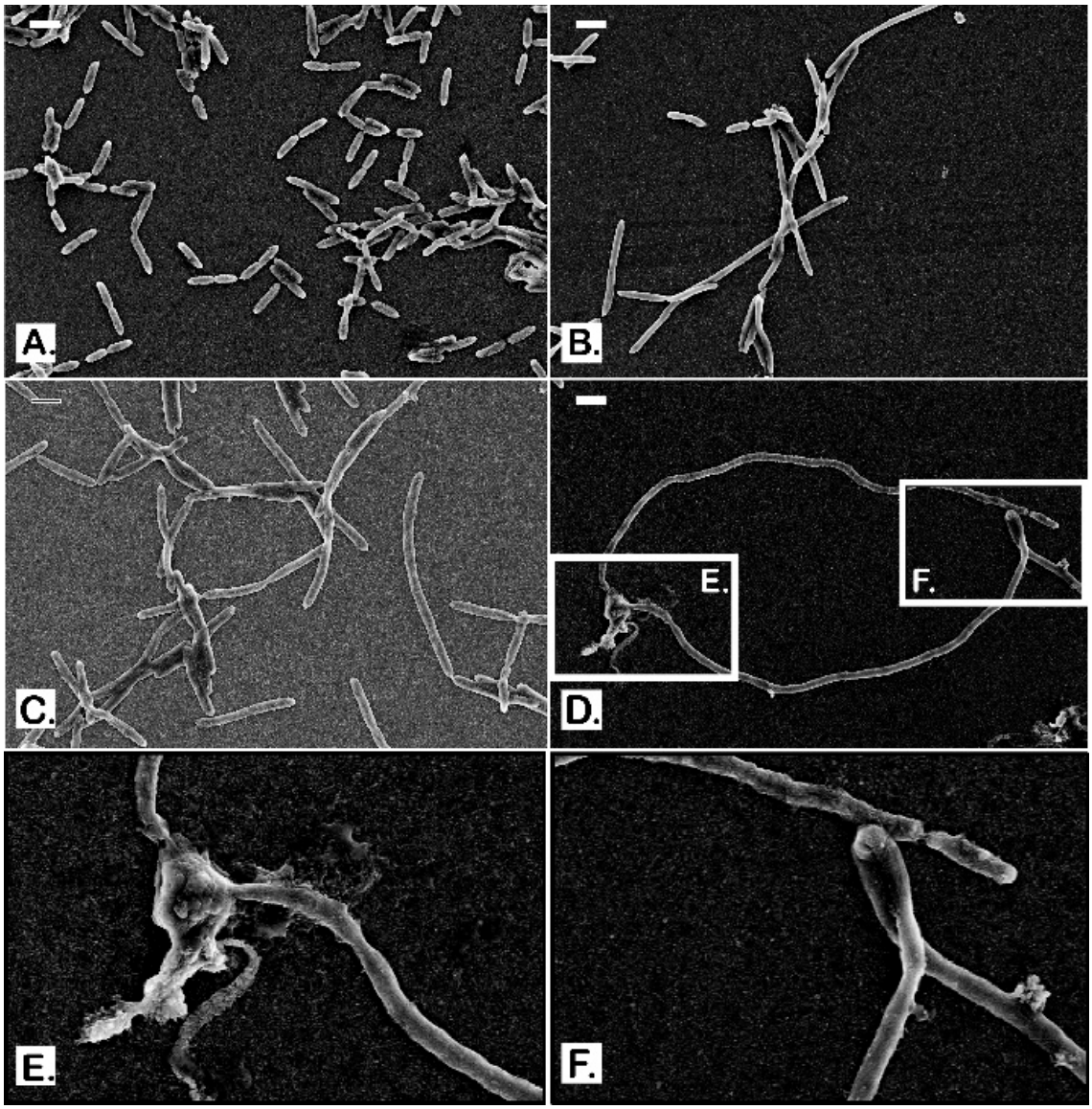


Figure 47. Scanning electron micrograph images of PA BAA-47. Untreated control cells appear with regular rod-shape of about 2-3 µm long (A). 600-Da BPEI treated cells (B) and piperacillin treated cells (C) show inconsistency in their size with longer lengths but the rod-shape remains. Combination of 600-Da BPEI + piperacillin treated cells (D) show extreme distortions both in size and shape with insets (E) and (F) for higher magnifications. Scale bars = 2µm.

Eradicating P. aeruginosa biofilms

Biofilms are accumulations of microorganisms embedded in a polysaccharide matrix known as extracellular polymeric substance (EPS), which protects the bacteria from antimicrobial agents.[169, 177] Current in-patient treatments include cleansing the wound, debridement, maintaining a moist tissue environment, and – when possible – eliminating the underlying factors that contributed to poor wound healing.[131] BPEI confronts the biofilm directly by disrupting the protective EPS. As shown in Figure 48, biofilms of *P. aeruginosa* BAA-47 create additional barriers that require 256 μg/mL of piperacillin to kill the bacteria. This minimum biofilm eradication concentration (MBEC) is significantly higher than the MIC of 4 μg/mL. Likewise, the MBEC of 600-Da BPEI is 512 μg/mL, compared to its MIC of 32 μg/mL. A combination treatment results in biofilm eradication with 16 μg/mL of BPEI and 8 μg/mL of piperacillin. As with the planktonic checkerboard assays, this data was collected without a β-lactamase inhibitor. The mechanism of action for disrupting the biofilm relies on the ability of cationic 600-Da BPEI to interact with anionic targets. Instead of binding with LPS in the planktonic cells, the biofilm targets are extracellular DNA, anionic polysaccharide Psl, and anionic polysaccharide alginic acid.[31, 65-67, 112-118] The presence of the cationic polysaccharide Pel in *P. aeruginosa* biofilms would repel BPEI, but this affect does not prevent 600-Da BPEI from disrupting the biofilm matrix and thus piperacillin can access to the underlying cells. The data in Figure 44 also confirms the paradigm that antibiotics effective against planktonic *P. aeruginosa* are nearly inert against biofilms and resistant strains. when 600-Da BPEI binds to EPS, the biofilm disperses because the intermolecular network of exopolymers, protein, and metals ions is disrupted.[2] As a result, quiescent bacteria are

released into solution where they become metabolically active and thus the antibiotic can kill the bacteria when additional BPEI molecules reduce LPS barriers to drug influx.

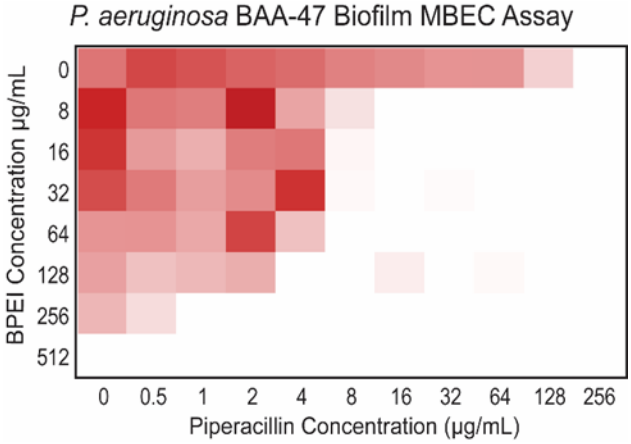


Figure 48. Biofilm eradication assay data using collected with the Calgary biofilm device. EPS creates additional barriers to piperacillin efficacy and thus 256 µg/mL are required to kill the bacteria. However, 600-Da BPEI disrupts the biofilm EPS and increases β-lactam access to the cells, reducing the MBEC to 8 µg/mL.

Conclusions

Multidrug resistance and biofilms of *Pseudomonas aeruginosa* were defeated by combination antibiotic therapy: existing β-lactam + 600-Da BPEI. Potentials of BPEI as a potentiator have shown to exceed what originally thought of only working against Gram-positive pathogens. Here, 600-Da BPEI targets LPS-mediated resistance in MDR-PA and restores piperacillin efficacy without the need for β-lactamase inhibitors. Additionally, 600-Da BPEI is attracted to anionic components of the bacterial biofilm, resulting in disruption of the extracellular matrix that dissolves the biofilms to enable anti-biofilm activity of piperacillin. Thus, 600-Da BPEI may improve patient care outcomes by restoring potency to existing antibiotics with a single potentiator. An advantage of 600-Da BPEI is that it does not need to cross the membrane itself to be

effective. By targeting the anionic inner-core and outer-core polysaccharides[141, 198] and biofilm EPS, 600-Da BPEI creates new avenues of access for antibiotics to reach their targets, Therefore, BPEI does not have to traverse the membrane for potentiation. This contrasts with other cationic antimicrobial agents, such as cationic peptides, aminoglycosides, and polymyxins, whose hydrophobic properties are required for membrane disruption. Its mechanisms of action on *P. aeruginosa* have been examined and documented to provide a strong foundation of understanding for future drug design and development.

Despite their tiny size, each pathogenic microorganism has an exquisite mechanism to survive, infect, and reproduce. For centuries, we coexist. Diseases are inevitable. Whether it's a virulent strain of *P. aeruginosa* or an opportunistic *S. epidermidis*, we never know when these bacteria would gene-transfer or mutate into a deadly one. The best way to mitigate is to study and research—an art that saves lives. And I am determined to be an artist!

References

1. Lam, A. K.; Hill, M. A.; Moen, E. L.; Pusavat, J.; Wouters, C. L.; Rice, C. V., Cationic Branched Polyethylenimine (BPEI) Disables Antibiotic Resistance in Methicillin-Resistant Staphylococcus epidermidis (MRSE). *ChemMedChem* **2018,** *13* (20), 2240-2248.
2. Lam, A. K.; Wouters, C. L.; Moen, E. L.; Pusavat, J.; Rice, C. V., Antibiofilm Synergy of beta-Lactams and Branched Polyethylenimine against Methicillin-Resistant Staphylococcus epidermidis. *Biomacromolecules* **2019,** *20* (10), 3778-3785.
3. Lam, A. K.; Panlilio, H.; Pusavat, J.; Wouters, C. L.; Moen, E. L.; Brennan, R. E.; Rice, C., Expanding the spectrum of antibiotics capable of killing multi-drug resistant Staphylococcus aureus and Pseudomonas aeruginosa. *ChemMedChem* **2020**.
4. Lam, A. K.; Panlilio, H.; Pusavat, J.; Wouters, C. L.; Moen, E. L.; Neel, A. J.; Rice, C. V., Low-molecular-weight Branched Polyethylenimine Potentiates Ampicillin against MRSA Biofilms. *ACS Medicinal Chemistry Letters* **2020**.
5. Lam, A. K.; Panlilio, H.; Pusavat, J.; Wouters, C. L.; Moen, E. L.; Rice, C. V., Overcoming Multidrug Resistance and Biofilms of Pseudomonas aeruginosa with a Single Dual-Function Potentiator of β-Lactams. *ACS Infectious Diseases* **2020**.
6. CDC, Antibiotic Resistance Threats in the United States 2019. Atlanta, GA: U.S Department of Health and Human Services, CDC;. **2019**.
7. de Kraker, M. E.; Stewardson, A. J.; Harbarth, S., Will 10 million people die a year due to antimicrobial resistance by 2050? *PLoS medicine* **2016,** *13* (11), e1002184.
8. Bennett, J. W.; Chung, K.-T., Alexander Fleming and the discovery of penicillin. **2001**.
9. Debono, M.; Barnhart, M.; Carrell, C.; Hoffmann, J.; Occolowitz, J.; Abbott, B.; Fukuda, D.; Hamill, R.; Biemann, K.; Herlihy, W., A21978C, a complex of new acidic peptide antibiotics: isolation, chemistry, and mass spectral structure elucidation. *The Journal of antibiotics* **1987,** *40* (6), 761-777.
10. Silver, L. L., Challenges of antibacterial discovery. *Clin Microbiol Rev* **2011,** *24* (1), 71-109.
11. Tortora, G. J.; Funke, B. R.; Case, C. L.; Johnson, T. R., *Microbiology: an introduction*. Benjamin Cummings San Francisco, CA: 2004; Vol. 9.
12. Kohanski, M. A.; Dwyer, D. J.; Collins, J. J., How antibiotics kill bacteria: from targets to networks. *Nat Rev Microbiol* **2010,** *8* (6), 423-35.
13. Grace, D., Review of evidence on antimicrobial resistance and animal agriculture in developing countries. **2015**.
14. Santajit, S.; Indrawattana, N., Mechanisms of Antimicrobial Resistance in ESKAPE Pathogens. *Biomed Res Int* **2016,** *2016*, 2475067.
15. Vestergaard, M.; Frees, D.; Ingmer, H., Antibiotic Resistance and the MRSA Problem. *Microbiology spectrum* **2019,** *7* (2).
16. Grice, E. A.; Kong, H. H.; Conlan, S.; Deming, C. B.; Davis, J.; Young, A. C.; Bouffard, G. G.; Blakesley, R. W.; Murray, P. R.; Green, E. D., Topographical and temporal diversity of the human skin microbiome. *science* **2009,** *324* (5931), 1190-1192.
17. Percival, S. L.; Suleman, L.; Vuotto, C.; Donelli, G., Healthcare-associated infections, medical devices and biofilms: risk, tolerance and control. *J Med Microbiol* **2015,** *64* (Pt 4), 323-34.
18. Otto, M., Staphylococcus epidermidis--the 'accidental' pathogen. *Nat Rev Microbiol* **2009,** *7* (8), 555-67.
19. Neely, A. N.; Maley, M. P., Survival of enterococci and staphylococci on hospital fabrics and plastic. *Journal of clinical microbiology* **2000,** *38* (2), 724-726.
20. Chu, V.; Miro, J. M.; Hoen, B.; Cabell, C. H.; Pappas, P. A.; Jones, P.; Stryjewski, M. E.; Anguera, I.; Braun, S.; Munoz, P., Coagulase-negative staphylococcal prosthetic valve

endocarditis—a contemporary update based on the International Collaboration on Endocarditis: prospective cohort study. *Heart* **2009,** *95* (7), 570-576.
21. Sidhu, M. S.; Heir, E.; Leegaard, T.; Wiger, K.; Holck, A., Frequency of disinfectant resistance genes and genetic linkage with beta-lactamase transposon Tn552 among clinical staphylococci. *Antimicrob Agents Chemother* **2002,** *46* (9), 2797-803.
22. Zhang, M.; O'Donoghue, M. M.; Ito, T.; Hiramatsu, K.; Boost, M. V., Prevalence of antiseptic-resistance genes in Staphylococcus aureus and coagulase-negative staphylococci colonising nurses and the general population in Hong Kong. *J Hosp Infect* **2011,** *78* (2), 113-7.
23. Becker, K.; Heilmann, C.; Peters, G., Coagulase-negative staphylococci. *Clin Microbiol Rev* **2014,** *27* (4), 870-926.
24. Magner, L. N., *A history of infectious diseases and the microbial world*. Praeger: Westport, Conn., 2009; p xxiv, 225 p.
25. Cowan, M. K.; Talaro, K. P., *Microbiology : a systems approach*. 2nd ed.; McGraw-Hill: Boston, 2009; p xxi, 869 p.
26. Ramachandran, G., Gram-positive and gram-negative bacterial toxins in sepsis: a brief review. *Virulence* **2014,** *5* (1), 213-8.
27. Fleming, A., Penicillin. *British medical journal* **1941,** *2* (4210), 386.
28. Hicks, L. A.; Bartoces, M. G.; Roberts, R. M.; Suda, K. J.; Hunkler, R. J.; Taylor Jr, T. H.; Schrag, S. J., US outpatient antibiotic prescribing variation according to geography, patient population, and provider specialty in 2011. *Clinical Infectious Diseases* **2015,** *60* (9), 1308-1316.
29. Ventola, C. L., The antibiotic resistance crisis: part 1: causes and threats. *Pharmacy and therapeutics* **2015,** *40* (4), 277.
30. Diep, B. A.; Gill, S. R.; Chang, R. F.; Phan, T. H.; Chen, J. H.; Davidson, M. G.; Lin, F.; Lin, J.; Carleton, H. A.; Mongodin, E. F.; Sensabaugh, G. F.; Perdreau-Remington, F., Complete genome sequence of USA300, an epidemic clone of community-acquired meticillin-resistant Staphylococcus aureus. *Lancet* **2006,** *367* (9512), 731-9.
31. Wagstaff, J. L.; Sadovskaya, I.; Vinogradov, E.; Jabbouri, S.; Howard, M. J., Poly-N-acetylglucosamine and poly(glycerol phosphate) teichoic acid identification from staphylococcal biofilm extracts using excitation sculptured TOCSY NMR. *Mol Biosyst* **2008,** *4* (2), 170-4.
32. Schaeffer, C. R.; Hoang, T. N.; Sudbeck, C. M.; Alawi, M.; Tolo, I. E.; Robinson, D. A.; Horswill, A. R.; Rohde, H.; Fey, P. D., Versatility of Biofilm Matrix Molecules in Staphylococcus epidermidis Clinical Isolates and Importance of Polysaccharide Intercellular Adhesin Expression during High Shear Stress. *mSphere* **2016,** *1* (5), e00165-16.
33. Chokr, A.; Leterme, D.; Watier, D.; Jabbouri, S., Neither the presence of ica locus, nor in vitro-biofilm formation ability is a crucial parameter for some Staphylococcus epidermidis strains to maintain an infection in a guinea pig tissue cage model. *Microb Pathog* **2007,** *42* (2-3), 94-7.
34. Rupp, M. E.; Ulphani, J. S.; Fey, P. D.; Mack, D., Characterization of Staphylococcus epidermidisPolysaccharide Intercellular Adhesin/Hemagglutinin in the Pathogenesis of Intravascular Catheter-Associated Infection in a Rat Model. *Infection and Immunity* **1999,** *67* (5), 2656-2659.
35. Rupp, M. E.; Fey, P. D.; Heilmann, C.; Gotz, F., Characterization of the importance of Staphylococcus epidermidis autolysin and polysaccharide intercellular adhesin in the pathogenesis of intravascular catheter-associated infection in a rat model. *J Infect Dis* **2001,** *183* (7), 1038-42.
36. Zhuk, D. S.; Gembitskii, P. A.; Kargin, V. A., Advances in the chemistry of polyethyleneimine (polyaziridine). *Russian Chemical Reviews* **1965,** *34* (7), 515.
37. Steuerle, U.; Feuerhake, R., Aziridines. In *Ullmann's Encyclopedia of Industrial Chemistry*, 2006.

38. Parhamifar, L.; Larsen, A. K.; Hunter, A. C.; Andresen, T. L.; Moghimi, S. M., Polycation cytotoxicity: a delicate matter for nucleic acid therapy—focus on polyethylenimine. *Soft Matter* **2010,** *6* (17), 4001-4009.
39. Jager, M.; Schubert, S.; Ochrimenko, S.; Fischer, D.; Schubert, U. S., Branched and linear poly(ethylene imine)-based conjugates: synthetic modification, characterization, and application. *Chem Soc Rev* **2012,** *41* (13), 4755-67.
40. Thomas, K. J.; Rice, C. V., Equilibrium binding behavior of magnesium to wall teichoic acid. *Bba-Biomembranes* **2015,** *1848* (10), 1981-1987.
41. Foxley, M., Branched polyethylenimine re-sensitizes methicillin-resistant Staphylococcus aureus to beta-lactam antibioitics through a novel mechanism of action. **2018**.
42. Dick, C. R.; Potter, J. L.; Coker, W. P., Process for the selective alkylation of polyalkylene polyamines. Google Patents: 1971.
43. Wightman, L.; Kircheis, R.; Rossler, V.; Carotta, S.; Ruzicka, R.; Kursa, M.; Wagner, E., Different behavior of branched and linear polyethylenimine for gene delivery in vitro and in vivo. *J Gene Med* **2001,** *3* (4), 362-72.
44. Zhang, C.; Wu, F.-G.; Hu, P.; Chen, Z., Interaction of Polyethylenimine with Model Cell Membranes Studied by Linear and Nonlinear Spectroscopic Techniques. *The Journal of Physical Chemistry C* **2014,** *118* (23), 12195-12205.
45. Foxley, M. A.; Wright, S. N.; Lam, A. K.; Friedline, A. W.; Strange, S. J.; Xiao, M. T.; Moen, E. L.; Rice, C. V., Targeting Wall Teichoic Acid in Situ with Branched Polyethylenimine Potentiates beta-Lactam Efficacy against MRSA. *ACS Med Chem Lett* **2017,** *8* (10), 1083-1088.
46. Wiegand, C.; Bauer, M.; Hipler, U. C.; Fischer, D., Poly(ethyleneimines) in dermal applications: biocompatibility and antimicrobial effects. *Int J Pharm* **2013,** *456* (1), 165-74.
47. Claessens, H.; Van Straten, M., Review on the chemical and thermal stability of stationary phases for reversed-phase liquid chromatography. *Journal of Chromatography A* **2004,** *1060* (1-2), 23-41.
48. Krstulovic, A.; Brown, P. R., Reversed-phase high-performance liquid chromatography. In *Theory, Practice, and Biomedical Applications*, Wiley New York: 1982.
49. Behm, B.; Babilas, P.; Landthaler, M.; Schreml, S., Cytokines, chemokines and growth factors in wound healing. *Journal of the European Academy of Dermatology and Venereology* **2012,** *26* (7), 812-820.
50. Mast, B. A.; Schultz, G. S., Interactions of cytokines, growth factors, and proteases in acute and chronic wounds. *Wound Repair and Regeneration* **1996,** *4* (4), 411-420.
51. Gillitzer, R.; Goebeler, M., Chemokines in cutaneous wound healing. *Journal of leukocyte biology* **2001,** *69* (4), 513-521.
52. Ferreira, V. L.; Borba, H. H.; Bonetti, A. d. F.; Leonart, L. P.; Pontarolo, R., Cytokines and interferons: types and functions. In *Autoantibodies and Cytokines*, IntechOpen: 2018.
53. Gerard, C.; Rollins, B. J., Chemokines and disease. *Nature immunology* **2001,** *2* (2), 108-115.
54. McDonald, C.; Inohara, N.; Nuñez, G., Peptidoglycan signaling in innate immunity and inflammatory disease. *Journal of Biological Chemistry* **2005,** *280* (21), 20177-20180.
55. Jones, R. E.; Foster, D. S.; Longaker, M. T., Management of Chronic Wounds-2018. *JAMA* **2018,** *320* (14), 1481-1482.
56. Sen, C. K.; Gordillo, G. M.; Roy, S.; Kirsner, R.; Lambert, L.; Hunt, T. K.; Gottrup, F.; Gurtner, G. C.; Longaker, M. T., Human skin wounds: a major and snowballing threat to public health and the economy. *Wound Repair Regen* **2009,** *17* (6), 763-71.
57. Omar, A.; Wright, J. B.; Schultz, G.; Burrell, R.; Nadworny, P., Microbial Biofilms and Chronic Wounds. *Microorganisms* **2017,** *5* (1).
58. Wolcott, R., Disrupting the biofilm matrix improves wound healing outcomes. *J Wound Care* **2015,** *24* (8), 366-71.

59. Cherifi, S.; Byl, B.; Deplano, A.; Nonhoff, C.; Denis, O.; Hallin, M., Comparative epidemiology of Staphylococcus epidermidis isolates from patients with catheter-related bacteremia and from healthy volunteers. *J Clin Microbiol* **2013,** *51* (5), 1541-7.
60. Snowden, J. N.; Beaver, M.; Smeltzer, M. S.; Kielian, T., Biofilm-infected intracerebroventricular shunts elicit inflammation within the central nervous system. *Infection and immunity* **2012,** *80* (9), 3206-3214.
61. Farha, M. A.; Leung, A.; Sewell, E. W.; D'Elia, M. A.; Allison, S. E.; Ejim, L.; Pereira, P. M.; Pinho, M. G.; Wright, G. D.; Brown, E. D., Inhibition of WTA synthesis blocks the cooperative action of PBPs and sensitizes MRSA to beta-lactams. *ACS Chem Biol* **2013,** *8* (1), 226-33.
62. European Committee for Antimicrobial Susceptibility Testing of the European Society of Clinical, M.; Infectious, D., EUCAST Definitive Document E.Def 1.2, May 2000: Terminology relating to methods for the determination of susceptibility of bacteria to antimicrobial agents. *Clin Microbiol Infect* **2000,** *6* (9), 503-8.
63. Knox, J. R.; Pratt, R. F., Different modes of vancomycin and D-alanyl-D-alanine peptidase binding to cell wall peptide and a possible role for the vancomycin resistance protein. *Antimicrob Agents Chemother* **1990,** *34* (7), 1342-7.
64. Mann, P. A.; Muller, A.; Wolff, K. A.; Fischmann, T.; Wang, H.; Reed, P.; Hou, Y.; Li, W.; Muller, C. E.; Xiao, J.; Murgolo, N.; Sher, X.; Mayhood, T.; Sheth, P. R.; Mirza, A.; Labroli, M.; Xiao, L.; McCoy, M.; Gill, C. J.; Pinho, M. G.; Schneider, T.; Roemer, T., Chemical Genetic Analysis and Functional Characterization of Staphylococcal Wall Teichoic Acid 2-Epimerases Reveals Unconventional Antibiotic Drug Targets. *PLoS Pathog* **2016,** *12* (5), e1005585.
65. Arciola, C. R.; Campoccia, D.; Speziale, P.; Montanaro, L.; Costerton, J. W., Biofilm formation in Staphylococcus implant infections. A review of molecular mechanisms and implications for biofilm-resistant materials. *Biomaterials* **2012,** *33* (26), 5967-82.
66. Bucher, T.; Oppenheimer-Shaanan, Y.; Savidor, A.; Bloom-Ackermann, Z.; Kolodkin-Gal, I., Disturbance of the bacterial cell wall specifically interferes with biofilm formation. *Environ Microbiol Rep* **2015,** *7* (6), 990-1004.
67. Holland, L. M.; Conlon, B.; O'Gara, J. P., Mutation of tagO reveals an essential role for wall teichoic acids in Staphylococcus epidermidis biofilm development. *Microbiology* **2011,** *157* (Pt 2), 408-18.
68. Foxley, M. A.; Friedline, A. W.; Jensen, J. M.; Nimmo, S. L.; Scull, E. M.; King, J. B.; Strange, S.; Xiao, M. T.; Smith, B. E.; Thomas Iii, K. J.; Glatzhofer, D. T.; Cichewicz, R. H.; Rice, C. V., Efficacy of ampicillin against methicillin-resistant Staphylococcus aureus restored through synergy with branched poly(ethylenimine). *J Antibiot (Tokyo)* **2016,** *69* (12), 871-878.
69. CDC Antibiotic resistance threats in the United States 2013. http://www.cdc.gov/drugresistance/threat-report-2013/.
70. Vuong, C.; Otto, M., Staphylococcus epidermidis infections. *Microbes and Infection* **2002,** *4* (4), 481-489.
71. Farha, M. A.; Leung, A.; Sewell, E. W.; D'Elia, M. A.; Allison, S. E.; Ejim, L.; Pereira, P. M.; Pinho, M. G.; Wright, G. D.; Brown, E. D., Inhibition of WTA Synthesis Blocks the Cooperative Action of PBPs and Sensitizes MRSA to β-Lactams. *ACS Chemical Biology* **2012,** *8* (1), 226-233.
72. Wang, H.; Gill, Charles J.; Lee, Sang H.; Mann, P.; Zuck, P.; Meredith, Timothy C.; Murgolo, N.; She, X.; Kales, S.; Liang, L.; Liu, J.; Wu, J.; Santa Maria, J.; Su, J.; Pan, J.; Hailey, J.; McGuinness, D.; Tan, Christopher M.; Flattery, A.; Walker, S.; Black, T.; Roemer, T., Discovery of Wall Teichoic Acid Inhibitors as Potential Anti-MRSA β-Lactam Combination Agents. *Chemistry & Biology* **2013,** *20* (2), 272-284.
73. Pasquina, L. W.; Santa Maria, J. P.; Walker, S., Teichoic acid biosynthesis as an antibiotic target. *Current Opinion in Microbiology* **2013,** *16* (5), 531-537.

74. Campbell, J.; Singh, A. K.; Santa Maria, J. P.; Kim, Y.; Brown, S.; Swoboda, J. G.; Mylonakis, E.; Wilkinson, B. J.; Walker, S., Synthetic Lethal Compound Combinations Reveal a Fundamental Connection between Wall Teichoic Acid and Peptidoglycan Biosyntheses inStaphylococcus aureus. *ACS Chemical Biology* **2011,** *6* (1), 106-116.
75. Swoboda, J. G.; Meredith, T. C.; Campbell, J.; Brown, S.; Suzuki, T.; Bollenbach, T.; Malhowski, A. J.; Kishony, R.; Gilmore, M. S.; Walker, S., Discovery of a Small Molecule that Blocks Wall Teichoic Acid Biosynthesis inStaphylococcus aureus. *ACS Chemical Biology* **2009,** *4* (10), 875-883.
76. D'Elia, M. A.; Millar, K. E.; Beveridge, T. J.; Brown, E. D., Wall Teichoic Acid Polymers Are Dispensable for Cell Viability in Bacillus subtilis. *Journal of Bacteriology* **2006,** *188* (23), 8313-8316.
77. Bhavsar, A. P.; Erdman, L. K.; Schertzer, J. W.; Brown, E. D., Teichoic Acid Is an Essential Polymer in Bacillus subtilis That Is Functionally Distinct from Teichuronic Acid. *Journal of Bacteriology* **2004,** *186* (23), 7865-7873.
78. Lee, S. H.; Wang, H.; Labroli, M.; Koseoglu, S.; Zuck, P.; Mayhood, T.; Gill, C.; Mann, P.; Sher, X.; Ha, S.; Yang, S.-W.; Mandal, M.; Yang, C.; Liang, L.; Tan, Z.; Tawa, P.; Hou, Y.; Kuvelkar, R.; DeVito, K.; Wen, X.; Xiao, J.; Batchlett, M.; Balibar, C. J.; Liu, J.; Xiao, J.; Murgolo, N.; Garlisi, C. G.; Sheth, P. R.; Flattery, A.; Su, J.; Tan, C.; Roemer, T., TarO-specific inhibitors of wall teichoic acid biosynthesis restore β-lactam efficacy against methicillin-resistant staphylococci. *Science Translational Medicine* **2016,** *8* (329), 329ra32-329ra32.
79. Mandal, M.; Tan, Z.; Madsen-Duggan, C.; Buevich, A. V.; Caldwell, J. P.; Dejesus, R.; Flattery, A.; Garlisi, C. G.; Gill, C.; Ha, S. N.; Ho, G.; Koseoglu, S.; Labroli, M.; Basu, K.; Lee, S. H.; Liang, L.; Liu, J.; Mayhood, T.; McGuinness, D.; McLaren, D. G.; Wen, X.; Parmee, E.; Rindgen, D.; Roemer, T.; Sheth, P.; Tawa, P.; Tata, J.; Yang, C.; Yang, S.-W.; Xiao, L.; Wang, H.; Tan, C.; Tang, H.; Walsh, P.; Walsh, E.; Wu, J.; Su, J., Can We Make Small Molecules Lean? Optimization of a Highly Lipophilic TarO Inhibitor. *Journal of Medicinal Chemistry* **2017,** *60* (9), 3851-3865.
80. Foxley, M. A.; Wright, S. N.; Lam, A. K.; Friedline, A. W.; Strange, S. J.; Xiao, M. T.; Moen, E. L.; Rice, C. V., Targeting Wall Teichoic Acid in Situ with Branched Polyethylenimine Potentiates β-Lactam Efficacy against MRSA. *ACS Medicinal Chemistry Letters* **2017,** *8* (10), 1083-1088.
81. Foxley, M. A.; Friedline, A. W.; Jensen, J. M.; Nimmo, S. L.; Scull, E. M.; King, J. B.; Strange, S.; Xiao, M. T.; Smith, B. E.; Thomas Iii, K. J.; Glatzhofer, D. T.; Cichewicz, R. H.; Rice, C. V., Efficacy of ampicillin against methicillin-resistant Staphylococcus aureus restored through synergy with branched poly(ethylenimine). *The Journal of Antibiotics* **2016,** *69* (12), 871-878.
82. Diep, B. A.; Gill, S. R.; Chang, R. F.; Phan, T. H.; Chen, J. H.; Davidson, M. G.; Lin, F.; Lin, J.; Carleton, H. A.; Mongodin, E. F.; Sensabaugh, G. F.; Perdreau-Remington, F., Complete genome sequence of USA300, an epidemic clone of community-acquired meticillin-resistant Staphylococcus aureus. *The Lancet* **2006,** *367* (9512), 731-739.
83. Hanssen, A. M.; Kjeldsen, G.; Sollid, J. U. E., Local Variants of Staphylococcal Cassette Chromosome mec in Sporadic Methicillin-Resistant Staphylococcus aureus and Methicillin-Resistant Coagulase-Negative Staphylococci: Evidence of Horizontal Gene Transfer? *Antimicrob. Agents Chemother.* **2003,** *48* (1), 285-296.
84. Marraffini, L. A.; Sontheimer, E. J., CRISPR Interference Limits Horizontal Gene Transfer in Staphylococci by Targeting DNA. *Science* **2008,** *322* (5909), 1843-1845.
85. Raad, I.; Hanna, H.; Maki, D., Intravascular catheter-related infections: advances in diagnosis, prevention, and management. *The Lancet Infectious Diseases* **2007,** *7* (10), 645-657.
86. Gagnon, R. F.; Richards, G. K.; Subang, R., Experimental Staphylococcus epidermidis Implant Infection in the Mouse. *ASAIO Journal* **1992,** *38* (3), M596-M599.

87. Raad, I.; Hanna, H.; Jiang, Y.; Dvorak, T.; Reitzel, R.; Chaiban, G.; Sherertz, R.; Hachem, R., Comparative Activities of Daptomycin, Linezolid, and Tigecycline against Catheter-Related Methicillin-Resistant Staphylococcus Bacteremic Isolates Embedded in Biofilm. *Antimicrob. Agents Chemother.* **2007,** *51* (5), 1656-1660.
88. Sieradzki, K.; Roberts, R. B.; Serur, D.; Hargrave, J.; Tomasz, A., Heterogeneously vancomycin-resistant Staphylococcus epidermidis strain causing recurrent peritonitis in a dialysis patient during vancomycin therapy. *J Clin Microbiol* **1999,** *37* (1), 39-44.
89. Schwalbe, R. S.; Stapleton, J. T.; Gilligan, P. H., Emergence of Vancomycin Resistance in Coagulase-Negative Staphylococci. *New England Journal of Medicine* **1987,** *316* (15), 927-931.
90. Nery, P. B.; Fernandes, R.; Nair, G. M.; Sumner, G. L.; Ribas, C. S.; Menon, S. M.; Wang, X.; Krahn, A. D.; Morillo, C. A.; Connolly, S. J.; Healey, J. S., Device-related infection among patients with pacemakers and implantable defibrillators: incidence, risk factors, and consequences. *J Cardiovasc Electrophysiol* **2010,** *21* (7), 786-90.
91. Maki, D. G.; Kluger, D. M.; Crnich, C. J., The risk of bloodstream infection in adults with different intravascular devices: a systematic review of 200 published prospective studies. *Mayo Clin Proc* **2006,** *81* (9), 1159-71.
92. Romling, U.; Balsalobre, C., Biofilm infections, their resilience to therapy and innovative treatment strategies. *J Intern Med* **2012,** *272* (6), 541-61.
93. Wolfmeier, H.; Pletzer, D.; Mansour, S. C.; Hancock, R. E. W., New Perspectives in Biofilm Eradication. *ACS Infect Dis* **2018,** *4* (2), 93-106.
94. James, G. A.; Swogger, E.; Wolcott, R.; Pulcini, E.; Secor, P.; Sestrich, J.; Costerton, J. W.; Stewart, P. S., Biofilms in chronic wounds. *Wound Repair Regen* **2008,** *16* (1), 37-44.
95. Ceri, H.; Olson, M.; Morck, D.; Storey, D.; Read, R.; Buret, A.; Olson, B., The MBEC assay system: Multiple equivalent biofilms for antibiotic and biocide susceptibility testing. In *Methods in enzymology*, Elsevier: 2001; Vol. 337, pp 377-385.
96. Ceri, H.; Olson, M. E.; Stremick, C.; Read, R. R.; Morck, D.; Buret, A., The Calgary Biofilm Device: New Technology for Rapid Determination of Antibiotic Susceptibilities of Bacterial Biofilms. *J. CLIN. MICROBIOL.* **1999,** *37*, 6.
97. Olson, M. E.; Ceri, H.; Morck, D. W.; Buret, A. G.; Read, R. R., Biofilm bacteria: formation and comparative susceptibility to antibiotics. *Can J Vet Res* **2002,** *66* (2), 86-92.
98. Odds, F. C., Synergy, antagonism, and what the chequerboard puts between them. *J Antimicrob Chemother* **2003,** *52* (1), 1.
99. Schuch, R.; Khan, B. K.; Raz, A.; Rotolo, J. A.; Wittekind, M., Bacteriophage Lysin CF-301, a Potent Antistaphylococcal Biofilm Agent. *Antimicrob Agents Chemother* **2017,** *61* (7), e02666-16, /aac/61/7/e02666-16.atom.
100. Pabst, B.; Pitts, B.; Lauchnor, E.; Stewart, P. S., Gel-Entrapped Staphylococcus aureus Bacteria as Models of Biofilm Infection Exhibit Growth in Dense Aggregates, Oxygen Limitation, Antibiotic Tolerance, and Heterogeneous Gene Expression. *Antimicrob Agents Chemother* **2016,** *60* (10), 6294-301.
101. *Bacterial biofilms*. Springer: Berlin, 2008; p 293.
102. Pourmand, M. R.; Clarke, S. R.; Schuman, R. F.; Mond, J. J.; Foster, S. J., Identification of antigenic components of Staphylococcus epidermidis expressed during human infection. *Infect Immun* **2006,** *74* (8), 4644-54.
103. Heilmann, C.; Gerke, C.; Perdreau-Remington, F.; Tz, F. G., Characterization of Tn917 Insertion Mutants of Staphylococcus epidermidis Affected in Biofilm Formation. *INFECT. IMMUN.* **1996,** *64*, 8.
104. Heilmann, C.; Schweitzer, O.; Gerke, C.; Vanittanakom, N.; Mack, D.; Gotz, F., Molecular basis of intercellular adhesion in the biofilm-forming Staphylococcus epidermidis. *Mol Microbiol* **1996,** *20* (5), 1083-91.

105. Rupp, M. E.; Ulphani, J. S.; Fey, P. D.; Mack, D., Characterization of Staphylococcus epidermidis polysaccharide intercellular adhesin/hemagglutinin in the pathogenesis of intravascular catheter-associated infection in a rat model. *Infect Immun* **1999,** *67* (5), 2656-9.
106. Kocianova, S.; Vuong, C.; Yao, Y.; Voyich, J. M.; Fischer, E. R.; DeLeo, F. R.; Otto, M., Key role of poly-gamma-DL-glutamic acid in immune evasion and virulence of Staphylococcus epidermidis. *J Clin Invest* **2005,** *115* (3), 688-94.
107. Wiegand, C.; Bauer, M.; Hipler, U.-C.; Fischer, D., Poly (ethyleneimines) in dermal applications: biocompatibility and antimicrobial effects. *International journal of pharmaceutics* **2013,** *456* (1), 165-174.
108. Zimmerli, W.; Waldvogel, F. A.; Vaudaux, P.; Nydegger, U. E., Pathogenesis of foreign body infection: description and characteristics of an animal model. *J Infect Dis* **1982,** *146* (4), 487-97.
109. Bottcher, T.; Kolodkin-Gal, I.; Kolter, R.; Losick, R.; Clardy, J., Synthesis and activity of biomimetic biofilm disruptors. *J Am Chem Soc* **2013,** *135* (8), 2927-30.
110. Donlan, R. M., Biofilms: microbial life on surfaces. *Emerg Infect Dis* **2002,** *8* (9), 881-90.
111. Okajima, Y.; Kobayakawa, S.; Tsuji, A.; Tochikubo, T., Biofilm formation by Staphylococcus epidermidis on intraocular lens material. *Invest Ophthalmol Vis Sci* **2006,** *47* (7), 2971-5.
112. Jennings, L. K.; Storek, K. M.; Ledvina, H. E.; Coulon, C.; Marmont, L. S.; Sadovskaya, I.; Secor, P. R.; Tseng, B. S.; Scian, M.; Filloux, A.; Wozniak, D. J.; Howell, P. L.; Parsek, M. R., Pel is a cationic exopolysaccharide that cross-links extracellular DNA in the Pseudomonas aeruginosa biofilm matrix. *Proc Natl Acad Sci U S A* **2015,** *112* (36), 11353-8.
113. Sadovskaya, I.; Vinogradov, E.; Li, J.; Jabbouri, S., Structural elucidation of the extracellular and cell-wall teichoic acids of Staphylococcus epidermidis RP62A, a reference biofilm-positive strain. *Carbohydr Res* **2004,** *339* (8), 1467-73.
114. Vinogradov, E.; Sadovskaya, I.; Li, J.; Jabbouri, S., Structural elucidation of the extracellular and cell-wall teichoic acids of Staphylococcus aureus MN8m, a biofilm forming strain. *Carbohydr Res* **2006,** *341* (6), 738-43.
115. Joo, H. S.; Otto, M., Mechanisms of resistance to antimicrobial peptides in staphylococci. *Biochim Biophys Acta* **2015,** *1848* (11 Pt B), 3055-61.
116. Krismer, B.; Weidenmaier, C.; Zipperer, A.; Peschel, A., The commensal lifestyle of Staphylococcus aureus and its interactions with the nasal microbiota. *Nat Rev Microbiol* **2017,** *15* (11), 675-687.
117. Laverty, G.; Gorman, S. P.; Gilmore, B. F., Biomolecular mechanisms of staphylococcal biofilm formation. *Future Microbiol* **2013,** *8* (4), 509-24.
118. O'Neill, E.; Pozzi, C.; Houston, P.; Smyth, D.; Humphreys, H.; Robinson, D. A.; O'Gara, J. P., Association between methicillin susceptibility and biofilm regulation in Staphylococcus aureus isolates from device-related infections. *J Clin Microbiol* **2007,** *45* (5), 1379-88.
119. Hill, M. A.; Lam, A. K.; Reed, P.; Harney, M. C.; Wilson, B. A.; Moen, E. L.; Wright, S. N.; Pinho, M. G.; Rice, C. V., BPEI-Induced Delocalization of PBP4 Potentiates β-Lactams against MRSA. *Biochemistry* **2019,** *58* (36), 3813-3822.
120. Malone, M.; Bjarnsholt, T.; McBain, A. J.; James, G. A.; Stoodley, P.; Leaper, D.; Tachi, M.; Schultz, G.; Swanson, T.; Wolcott, R. D., The prevalence of biofilms in chronic wounds: a systematic review and meta-analysis of published data. *Journal of Wound Care* **2017,** *26* (1), 20-25.
121. Roy, S.; Santra, S.; Das, A.; Dixith, S.; Sinha, M.; Ghatak, S.; Ghosh, N.; Banerjee, P.; Khanna, S.; Mathew-Steiner, S.; Ghatak, P. D.; Blackstone, B. N.; Powell, H. M.; Bergdall, V. K.; Wozniak, D. J.; Sen, C. K., Staphylococcus aureus Biofilm Infection Compromises Wound Healing by Causing Deficiencies in Granulation Tissue Collagen. *Ann Surg* **2019**.

122. Malani, P. N., National burden of invasive methicillin-resistant Staphylococcus aureus infection. *JAMA* **2014,** *311* (14), 1438-1439.
123. Dantes, R.; Mu, Y.; Belflower, R.; Aragon, D.; Dumyati, G.; Harrison, L. H.; Lessa, F. C.; Lynfield, R.; Nadle, J.; Petit, S., National burden of invasive methicillin-resistant Staphylococcus aureus infections, United States, 2011. *JAMA internal medicine* **2013,** *173* (21), 1970-1978.
124. Atilano, M. L.; Pereira, P. M.; Yates, J.; Reed, P.; Veiga, H.; Pinho, M. G.; Filipe, S. R., Teichoic acids are temporal and spatial regulators of peptidoglycan cross-linking in Staphylococcus aureus. *Proc Natl Acad Sci U S A* **2010,** *107* (44), 18991-6.
125. Garimella, R.; Halye, J. L.; Harrison, W.; Klebba, P. E.; Rice, C. V., Conformation of the Phosphate D-Alanine Zwitterion in Bacterial Teichoic Acid from Nuclear Magnetic Resonance Spectroscopy. *Biochemistry* **2009,** *48* (39), 9242-9249.
126. Halye, J. L.; Rice, C. V., Cadmium Chelation by Bacterial Teichoic Acid from Solid-State Nuclear Magnetic Resonance Spectroscopy. *Biomacromolecules* **2010,** *11* (2), 333-340.
127. Thomas, K. J.; Rice, C. V., Revised model of calcium and magnesium binding to the bacterial cell wall. *Biometals* **2014,** *27* (6), 1361-1370.
128. Wickham, J. R.; Halye, J. L.; Kashtanov, S.; Khandogin, J.; Rice, C. V., Revisiting Magnesium Chelation by Teichoic Acid with Phosphorus Solid-State NMR and Theoretical Calculations. *J Phys Chem B* **2009,** *113* (7), 2177-2183.
129. Gross, M.; Cramton, S. E.; Gotz, F.; Peschel, A., Key role of teichoic acid net charge in Staphylococcus aureus colonization of artificial surfaces. *Infect Immun* **2001,** *69* (5), 3423-6.
130. Lim, H. W.; Collins, S. A.; Resneck Jr, J. S.; Bolognia, J. L.; Hodge, J. A.; Rohrer, T. A.; Van Beek, M. J.; Margolis, D. J.; Sober, A. J.; Weinstock, M. A., The burden of skin disease in the United States. *Journal of the American Academy of Dermatology* **2017,** *76* (5), 958-972. e2.
131. Stevens, D. L.; Bisno, A. L.; Chambers, H. F.; Dellinger, E. P.; Goldstein, E. J.; Gorbach, S. L.; Hirschmann, J. V.; Kaplan, S. L.; Montoya, J. G.; Wade, J. C., Practice guidelines for the diagnosis and management of skin and soft tissue infections: 2014 update by the infectious diseases society of America. *Clin Infect Dis* **2014,** *59* (2), 147-59.
132. Therien, A. G.; Huber, J. L.; Wilson, K. E.; Beaulieu, P.; Caron, A.; Claveau, D.; Deschamps, K.; Donald, R. G.; Galgoci, A. M.; Gallant, M.; Gu, X.; Kevin, N. J.; Lafleur, J.; Leavitt, P. S.; Lebeau-Jacob, C.; Lee, S. S.; Lin, M. M.; Michels, A. A.; Ogawa, A. M.; Painter, R. E.; Parish, C. A.; Park, Y. W.; Benton-Perdomo, L.; Petcu, M.; Phillips, J. W.; Powles, M. A.; Skorey, K. I.; Tam, J.; Tan, C. M.; Young, K.; Wong, S.; Waddell, S. T.; Miesel, L., Broadening the spectrum of beta-lactam antibiotics through inhibition of signal peptidase type I. *Antimicrob Agents Ch* **2012,** *56* (9), 4662-70.
133. Tan, C. M.; Therien, A. G.; Lu, J.; Lee, S. H.; Caron, A.; Gill, C. J.; Lebeau-Jacob, C.; Benton-Perdomo, L.; Monteiro, J. M.; Pereira, P. M.; Elsen, N. L.; Wu, J.; Deschamps, K.; Petcu, M.; Wong, S.; Daigneault, E.; Kramer, S.; Liang, L.; Maxwell, E.; Claveau, D.; Vaillancourt, J.; Skorey, K.; Tam, J.; Wang, H.; Meredith, T. C.; Sillaots, S.; Wang-Jarantow, L.; Ramtohul, Y.; Langlois, E.; Landry, F.; Reid, J. C.; Parthasarathy, G.; Sharma, S.; Baryshnikova, A.; Lumb, K. J.; Pinho, M. G.; Soisson, S. M.; Roemer, T., Restoring methicillin-resistant Staphylococcus aureus susceptibility to beta-lactam antibiotics. *Sci Transl Med* **2012,** *4* (126), 126ra35.
134. Xia, G.; Kohler, T.; Peschel, A., The wall teichoic acid and lipoteichoic acid polymers of Staphylococcus aureus. *Int J Med Microbiol* **2010,** *300* (2-3), 148-54.
135. Pinho, M. G.; de Lencastre, H.; Tomasz, A., An acquired and a native penicillin-binding protein cooperate in building the cell wall of drug-resistant staphylococci. *P Natl Acad Sci USA* **2001,** *98* (19), 10886-91.

136. Komatsuzawa, H.; Suzuki, J.; Sugai, M.; Miyake, Y.; Suginaka, H., Effect of Combination of Oxacillin and Non-Beta-Lactam Antibiotics on Methicillin-Resistant Staphylococcus-Aureas. *J Antimicrob Chemoth* **1994,** *33* (6), 1155-1163.
137. Clements, J. M.; Coignard, F.; Johnson, I.; Chandler, S.; Palan, S.; Waller, A.; Wijkmans, J.; Hunter, M. G., Antibacterial activities and characterization of novel inhibitors of LpxC. *Antimicrob Agents Ch* **2002,** *46* (6), 1793-9.
138. Jackman, J. E.; Fierke, C. A.; Tumey, L. N.; Pirrung, M.; Uchiyama, T.; Tahir, S. H.; Hindsgaul, O.; Raetz, C. R. H., Antibacterial agents that target lipid A biosynthesis in Gram-negative bacteria - Inhibition of diverse UDP-3-O-(R-3-hydroxymyristoyl)-N-acetyglucosamine deacetylases by substrate analogs containing zinc binding motifs. *J Biol Chem* **2000,** *275* (15), 11002-11009.
139. Nayar, A. S.; Dougherty, T. J.; Ferguson, K. E.; Granger, B. A.; McWilliams, L.; Stacey, C.; Leach, L. J.; Narita, S.; Tokuda, H.; Miller, A. A.; Brown, D. G.; McLeod, S. M., Novel antibacterial targets and compounds revealed by a high-throughput cell wall reporter assay. *J Bacteriol* **2015,** *197* (10), 1726-34.
140. Wei, J. R.; Richie, D. L.; Mostafavi, M.; Metzger, L. E. t.; Rath, C. M.; Sawyer, W. S.; Takeoka, K. T.; Dean, C. R., LpxK Is Essential for Growth of Acinetobacter baumannii ATCC 19606: Relationship to Toxic Accumulation of Lipid A Pathway Intermediates. *mSphere* **2017,** *2* (4).
141. Clifton, L. A.; Ciesielski, F.; Skoda, M. W.; Paracini, N.; Holt, S. A.; Lakey, J. H., The Effect of Lipopolysaccharide Core Oligosaccharide Size on the Electrostatic Binding of Antimicrobial Proteins to Models of the Gram Negative Bacterial Outer Membrane. *Langmuir* **2016,** *32* (14), 3485-94.
142. Snyder, S.; Kim, D.; McIntosh, T. J., Lipopolysaccharide bilayer structure: effect of chemotype, core mutations, divalent cations, and temperature. *Biochemistry* **1999,** *38* (33), 10758-67.
143. Wang, H.; Gill, C. J.; Lee, S. H.; Mann, P.; Zuck, P.; Meredith, T. C.; Murgolo, N.; She, X.; Kales, S.; Liang, L.; Liu, J.; Wu, J.; Santa Maria, J.; Su, J.; Pan, J.; Hailey, J.; McGuinness, D.; Tan, C. M.; Flattery, A.; Walker, S.; Black, T.; Roemer, T., Discovery of wall teichoic acid inhibitors as potential anti-MRSA beta-lactam combination agents. *Chem Biol* **2013,** *20* (2), 272-84.
144. Pasquina, L. W.; Santa Maria, J. P.; Walker, S., Teichoic acid biosynthesis as an antibiotic target. *Curr Opin Microbiol* **2013,** *16* (5), 531-7.
145. Mermel, L. A.; Allon, M.; Bouza, E., Clinical practice guidelines for the diagnosis and management of intravascular catheter-related infection: 2009 update by the Infectious Diseases Society of America (vol 49, pg 1, 2009). *Clinical Infectious Diseases* **2010,** *50* (7), 1079-1079.
146. Baddour, L. M.; Wilson, W. R.; Bayer, A. S.; Fowler, V. G., Jr.; Tleyjeh, I. M.; Rybak, M. J.; Barsic, B.; Lockhart, P. B.; Gewitz, M. H.; Levison, M. E.; Bolger, A. F.; Steckelberg, J. M.; Baltimore, R. S.; Fink, A. M.; O'Gara, P.; Taubert, K. A.; American Heart Association Committee on Rheumatic Fever, E.; Kawasaki Disease of the Council on Cardiovascular Disease in the Young, C. o. C. C. C. o. C. S.; Anesthesia; Stroke, C., Infective Endocarditis in Adults: Diagnosis, Antimicrobial Therapy, and Management of Complications: A Scientific Statement for Healthcare Professionals From the American Heart Association. *Circulation* **2015,** *132* (15), 1435-86.
147. McDanel, J. S.; Roghmann, M. C.; Perencevich, E. N.; Ohl, M. E.; Goto, M.; Livorsi, D. J.; Jones, M.; Albertson, J. P.; Nair, R.; O'Shea, A. M. J.; Schweizer, M. L., Comparative Effectiveness of Cefazolin Versus Nafcillin or Oxacillin for Treatment of Methicillin-Susceptible Staphylococcus aureus Infections Complicated by Bacteremia: A Nationwide Cohort Study. *Clin Infect Dis* **2017,** *65* (1), 100-106.
148. Blumenthal, K. G.; Shenoy, E. S., Editorial Commentary: Fortune Favors the Bold: Give a Beta-Lactam! *Clin Infect Dis* **2016,** *63* (7), 911-3.

149. Klein, J. O., History of macrolide use in pediatrics. *The Pediatric infectious disease journal* **1997,** *16* (4), 427-431.
150. Ross, J.; Eady, E.; Cove, J.; Cunliffe, W.; Baumberg, S.; Wootton, J., Inducible erythromycin resistance in staphlyococci is encoded by a member of the ATP-binding transport super-gene family. *Molecular microbiology* **1990,** *4* (7), 1207-1214.
151. Guay, G. G.; Khan, S. A.; Rothstein, D. M., The tet (K) gene of plasmid pT181 of Staphylococcus aureus encodes an efflux protein that contains 14 transmembrane helices. *Plasmid* **1993,** *30* (2), 163-166.
152. Ng, E.; Trucksis, M.; Hooper, D. C., Quinolone resistance mediated by norA: physiologic characterization and relationship to flqB, a quinolone resistance locus on the Staphylococcus aureus chromosome. *Antimicrob. Agents Chemother.* **1994,** *38* (6), 1345-1355.
153. Scott, M. G.; Gold, M. R.; Hancock, R. E., Interaction of cationic peptides with lipoteichoic acid and gram-positive bacteria. *Infection and immunity* **1999,** *67* (12), 6445-6453.
154. Falagas, M. E.; Kasiakou, S. K., Toxicity of polymyxins: a systematic review of the evidence from old and recent studies. *Crit Care* **2006,** *10* (1), R27.
155. Gibney, K. A.; Sovadinova, I.; Lopez, A. I.; Urban, M.; Ridgway, Z.; Caputo, G. A.; Kuroda, K., Poly(ethylene imine)s as antimicrobial agents with selective activity. *Macromol Biosci* **2012,** *12* (9), 1279-89.
156. Boussif, O.; Lezoualc'h, F.; Zanta, M. A.; Mergny, M. D.; Scherman, D.; Demeneix, B.; Behr, J.-P., A versatile vector for gene and oligonucleotide transfer into cells in culture and in vivo: polyethylenimine. *Proc Natl Acad Sci USA* **1995,** *92* (16), 7297-7301.
157. Boussif, O.; Zanta, M.; Behr, J., Optimized galenics improve in vitro gene transfer with cationic molecules up to 1000-fold. *Gene therapy* **1996,** *3* (12), 1074-1080.
158. Zanta, M.-A.; Boussif, O.; Adib, A.; Behr, J.-P., In vitro gene delivery to hepatocytes with galactosylated polyethylenimine. *Bioconjugate Chemistry* **1997,** *8* (6), 839-844.
159. Fischer, D.; Bieber, T.; Li, Y.; Elsässer, H.-P.; Kissel, T., A novel non-viral vector for DNA delivery based on low molecular weight, branched polyethylenimine: effect of molecular weight on transfection efficiency and cytotoxicity. *Pharmaceutical research* **1999,** *16* (8), 1273-1279.
160. Motley, M. P.; Banerjee, K.; Fries, B. C., Monoclonal antibody-based therapies for bacterial infections. *Curr Opin Infect Dis* **2019,** *32* (3), 210-216.
161. van Riet, E.; Everts, B.; Retra, K.; Phylipsen, M.; van Hellemond, J. J.; Tielens, A. G.; van der Kleij, D.; Hartgers, F. C.; Yazdanbakhsh, M., Combined TLR2 and TLR4 ligation in the context of bacterial or helminth extracts in human monocyte derived dendritic cells: molecular correlates for Th1/Th2 polarization. *BMC Immunol* **2009,** *10*, 9.
162. Strunk, T.; Power Coombs, M. R.; Currie, A. J.; Richmond, P.; Golenbock, D. T.; Stoler-Barak, L.; Gallington, L. C.; Otto, M.; Burgner, D.; Levy, O., TLR2 mediates recognition of live Staphylococcus epidermidis and clearance of bacteremia. *PLoS One* **2010,** *5* (4), e10111.
163. Netea, M. G.; Nold-Petry, C. A.; Nold, M. F.; Joosten, L. A.; Opitz, B.; van der Meer, J. H.; van de Veerdonk, F. L.; Ferwerda, G.; Heinhuis, B.; Devesa, I.; Funk, C. J.; Mason, R. J.; Kullberg, B. J.; Rubartelli, A.; van der Meer, J. W.; Dinarello, C. A., Differential requirement for the activation of the inflammasome for processing and release of IL-1beta in monocytes and macrophages. *Blood* **2009,** *113* (10), 2324-35.
164. Takeuchi, O.; Hoshino, K.; Akira, S., Cutting edge: TLR2-deficient and MyD88-deficient mice are highly susceptible to Staphylococcus aureus infection. *J Immunol* **2000,** *165* (10), 5392-6.
165. Lembo, A.; Kalis, C.; Kirschning, C. J.; Mitolo, V.; Jirillo, E.; Wagner, H.; Galanos, C.; Freudenberg, M. A., Differential contribution of Toll-like receptors 4 and 2 to the cytokine response to Salmonella enterica serovar Typhimurium and Staphylococcus aureus in mice. *Infect Immun* **2003,** *71* (10), 6058-62.

166. Schwandner, R.; Dziarski, R.; Wesche, H.; Rothe, M.; Kirschning, C. J., Peptidoglycan- and lipoteichoic acid-induced cell activation is mediated by toll-like receptor 2. *J Biol Chem* **1999,** *274* (25), 17406-9.
167. Schultz, G.; Bjarnsholt, T.; James, G. A.; Leaper, D. J.; McBain, A. J.; Malone, M.; Stoodley, P.; Swanson, T.; Tachi, M.; Wolcott, R. D.; Global Wound Biofilm Expert, P., Consensus guidelines for the identification and treatment of biofilms in chronic nonhealing wounds. *Wound Repair Regen* **2017,** *25* (5), 744-757.
168. Zhao, G.; Usui, M. L.; Lippman, S. I.; James, G. A.; Stewart, P. S.; Fleckman, P.; Olerud, J. E., Biofilms and Inflammation in Chronic Wounds. *Adv Wound Care (New Rochelle)* **2013,** *2* (7), 389-399.
169. Lavery, L. A.; Armstrong, D. G.; Murdoch, D. P.; Peters, E. J.; Lipsky, B. A., Validation of the Infectious Diseases Society of America's diabetic foot infection classification system. *Clin Infect Dis* **2007,** *44* (4), 562-5.
170. Driscoll, J. A.; Brody, S. L.; Kollef, M. H., The epidemiology, pathogenesis and treatment of Pseudomonas aeruginosa infections. *Drugs* **2007,** *67* (3), 351-368.
171. Richards, M. J.; Edwards, J. R.; Culver, D. H.; Gaynes, R. P.; System, N. N. I. S., Nosocomial infections in pediatric intensive care units in the United States. *Pediatrics* **1999,** *103* (4), e39-e39.
172. Burns, J. L.; Gibson, R. L.; McNamara, S.; Yim, D.; Emerson, J.; Rosenfeld, M.; Hiatt, P.; McCoy, K.; Castile, R.; Smith, A. L., Longitudinal assessment of Pseudomonas aeruginosa in young children with cystic fibrosis. *The Journal of infectious diseases* **2001,** *183* (3), 444-452.
173. Lyczak, J. B.; Cannon, C. L.; Pier, G. B., Establishment of Pseudomonas aeruginosa infection: lessons from a versatile opportunist1*Address for correspondence: Channing Laboratory, 181 Longwood Avenue, Boston, MA 02115, USA. *Microbes and Infection* **2000,** *2* (9), 1051-1060.
174. Branski, L. K.; Al-Mousawi, A.; Rivero, H.; Jeschke, M. G.; Sanford, A. P.; Herndon, D. N., Emerging infections in burns. *Surg Infect (Larchmt)* **2009,** *10* (5), 389-97.
175. Lim, H. W.; Collins, S. A. B.; Resneck, J. S., Jr.; Bolognia, J. L.; Hodge, J. A.; Rohrer, T. A.; Van Beek, M. J.; Margolis, D. J.; Sober, A. J.; Weinstock, M. A.; Nerenz, D. R.; Smith Begolka, W.; Moyano, J. V., The burden of skin disease in the United States. *J Am Acad Dermatol* **2017,** *76* (5), 958-972 e2.
176. Centers for Disease Control and Prevention. National Diabetes Statistics Report, A., GA: Centers for Disease Control and Prevention, US Department of Health and Human Services; 2017.
177. Swanson, T.; Wolcott, R. D.; Wallis, H.; Woodmansey, E. J., Understanding biofilm in practice: a global survey of health professionals. *J Wound Care* **2017,** *26* (8), 426-440.
178. Fazli, M.; Bjarnsholt, T.; Kirketerp-Moller, K.; Jorgensen, B.; Andersen, A. S.; Krogfelt, K. A.; Givskov, M.; Tolker-Nielsen, T., Nonrandom distribution of Pseudomonas aeruginosa and Staphylococcus aureus in chronic wounds. *J Clin Microbiol* **2009,** *47* (12), 4084-9.
179. Malic, S.; Hill, K. E.; Hayes, A.; Percival, S. L.; Thomas, D. W.; Williams, D. W., Detection and identification of specific bacteria in wound biofilms using peptide nucleic acid fluorescent in situ hybridization (PNA FISH). *Microbiology* **2009,** *155* (Pt 8), 2603-11.
180. Gjodsbol, K.; Christensen, J. J.; Karlsmark, T.; Jorgensen, B.; Klein, B. M.; Krogfelt, K. A., Multiple bacterial species reside in chronic wounds: a longitudinal study. *Int Wound J* **2006,** *3* (3), 225-31.
181. Stover, C. K.; Pham, X. Q.; Erwin, A. L.; Mizoguchi, S. D.; Warrener, P.; Hickey, M. J.; Brinkman, F. S.; Hufnagle, W. O.; Kowalik, D. J.; Lagrou, M.; Garber, R. L.; Goltry, L.; Tolentino, E.; Westbrock-Wadman, S.; Yuan, Y.; Brody, L. L.; Coulter, S. N.; Folger, K. R.; Kas, A.; Larbig, K.; Lim, R.; Smith, K.; Spencer, D.; Wong, G. K.; Wu, Z.; Paulsen, I. T.;

Reizer, J.; Saier, M. H.; Hancock, R. E.; Lory, S.; Olson, M. V., Complete genome sequence of Pseudomonas aeruginosa PAO1, an opportunistic pathogen. *Nature* **2000,** *406* (6799), 959-64.
182. Dongari-Bagtzoglou, A., Pathogenesis of mucosal biofilm infections: challenges and progress. *Expert Rev Anti-Infe* **2008,** *6* (2), 201-8.
183. Vermote, A.; Van Calenbergh, S., Small-Molecule Potentiators for Conventional Antibiotics against Staphylococcus aureus. *ACS Infect Dis* **2017,** *3* (11), 780-796.
184. Hill, M. A.; Lam, A. K.; Reed, P.; Harney, M. C.; Wilson, B. A.; Moen, E. L.; Wright, S. N.; Pinho, M. G.; Rice, C. V., BPEI-Induced Delocalization of PBP4 Potentiates beta-Lactams against MRSA. *Biochemistry* **2019,** *58* (36), 3813-3822.
185. (USCAST)., T. U. S. C. o. A. S. T. Breakpoint tables for interpretation of MICs and zone diameters Version 3.0. http://www.uscast.org.
186. Kojima, S.; Nikaido, H., Permeation rates of penicillins indicate that Escherichia coli porins function principally as nonspecific channels. *Proc Natl Acad Sci U S A* **2013,** *110* (28), E2629-34.
187. Zgurskaya, H. I.; Lopez, C. A.; Gnanakaran, S., Permeability Barrier of Gram-Negative Cell Envelopes and Approaches To Bypass It. *ACS Infect Dis* **2015,** *1* (11), 512-522.
188. Nascimento, A., Jr.; Pontes, F. J.; Lins, R. D.; Soares, T. A., Hydration, ionic valence and cross-linking propensities of cations determine the stability of lipopolysaccharide (LPS) membranes. *Chem Commun (Camb)* **2014,** *50* (2), 231-3.
189. Krishnamoorthy, G.; Leus, I. V.; Weeks, J. W.; Wolloscheck, D.; Rybenkov, V. V.; Zgurskaya, H. I., Synergy between Active Efflux and Outer Membrane Diffusion Defines Rules of Antibiotic Permeation into Gram-Negative Bacteria. *Mbio* **2017,** *8* (5).
190. Rampersad, S. N., Multiple Applications of Alamar Blue as an Indicator of Metabolic Function and Cellular Health in Cell Viability Bioassays. *Sensors-Basel* **2012,** *12* (9), 12347-12360.
191. Jo, S.; Wu, E. L.; Stuhlsatz, D.; Klauda, J. B.; MacKerell, A. D.; Widmalm, G.; Im, W., Lipopolysaccharide Membrane Building and Simulation. In *Glycoinformatics*, Lütteke, T.; Frank, M., Eds. Springer New York: New York, NY, 2015; pp 391-406.
192. Knirel, Y. A.; Bystrova, O. V.; Kocharova, N. A.; Zahringer, U.; Pier, G. B., Conserved and variable structural features in the lipopolysaccharide of Pseudomonas aeruginosa. *J Endotoxin Res* **2006,** *12* (6), 324-36.
193. Hancock, R. E.; Farmer, S. W.; Li, Z. S.; Poole, K., Interaction of aminoglycosides with the outer membranes and purified lipopolysaccharide and OmpF porin of Escherichia coli. *Antimicrob Agents Chemother* **1991,** *35* (7), 1309-14.
194. Gill, E. E.; Franco, O. L.; Hancock, R. E., Antibiotic adjuvants: diverse strategies for controlling drug-resistant pathogens. *Chem Biol Drug Des* **2015,** *85* (1), 56-78.
195. Trimble, M. J.; Mlynarcik, P.; Kolar, M.; Hancock, R. E., Polymyxin: Alternative Mechanisms of Action and Resistance. *Cold Spring Harb Perspect Med* **2016,** *6* (10).
196. Lutkenhaus, J.; Pichoff, S.; Du, S., Bacterial cytokinesis: From Z ring to divisome. *Cytoskeleton* **2012,** *69* (10), 778-90.
197. de Boer, P. A., Advances in understanding E. coli cell fission. *Curr Opin Microbiol* **2010,** *13* (6), 730-7.
198. Goldberg, J. B.; Hatano, K.; Pier, G. B., Synthesis of lipopolysaccharide O side chains by Pseudomonas aeruginosa PAO1 requires the enzyme phosphomannomutase. *J Bacteriol* **1993,** *175* (6), 1605-11.